HEINRICH HEINE
UNIVERSITÄT DÜSSELDORF

Biochemical studies on Pdr5 – an ABC transporter from *Saccharomyces cerevisiae*

Inaugural dissertation

for the attainment of the title of doctor
in the Faculty of Mathematics and Natural Sciences
at the Heinrich Heine University Düsseldorf

presented by

Rakeshkumar P. Gupta
from Pune

Düsseldorf, February 2014

from the Institute of Biochemistry
at the Heinrich Heine University Düsseldorf

Published by permission of the
Faculty of Mathematics and Natural Sciences at
Heinrich Heine University Düsseldorf

Supervisor: Prof. Lutz Schmitt
Co-supervisor: Prof. Georg Groth

Date of the oral examination:

'Imagination is more important than knowledge'
-Albert Einstein

Summary

Pdr5 is an ATP binding cassette (ABC) transporter from *Saccharomyces cerevisiae* involved in the phenomena of pleiotropic drug resistance (PDR). Its primary function is to protect the yeast cell by pumping out toxic compounds to the extracellular surface. To carry out its function Pdr5 utilizes ATP as an energy source, which is bound and hydrolyzed intracellularly by the nucleotide binding domains (NBDs). Full size ABC transporters such as Pdr5 possess two such domains that are capable of binding two ATP molecules. Unlike most human ABC transporters Pdr5 possesses one degenerate nucleotide binding site (NBS) and one canonical binding site. This feature renders Pdr5 and other yeast ABC transporters unable to hydrolyze ATP at the degenerate site. To understand the relevance of this degeneracy we mutated the non-consensus amino acid residues with their consensus counterparts and studied the impact on cell survival when challenged with toxic compounds and in vitro activity of Pdr5. Our findings suggest that artificially introducing a second consensus site completely disrupts Pdr5 function, which is displayed by increased drug sensitivity, drastically reduced ATPase activity and no substrate transport. This supports our hypothesis that yeast ABC transporters have evolved and maintained a degenerate NBS that function as a structural platform for ATP hydrolysis to take place at the consensus site. This would also explain the high level basal ATPase activity, which keeps Pdr5 active at all the times to pump out substrate immediately upon encountering it.

Second part of the work deals with determining stoichiometry of rhodamine 6g transport mediated by Pdr5 in crude membrane vesicle preparations. Coupling of ATP hydrolysis to substrate transport is an essential feature of ABC transporter function. Most human ABC transporters have a strict coupling and display substrate stimulated ATPase activity. Pdr5 on the other hand is an uncoupled transporter and has so far not displayed any substrate stimulation. We tried to determine the stoichiometry of transport of a fluorescent substrate rhodamine 6g by measuring the amount of ATP hydrolyzed while transport is being quantitatively measured. The ratio we obtained was 0.3 moles of substrate transported per mole of ATP hydrolyzed. But this ratio was stochastic in the sense that Pdr5 being an uncoupled

transporter it is only a matter of chance that it encounters a substrate during ATP hydrolysis. The optimum rhodamine 6g concentration was determined to be 600nM beyond which the substrate becomes inhibitory to protein activity and reduces the stoichiometric ratio.

The third and last part of the work was focussed on determining alternate mechanisms of drug resistance in particular mutants of Pdr5. It was observed with some NBD mutants of Pdr5 that they display increased resistance towards rhodamine 6g in liquid drug assays when compared to the wildtype protein. But, these mutants lacked functional Pdr5 and were incapable of transporting rhodamine 6g. This is supported by laser scanning confocal microscopy data that displays accumulation of the fluorescent dye within the cells of these mutants, who can withstand twice as much rhodamine 6g as compared to the wildtype cells. To determine the reason for this behaviour we subjected the mutants to complete proteome analysis and discovered that in the presence of rhodamine 6g the mutants have significantly higher up-regulation of glycolytic enzymes in the background of lack of mitochondrial function. These results are supported by liquid drug assays with varying glucose concentrations where the mutants display higher efficiency in growth at lower (1%) and higher (3-4%) glucose concentrations than the wildtype cells. It also points in the direction of post-translational modifications of Pdr5 that might be involved in its interaction with other membrane proteins and in turn lead to glucose import within the cells.

In short the entire work can be summarized in three points:

1. The degenerate nucleotide binding site in yeast ABC transporters functions as a structural platform.
2. The stochastic stoichiometry for rhodamine 6g transport mediated by Pdr5 in membrane vesicles is 0.3.
3. Specific mutants of Pdr5 display alternate mechanisms of drug resistance in the presence of rhodamine 6g.

Zusammenfassung

Pdr5 ist ein ABC (*ATP-binding cassette*) -Transporter aus *Saccharomyces cerevisiae,* der eine Schlüsselstellung im Phänomen der pleiotropen Drogenresistenz (PDR) einnimmt. Seine primäre Funktion besteht darin Hefezellen durch aktive Ausschleusung toxischer Verbindungen zu schützen. Um diese lebenswichtige Funktion zu erfüllen nutzt Pdr5 ATP als Energiequelle, das durch zytosolische Nukleotidbindedomänen (NBDs) gebunden und hydrolysiert wird. '*Full size*' ABC-Transporter wie Pdr5 besitzen zwei dieser Domänen, die jeweils ein ATP Molekül binden können. Im Gegensatz zu humanen ABC-Transportern besitzt Pdr5 eine sogenannte degenerierte Nukleotidbindungsstelle (NBS) und eine kanonische Bindungsstelle. Pdr5 und andere ABC-Transporter der Hefe sind daher nicht in der Lage in der degenerierten Bindungsstelle ATP zu hydrolysieren. Um die Relevanz dieser Degenerierung molekular zu analysieren, wurden die nicht-kanonischen Aminosäuren der degenerierten Bindungsstelle zu ihren konservierten Analoga mutiert. Anschließend wurden die Auswirkungen auf die Zellviabilität in Gegenwart toxischer Verbindungen und auf die in vitro Aktivität von Pdr5 analysiert. Dabei zeigte sich eine erhöhte Sensitivität gegenüber Drogen, eine drastisch reduzierte ATPase-Aktivität und ein fehlender Substrattransport. Diese Ergebnisse belegen, dass die Einführung einer zweiten, künstlichen Konsensussequenz die Funktion von Pdr5 komplett inhibiert. Damit wird die Hypothese unterstützt, dass während der Evolution der Hefe die ABC Transporter eine degenerierte NBS entwickelten, die als strukturelle Plattform der ATP-Hydrolyse fungiert. Auch lässt sich somit die hohe basale ATPase-Aktivität erklären, denn die Degeneration stellt den funktionalen Zustand von Pdr5 zu Jederzeit sicher.

Der zweite Teil der Dissertation beschäftigt sich mit der Bestimmung der Stöchiometrie des rhodamin 6g Transports in Pdr5 Membranvesikeln und der dafür benötigen Anzahl hydrolysierter ATP Moleküle. Die Kopplung der ATP-Hydrolyse mit dem Substrattransport als Grundlage dieses Prozesses ist ein wesentliches Merkmal von ABC Transportern. Die meisten menschlichen ABC Transporter besitzen eine strikte, energetische Kopplung und zeigen Substrat-stimulierte ATPase Aktivität. Pdr5 hingegen ist ein entkoppelter Transporter, für den bisher

keine Substratstimulation gezeigt werden konnte. Für das fluoreszierende Substrat rhodamin 6g wurde durch Messung des benötigten ATP die Stöchiometrie des Transportes quantitativ bestimmt, dabei wurde ein Verhältnis von 0.3 mol transportiertem Substrat pro mol hydrolysiertem ATP ermittelt. Jedoch ist dieses Verhältnis stochastischer Natur und wird durch die Wahrscheinlichkeit bestimmt, ob der entkoppelte Transporter Pdr5 während eines Hydrolyseszyklus auf ein Substrat trifft. Die rhodamin 6g Konzentration, bei der eine maximale Stöchiometrie bestimmt wurde, beträgt 600 nM. Eine weitere Erhöhung der Substratkonzentration wirkt sich hemmend auf die Aktivität aus und reduziert das stöchiometrische Verhältnis.

Der dritte und letzte Teil der Arbeit widmet sich der Bestimmung alternativer Mechanismen der Drogenresistenz, die bei einzelnen Mutanten von Pdr5 auftraten. Bei Mutanten der Pdr5 NBD wurde eine erhöhte Resistenz gegenüber rhodamin 6g in Flüssigkultur-Assays festgestellt. Diesen fehlte aber jegliche Funktionalität und damit konnten sie auch nicht den Transport von rhodamin 6g katalysieren. Dies wird durch Laser-Scan-Mikroskop Messungen unterstützt. Um die Ursachen dieses völlig unerwarteten Verhaltens zu bestimmen, wurden Proteomanalysen des Wildtyps und der entsprechenden Mutante durchgeführt. In Gegenwart von rhodamin 6g konnte in der Mutante eine Erhöhung der Glykolyse und eine verringerte mitochondriale Aktivität bestimmt werden. Diese Ergebnisse wurden mit Untersuchungen in Gegenwart unterschiedlicher Glukosekonzentrationen verifiziert. Hier wies die Mutante ein verbessertes Wachstums bei niedriger (1%) und hoher (3-4%) Glukosekonzentration auf. Erste Ergebnisse belegen, dass Änderungen in der post-translationalen Modifikation von Pdr5 vorliegen, die eine Wechselwirkung mit anderen (Membran)proteinen induzieren könnten.

Abschließend kann diese Dissertation in drei essentiellen Punkten zusammengefasst werden:

1. Die degenerierte Nukleotidbindungsstelle in Hefe ABC transportern stellt eine strukturelle Plattform dar.

2. Die stochastische Stöchiometrie des durch Pdr5 vermittelten rhodamin 6g Transports in Membranvesikeln beträgt maximal 0.3.

3. Spezifische Mutanten von Pdr5 führen zu alternativen Mechanismen der Drogenresistenz in Gegenwart von rhodamin 6g.

Table of Contents

Introduction

Pleiotropic drug resistance in yeast

Multidrug resistance has proven to be a significant challenge in treatment of cancer by imparting resistance to chemotherapy. The main culprit was identified as MDR1 or P-gp. Since the identification a lot of effort has been invested to gain insight into the structure and function of P-gp (1). A similar protein CFTR (Cystic Fibrosis Transmembrane Conductance Regulator) is a chloride channel and mutations in which are responsible for the disease cystic fibrosis (2). In addition diseases caused by protozoans such as *Plasmodium falciparum* were also found to involve multidrug resistance proteins and are proving to be roadblocks in malaria treatment (3). In essence the multidrug proteins involved in clinically relevant diseases are ABC transporters.

Yeast being a single cell eukaryote shares many features with mammalian cells and has proven to be an excellent model organism. Since the handling and culturing of yeast is comparatively easier than mammalian cells it has proven useful in the study of many phenomena at a molecular level. *Saccharomyces cerevisiae* has been found to possess a number of ABC transporters that are part of the pleiotropic drug resistance (PDR) network (4). The term PDR is analogous to multidrug resistance observed in higher eukaryotes. The drug resistance observed in yeast can broadly be classified into three classes:

1. ABC superfamily, consisting of Pdr5, Snq2, Yor1
2. Major facilitator superfamily (MFS), consisting of Atr1 and Sge1

3. Transcriptional regulators, including Pdr1, Pdr3, Pdr7, Pdr9, Yap1 and Yap2

Among the transcriptional regulators Pdr1 and its paralog protein Pdr3 are important ones and are part of the GAL4 family of yeast transcription factors, and are characterized by a zinc-binding motif (5). Pdr1 and Pdr3 bind to the same DNA binding site called the Pdr response element (PDRE) (6). Despite their significant sequence identity both transcription factors play distinct roles. Pdr1 allele mutations affect the transcription of ABC proteins more than Pdr3 and in turn lead to difference in drug sensitivities (7). Figure 1 summarizes the downstream regulation exerted by Pdr1 and Pdr3 (6).

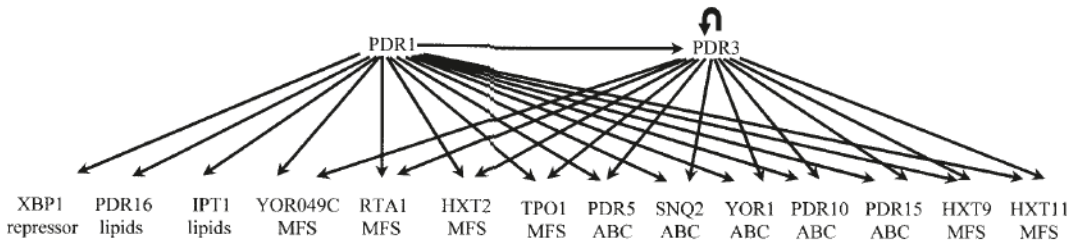

Figure 1. The major target genes of Pdr1 and Pdr3. Figure taken from Kolaczkowska A *et al*. (6).

The most notable observation from the mutants of Pdr1 allele (*pdr1-3*) was the over expression of the ABC transporter Pdr5 (8).

Pdr5, structure and function

Pdr5 is an ABC transporter from *Saccharomyces cerevisiae*. It is functionally similar to Pgp and has been studied well in the recent past. It is a 170-kDa full size transporter and is part of the PDR sub-family in yeast. For full size transporters such as Pdr5 the entire protein is encoded in a single polypeptide chain, whereas for half size

transporters such as LmrCD, TAP 1, TAP 2 etc. different genes encode for the respective halves of the protein (9, 10). The discovery that certain mutations in the transcription factor Pdr1 lead to constitutive over expression of Pdr5 opened new doors to the study of these intriguing proteins more closely (5). Pdr5 being an ABC transporter has two cytoplasmically located nucleotide binding domains (NBDs) and two trans-membrane domains (TMDs). So far the physiological substrate for Pdr5 has not been found, although it has been predicted to play a role in phospholipid transfer from the inner to the outer leaflet of the plasma membrane (11). Apart from this the spectrum of compounds Pdr5 can transport is very wide and includes hydrophobic substances, detergents and dyes among others (12, 13). Pdr5, Snq2 and Yor1 are part of the response proteins that swing into action when challenged with xenotoxic compounds and also have substrate overlap. They have also shown to undergo compensatory activation in case one of these proteins is missing (14). The energy source for the activity of Pdr5 is mainly ATP although other nucleotides may be used but with less efficiency (15). Figure 2 shows the basic architecture of a Pdr5 molecule in the membrane. ABC transporters in general are presumed to have similar architectures. ATP binding and hydrolysis takes place at the cytoplasmically located NBDs, which are two in number, while the substrate binding pocket lies in the TMDs. Two nucleotides are sandwiched in between the two NBDs. Several consensus residues are involved in this binding to the nucleotides as enlisted in Table 1. Walker A, Walker B, H loop of one NBD and the C loop from the other NBD are always involved in binding to one nucleotide (16).

	Walker A	Q loop	C loop	Walker B	D loop	H loop
Consensus	GXXGXGKST	XQX	LSGGQ	hhhhDE	SALD	H
NBD1	GRPGSGCTT	AEA	VSGGE	FQCWDN	RGLD	Y
NBD2	GASGAGKTT	QQQ	LNVEQ	LVFLDE	SGLD	H

Table 1. Residues involved in ATP binding and hydrolysis of Pdr5. X- any amino acid, h- any hydrophobic amino acid. Residues in red deviate from the consensus sequence.

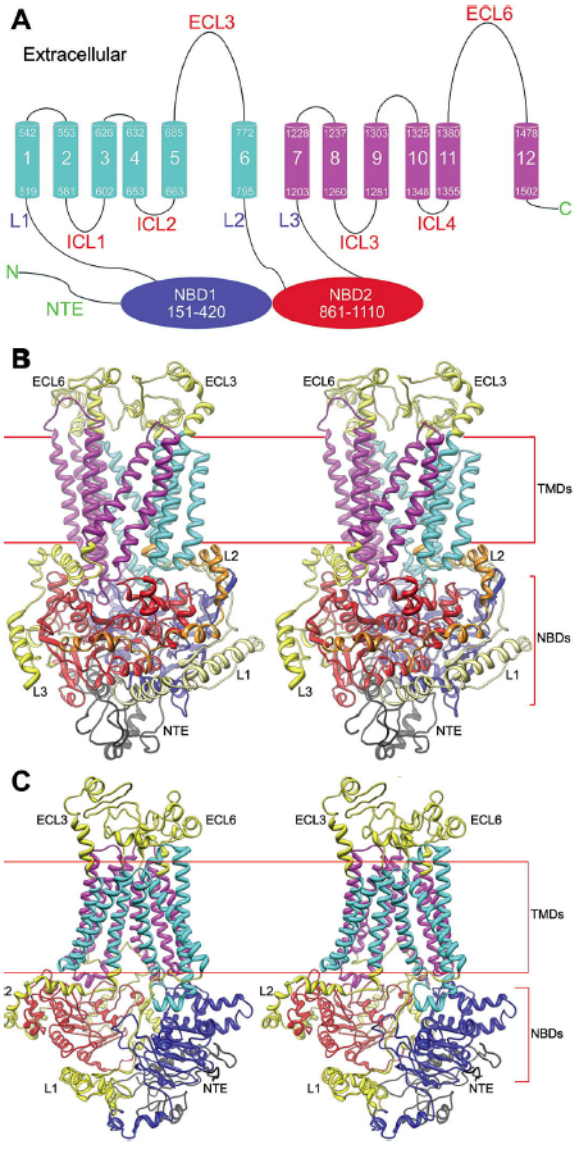

Figure 2. Structural model of the yeast ABC transporter Pdr5. (A) Predicted topology of Pdr5. Pdr5 is predicted to have 12 TMHs and 2 NBDs, organized in reverse order. The two NBDs are shown as blue and red ovals, respectively. Helices in TMD1 (519–795) are in cyan and those in TMD2 in magenta. Extracellular loops (ECLs), intracellular loops (ICLs), linkers (L1–L3), and the amino terminal extension (NTE) are indicated. (B) Stereoscopic view of the Pdr5 model based on the Sav1866 and hemolysin B

templates. The two modeled TMDs, colored magenta and cyan, are embedded in a membrane bilayer, which is indicated by the two horizontal lines. Underneath the TMDs are the NBDs (NBD1 in blue, NBD2 in red). The NBDs are surrounded by connecting loops L1–L3 in yellow and orange. The amino terminal extension (NTE) is located below the NBDs (black) and the extracellular loops (ECL3 and ECL6) sit above the TMDs (yellow). (C) Stereoscopic view of the Pdr5 model based on the P-gp template. The colors are the same as above. Figure taken from Rutledge *et al*. (17).

Mechanism of action of ABC transporters

ABC transporters couple ATP hydrolysis to substrate transport. A number of studies carried out with regards to this coupling propose a generally accepted mode of action (18-21). The resting state of the protein is the inward facing conformation; binding of substrate to the substrate binding pocket is followed by two nucleotides binding to the NBDs. This leads to closure of the NBD dimer. Hydrolysis of one nucleotide is the power stroke that changes the protein from inward facing to an outward facing conformation and leads to the substrate being released in the extracellular space. The second nucleotide hydrolysis is the step proposed to set the protein back to its resting state. Nucleotide binding and hydrolysis are the key steps in this entire process. A number of residues in the NBDs are key to achieving this goal and are summarized in Table 2:

	Consensus sequence	**Function**
Walker A	GXXGXGKST	Key residue Lysine : binds ATP.

C loop	LSGGQ	Key residues SGG : bind ATP.
Walker B	hhhhDE	Key residue Glutamate : forms catalytic dyad with Histidine of H loop.
H loop	H	Important for ATP hydrolysis.
Q loop	XQX	Communication between NBDs and TMDs.
D loop	SGLD	Communication between the two NBS.
X loop		Control access to the substrate-binding pocket.

Table 2. Summary of key residues of ABC transporters and their roles. X- any amino acid, h- any hydrophobic amino acid.

In terms of ABC transporters having all the consensus residues in place it is presumed that at least one nucleotide is hydrolyzed, which switches the protein from the inward to outward facing conformation. While the second nucleotide might be necessary to reset the protein to its resting state facing the inward conformation (22). Whether the second nucleotide is hydrolyzed or not is debatable.

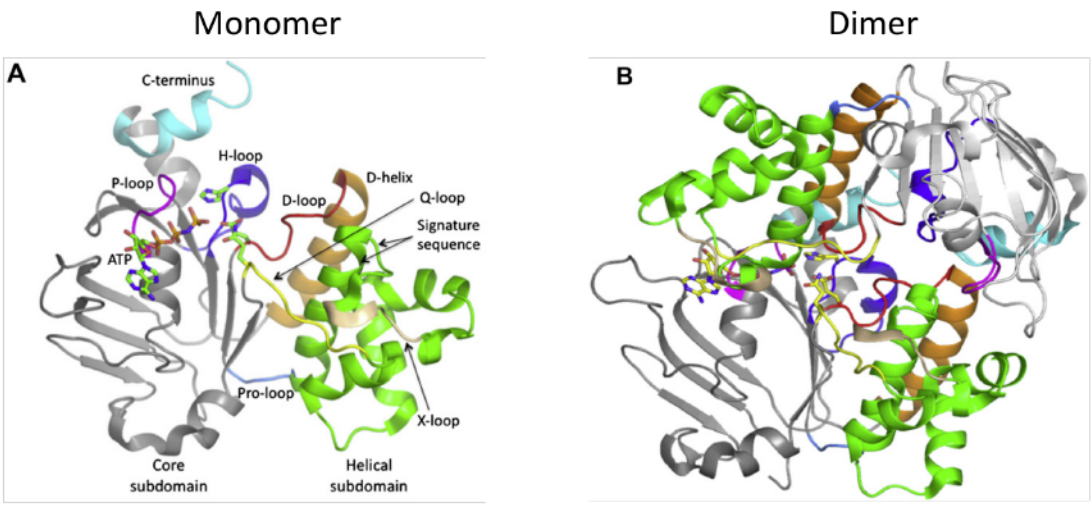

Figure 3. NBD monomer and dimer showing the major conserved motifs and residues. (A) NBD monomer in ribbon representation with ATP in stick format. The core sub-domain (CSD) is coloured grey and the helical subdomain (HSD) is green. The Walker A (P loop) motif is coloured magenta. The catalytic glutamate (in stick) is depicted at the start of the D loop (red) followed immediately by the D helix (orange). The Q loop is in yellow with the glutamine side chain in stick form. The H loop (histidine side chain in stick) is in dark blue; and the Pro loop is in light blue at the bottom of the figure connecting the two subdomains and leading into the signature sequence (vertical green helix and loop adjacent to the orange D helix). The C-terminus is coloured cyan. The short orange helix and loop in the centre of the HSD is the X loop. (B) The NBD dimer with the ATPs ''sandwiched' between the two protomers, with the ATP depicted on the left residing within the catalytic site of the lower monomer of the pair; and correspondingly for the right-side ATP in the catalytic site of the upper monomer. The colour coding is identical to that of Fig. 3A, with the CSD gray, HSD green, D loop red, D helix orange, H loop blue, P loop purple,

Q loop yellow, C-terminal helix cyan. ATP and residues Q422, E503, and H534 are in stick form, with carbon yellow, nitrogen blue, and oxygen red. Figure taken from George *et al*. (23).

Basically two models of ATP hydrolysis have been proposed.

1. Switch model where it is proposed that the two NBDs dissociate completely after hydrolysis of the two nucleotides, and
2. Constant contact model where it is presumed that the NBDs are in constant contact with each other at all times during ATP hydrolysis, which takes place at one site at a time. The two models are diagrammatically shown in Figure 4.

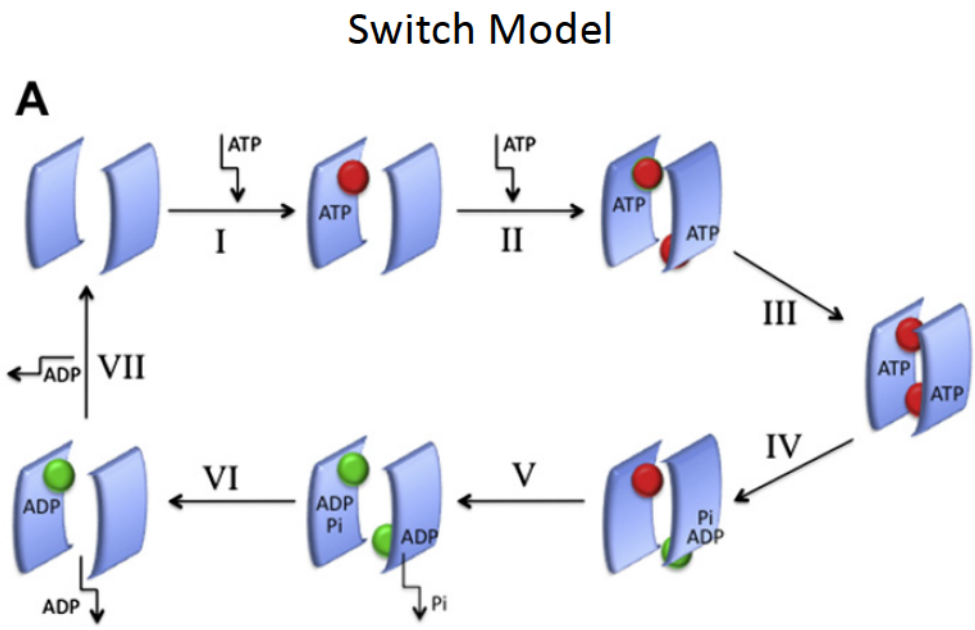

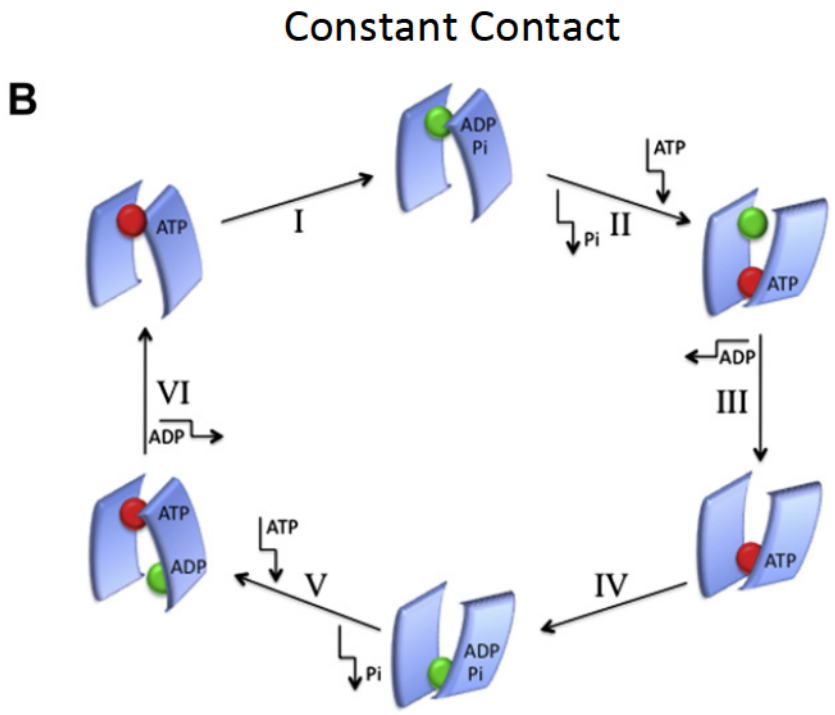

Figure 4. Models for the catalytic cycle of ATP binding and hydrolysis in the ABC transporter NBD dimer. (A) Switch Model: Step I is the resting state in which the ATP-binding cassette monomers are separated and nucleotide-free. Progression from Step I to Step II allows the monomers to become loaded processively with ATP, triggering the closure of the interface to form the sandwich dimer (Step III). Steps IV, V, and VI depict processive hydrolysis of ATP in each site followed by sequential release of Pi and ADP, returning the dimer to the nucleotide-free open state during Step VII, completing the cycle. (B) Constant Contact Model: For each catalytic site there are two distinct substates, either occluded (closed) or open (allowing nucleotide exchange); or in the case of the empty site, high or low affinity for nucleotide. The two active sites function 180° out of phase with respect to this cycle and ATP hydrolysis alternates between the opposite sites. The NBDs remain in contact throughout the cycle, with opening and

closing of the sites occurring by way of intrasubunit conformational changes within the NBD monomers. In Step I, the ATP-bound active site is closed and the opposite site is empty and ATP hydrolysis occurs. In Step II, with hydrolysis products still bound in the occluded active site, the empty, low-affinity site switches to high affinity, enabling ATP binding. In Step III, ATP binding to the empty site and Pi release from the occluded post-hydrolysis site promotes opening of the ADP-bound site, release of ADP and occlusion of the ATP-bound site. Step IV represents the 180° out of phase stage - the opposite of Step I - and cycling across Steps I, II, and III is repeated in the opposite active site during Steps IV, V, and VI, with ADP release in Step VI completing the cycle. In summary, each active site cycles in the sequence: ATP-open, ATP-occluded, ADP(+P_i)-occluded, ADP-open, empty-low affinity, empty-high affinity. Figure taken from George *et al*. (23).

Our theory is that the degenerate site of Pdr5 acts as a structural platform and supports ATP hydrolysis at the consensus site. Nucleotide exchange might occur at the degenerate site although less frequently. In order to better understand this we sequentially mutated each non-consensus amino acid in the degenerate site with its consensus counterpart and studied its effect on protein function and drug resistance.

Asymmetric ABC transporters – A case for Pdr5

On careful inspection it is noticed that Pdr5 has a number of mutations in very important conserved residues (24). Essentially only one nucleotide-binding site has all the residues necessary for proper

binding and hydrolysis, while the other NBS is lacking them. This is a very intriguing feature among ABC transporters of yeast and is markedly different from most human or bacterial counterparts. This is important keeping in mind the high basal ATPase activity of Pdr5 and absence of any substrate stimulation (24). In other words Pdr5 seems to always be in a 'on' state regardless of any threat posed by toxic compounds, and is ready to pump out the substrate immediately upon encountering. This poses a question upon the relevance of the degenerate nucleotide-binding site. To put this feature into perspective figure 5 compares the fungal and non-fungal conserved motifs of the NBS.

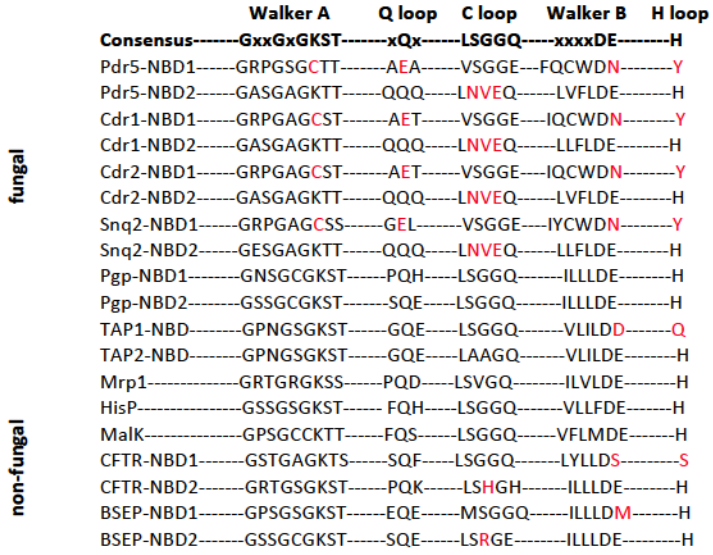

Figure 5. Comparison of conserved motifs of ABC transporters. Non-conserved amino acids are highlighted in red.

As can be seen from the figure above fungal ABC transporters distinctively possess degeneration in one NBS while the non-fungal transporters have much less of it.

Methods to study Pdr5

Liquid drug assay

This is usually the first biochemical assay to be undertaken on a cellular basis. It is a cell based assay which involves growing of the mutants in the presence of specific concentration of inhibitory drugs and evaluating the differences in their resistance patterns. Commonly we employ four drugs – cycloheximide, fluconazole, ketoconazole and rhodamine 6g. The assay is carried out in 96-well microplates and the cells are incubated with the drugs for 48 hours at 30°C. OD_{620} is measured using an elisa reader and evaluation is done by plotting the growth curves. A typical growth curve is depicted in figure 6. Here, the optical density at 620 nm was measured after 48 h at 30°C and served as a measure for cell survival.

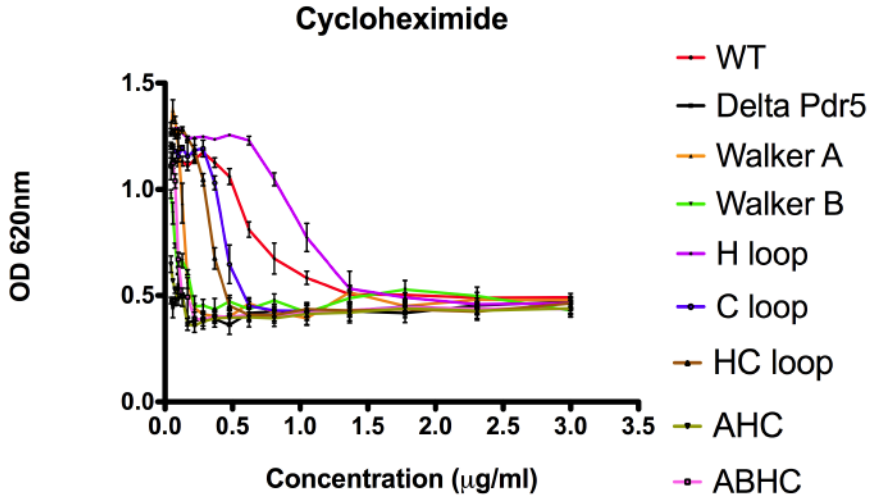

Figure 6. Representative growth curve displaying differences in resistance of various Pdr5 mutants in a typical liquid drug assay carried out with cycloheximide.

Oligomycin sensitive ATPase activity

Pdr5 is sensitive to the inhibitor oligomycin, and this feature is exploited to determine Pdr5 specific ATPase activity in crude membrane preparations (25). Yeast membrane preparations usually contain a number of ATP hydrolyzing proteins along with Pdr5 (26). To distinguish between Pdr5 specific ATPase activity from the others a number of inhibitors are used in this assay. We employ potassium nitrate, sodium azide and ammonium molybdate as inhibitors of other ATPases, while oligomycin acts as our negative control to inhibit Pdr5 ATPase activity. The difference in readings gives us the amount of ATP hydrolyzed specifically by Pdr5. The malachite green assay measures the amount of free inorganic phosphate generated by ATP hydrolysis. The assay is carried out for 20 minutes at 30^{o}C and the absorbance is measured using an elisa reader at 620nm.

Rhodamine 6G transport assay

To determine the functional integrity of Pdr5 this is the best-suited assay in our hands. The principle of the assay is based on Pdr5 mediated transport of the fluorescent substrate rhodamine 6g inside the vesicle in the presence of ATP (11, 25). Crude membrane preparations have an inside-out orientation of the Pdr5 molecules i.e the NBDs are facing the extracellular side and the substrate is transported into the inner leaflet and the lumen of the vesicle. In the

presence of a structurally and functionally active transporter and energy source like ATP the substrate transport can be monitored in real time using a fluorescence spectrofluorometer. A typical read-out is depicted in figure 7. The decrease in fluorescence is an indication of active transport and the slope determines the rate.

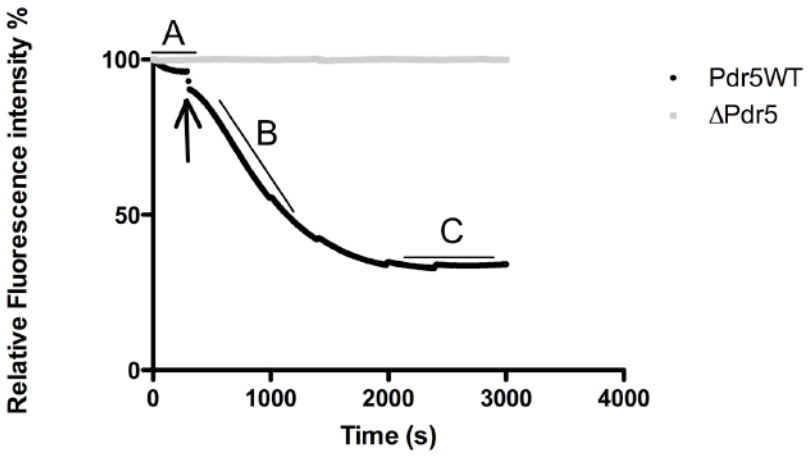

Figure 7. Representative graph displaying a typical R6G transport assay. Concentration of R6G in transport buffer, 30 μg/ml plasma membrane vesicles (see Materials and Methods section for details) Part A: equilibration phase without added energy source (0-290s), part B: phase of rapid decrease in fluorescence upon addition of 10mM ATP (310-2000s) and part C: saturation phase where active transport of R6G in the vesicle reaches its maximum (2000-3000s). The arrow represents point of addition of ATP.

Laser scanning confocal microscopy of immobilized membrane vesicles

This assay was developed to observe real time rhodamine 6g transport inside a single membrane vesicle. It provides a proof of principle for the data obtained using a fluorescence spectrofluorometer, which gives a read-out, based upon average thousands of such events taking place simultaneously. The cover slides for immobilization are prepared essentially as described by Toptygin *et al*. (27). Figure 8 gives the summary of the transport events happening in 600s.

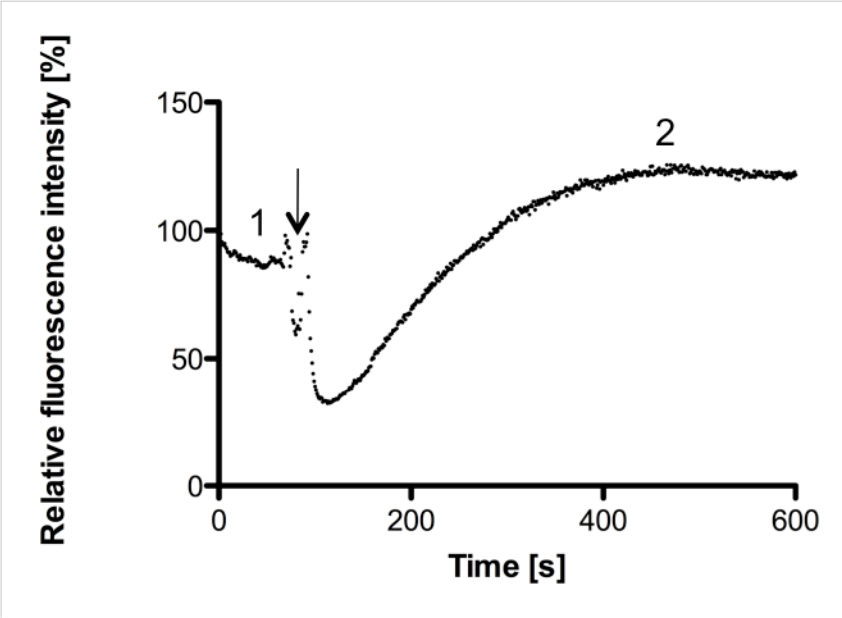

Figure 8. Trace of fluorescence intensity over time during observation of R6G transport in a single membrane vesicle. Phase 1 is the equilibration phase without ATP addition. An arrow represents the addition of 20mM ATP. Phase 2 displays rise in fluorescence intensity due to Pdr5 mediated active transport.

Aims

The aims of the dissertation work is enlisted as follows:

- To exchange non-consensus residues in the nucleotide binding site of Pdr5 with their consensus counterparts, and study the effect on protein function.
- To determine stoichiometry of rhodamine 6g transport mediated by Pdr5 in crude membrane vesicle preparations.
- To study alternate mechanisms of overcoming drug resistance with specific NBD mutants of Pdr5 using proteome analysis.

Publication I

Generating symmetry in the asymmetric ABC transporter Pdr5 from *Saccharomyces cerevisiae*

1: Institute of Biochemistry, Heinrich Heine University Düsseldorf, Universitätsstr. 1, 40225 Düsseldorf, Germany

Rakeshkumar P. Gupta [1], Petra Kueppers [1], Nils Hanekop [1] and Lutz Schmitt[1,*]

Running title: Role of degenerate nucleotide binding site in Pdr5

Final character count (with spaces): 30,812

*: To whom correspondence should be addressed:
Lutz Schmitt
Institute of Biochemistry
Heinrich Heine University Duesseldorf
Universitaetsstr. 1
40225 Duesseldorf, Germany
Phone: +49(0)211-81-10773
Fax: +49(0)211-81-15310
Email: lutz.schmitt@hhu.de

Abstract

Pdr5 is a plasma membrane bound ABC transporter from *Saccharomyces cerevisiae* and involved in the phenomenon of resistance against xenobiotics, which is clinically relevant in bacteria, fungi and humans. Many fungal ABC transporters such as Pdr5 display an inherent asymmetry in at least one of their nucleotide-binding site (NBS) unlike most of their human counterparts. This degeneracy of the NBSs is very intriguing and needs explanation in terms of structural and functional relevance. In this study we mutated non-consensus amino acid residues in the NBSs to its consensus counterpart and studied its effect on the function of the protein and effect on yeast cells. The completely 're-generated' Pdr5 protein was severely impaired in its function of ATP hydrolysis and of Rhodamine 6G transport. Moreover, we observe alternate compensatory mechanisms to counteract drug toxicity in some of the mutants. In essence, we here describe the first attempts in restoring complete symmetry in an asymmetric ABC transporter and to study its effects, which might be relevant to the entire class of asymmetric ABC transporters.

Keywords: ATPase activity / ATP binding cassette transporters / coupling mechanism / multidrug resistance / substrate transport.

Introduction

ABC transporters are found in all kingdoms of life, in prokaryotes they function as importers (Erkens et al, 2012) and exporters while they mainly act as exporters in eukaryotes (Hinz & Tampe, 2012; Klein et al, 2011). Multidrug resistance (MDR) during chemotherapy in the treatment of cancer or in immuno-compromised individuals has made the biochemical and structural study of these proteins essential. In fungi, many ATP binding cassette (ABC) transporters have been at the center of scientific investigation for example for their involvement in the phenomenon of pleiotropic drug resistance (Prasad & Goffeau, 2012) a phenomena similar to MDR.

Pdr5 is an ABC transporter localized in the plasma membrane of the baker's yeast *Saccharomyces cerevisiae*. It is a functional homologue of P-gp (MDR1 or ABCB1), which is the most widely studied ABC transporter from humans (Sharom, 2011). Pdr5 is involved in the extrusion of a wide variety of xenotoxic compounds from the cell (Ernst et al, 2005; Golin et al, 2007; Kolaczkowski et al, 1996). It is a full-size transporter having two nucleotide-binding domains (NBDs) and two transmembrane domains (TMDs) displaying a NBD-TMD-NBD-TMD membrane topology. This is inverse to that of the classic topology of ABC transporters (TMD-NBD-TMD-NBD). Since the discovery that a mutation in the transcription factor, which controls the expression of this membrane protein leads to over-expression of Pdr5 (Goffeau & Dufour, 1988), it has turned out to be an important model for studying multidrug resistance (MDR) or to be more precise pleiotropic drug resistance (PDR) as it is called in yeast.

Pdr5 displays a high basal ATPase activity, which unlike its other human counterparts such as P-gp does not seem to be stimulated in the presence of substrates (Ernst et al, 2005; Ernst et al, 2008). Such an uncoupling has important mechanistic consequences, because ATP hydrolysis is supposed to be the crucial step, which triggers the transport of substrates across the membrane and in the proper environment is strictly coupled to substrate

translocation (Shapiro & Ling, 1998). The NBDs play the role of harnessing chemical energy from ATP and converting it to mechanical energy by inducing structural changes in the TMDs to extrude the substrate to the exterior of the cell (Hanekop et al, 2006; Zaitseva et al, 2005b). The amino acid residues involved in binding and hydrolysis of ATP are essential for the proper functionality of the protein. A number of previous studies have investigated the roles of individual and groups of amino acids in the NBDs and shed light on their roles during ATP binding and hydrolysis. As per the generally accepted model, an ABC transporter binds two nucleotides in the two NBDs. This binding occurs in a head-to-tail fashion, i. e. consensus residues from the Walker A (GXGXXGKST, where X can be any amino acid) and Walker B (ΦΦΦΦDE, where Φ can be any hydrophobic amino acid) motifs as well as the H-loop (XHX) from one NBD and the C-loop (LSGGQ) from the other NBD sandwich one ATP molecule in-between them thereby forming the nucleotide-binding site (NBS) (Zaitseva et al, 2005b). Once both nucleotides are bound at the two NBSs, the transporter is supposed to switch from the so-called inward to the so-called outward facing conformation and as a consequence of this conformational change the substrate is extruded (Linton, 2007). Moreover, ATP hydrolysis has been suggested to be the step that sets the transporter back to the inward facing conformation ready to accept new substrate molecules for the next cycle of substrate translocation (Linton, 2007). However, there is debate about the number of ATP molecules that are hydrolyzed for one cycle of transport to be completed. But the pre-requisite for both bound ATP molecules to be hydrolyzed is the presence of key consensus residues in both NBSs. As seen in Figure 1, Pdr5 lacks key residues in one of the two NBSs. Although, this degenerate site could bind ATP, hydrolysis should be impossible or severely impaired due to the absence of these key residues. Some initial mutational studies supported this view (Ernst et al, 2008). This observation of a degenerate and a consensus site is common in yeast ABC transporters, but uncommon in ABC transporters of archaea and bacteria. In the case of human counterparts, only TAP1/2 (ABC B2 / B3) and many transporters of the subfamily C display this sort of degeneration (Lamping et al, 2010). A well-studied example of a eukaryotic protein possessing a degenerate NBS

is CFTR. Here, site 1 (degenerate) is proposed to be bound to ATP through many cycles of ATP hydrolysis occurring at site 2 (canonical) and thus play a supporting role (Csanady et al, 2013). This leads us to question the functional relevance for the protein and on a broader scale to the cell for maintaining a degenerate NBS, because such evolutionary conservation of this trait in yeast ABC transporters does need an explanation.

In this study, we systematically interchanged each degenerated amino acid residue in the NBSs and studied its effect on the functionality of the protein and in turn on the cellular consequences.

Results

A classic or canonical NBS of an ABC transporter is composed of residues of the Walker A and Walker B motifs, the Q-loop, D-loop and H-loop from one NBD and the C-loop of the opposing NBD forming a so-called composite ATP-binding site (Figure 1A). Based on structural studies of P-loop NTPases (Vetter & Wittinghofer, 1999), the lysine of the Walker A motif co-ordinates the β- and γ-phosphate moiety of ATP, the aspartate residue of the Walker B motif interacts with the cofactor Mg^{2+} (Chen et al, 2001; Smith et al, 2002; Zaitseva et al, 2005b), which is essential for hydrolytic activity. The glutamate residue of the Walker B motif and the histidine residue of the H-loop are essential for ATPase activity and were shown to form a catalytic dyad (Oldham & Chen, 2011; Zaitseva et al, 2005a). However, in the case of Pdr5, mutation of the histidine in NBS2 did not reduce or even abolish ATPase activity as shown for many other ABC systems (for references see Zaitseva et al., 2005), rather it selectively influenced the spectrum of transported substrates (Ernst et al, 2008). The serine and second glycine residue of the C-loop of the opposing NBD interact with the γ-phosphate moiety of ATP and complete the NBS. Furthermore, the glutamine residue of the Q-loop also coordinates directly or indirectly the cofactor Mg^{2+}, while the D-loop is thought to be involved in NBD-NBD communication in the composite dimer. Here, we excluded the D-loop and the Q-loop from our experiments. An elegant study already investigated the role of the Q-loop in NBD-TMD crosstalk of Pdr5 where it was seen that the mutation of Q loop residues from deviant and consensus part of NBDs led to drug hypersensitivity and displayed functional redundancy, while maintaining significant ATPase activity (Ananthaswamy et al, 2010). Hence, we focused only on the important residues of the Walker A and B motifs, the H-loop and the C-loop for this study.

Mutagenesis in Pdr5

Mutations to replace degenerate amino acid residues with their consensus counterparts were done in a step-wise fashion. The complete list of mutations is summarized in Table I. Site-directed mutagenesis was

performed in pRE5 plasmid after which the *pdr5* gene was subsequently excised and transformed into the *Saccharomyces* strain Δ*pdr5*Δ*pdr5prom* where through homologous recombination the *pdr5* gene is chromosomally integrated (Ernst et al, 2008). In this background, this leads to constitutive expression of Pdr5 under the strong Pdr5 promoter. In the following, restoration of the consensus sequence in the Walker A motif (C199K) located in NBD1 and forming NBS1 is called the 'Walker A' mutant, restoration of the consensus sequence in the Walker B motif (N334E; NBD1) in NBS1 is called the 'Walker B' mutant, restoration of the consensus sequence of the H-loop (Y367H, NBD1) in NBS1 is called the 'H-loop' mutant and restoration of the consensus sequence of the C-loop (N1011S / V1012G / E1013G, NBD2) in NBS1 is called the 'C-loop' mutant. The corresponding combinations are called 'HC-loop' (H- and C-loop mutations), AHC (H- and C-loop as well as Walker A mutations) and ABHC (H- and C-loop as well as Walker A and Walker B mutations). Please note that in the context of the combined mutations affecting the Walker A motif of NBS1, we also exchanged the proline residue at position 195 to a serine residue. We speculated that proline within the Walker A motif might hamper its functionality in wrapping around the phosphate moiety of the bound nucleotide. However, on the level of the single mutation no difference to the single C199K mutant was detected. Nevertheless, we kept this exchange in the combined mutations.

Liquid drug resistance assay

To determine the effects of mutations in key residues of the NBDs we investigated the changes in resistance towards specific drugs belonging to different classes. As an internal control and reference for the absence of resistance the Δpdr5 strain was employed. The response of the mutants towards these drugs was interestingly not uniform. For cycloheximide (Figure 2A), the H-loop and HC-loop mutants displayed a stronger resistance as compared to wild type, while for the azole drugs, ketoconazole and fluconazole (Figures 2B and 2C), the Walker A, Walker B, H-loop and HC-loop mutants displayed stronger resistance as compared to wild type. Finally, for R6G (Figure 2D), the Walker A, H-loop, C-loop, HC-loop and the

ABHC mutants were displaying higher resistance. Noticeably, the ABHC mutant, which contained all conserved residues and thereby restored a symmetrical architecture of the two NBSs, was severely impaired in providing better resistance towards all drugs except R6G.

In vitro oligomycin (OM)-sensitive ATPase assay

ATPase activity tests were carried out, in order to investigate the biochemical basis for such altered drug resistance of the mutants. For this purpose, Pdr5-enriched plasma membranes were isolated using the Serrano protocol (Serrano, 1988). Figure 3 demonstrated that the expression levels in the plasma membrane of all mutants were very similar if not identical to wild type levels. Therefore, the differences in resistance patterns observed in the liquid drug assay cannot be attributed to differences in the amounts of protein being expressed.

OM-sensitive ATPase activity was measured colorimetrically by determining the amount of inorganic phosphate released over time by the malachite green assay. The results are summarized in Figure 4. As seen clearly all mutants except the AHC and ABHC mutants displayed ATPase activity comparable to wild type with a 2-fold increase in apparent affinity at maximum for the H-loop mutant. Moreover, a quantitative analysis of the kinetic parameters of ATP hydrolysis revealed that the apparent affinity of these mutants towards ATP has not drastically changed (Table II). Only the AHC and ABHC mutants were severely impaired in their maximal reaction velocity, V_{max}, of ATP hydrolysis displayed values comparable to the negative control (Δ*pdr5* containing strains).

In vitro R6G transport assay

An *in vitro* R6G transport assay presents an elegant read out of the functional integrity of Pdr5 in inside-out membrane vesicles. The assay is based on the principle of transport of R6G molecules to the inner leaflet or the lumen of the vesicle in presence of an energy source, i.e. ATP in our case. The decrease in fluorescence intensity is a result of the formation of non-fluorescent excimers of R6G once transported inside the vesicle. As

summarized in Figure 5, all mutants except the HC-loop, AHC and ABHC mutants were able to efficiently transport R6G, although at different rates inside the vesicle. The affinities of these mutants towards R6G are summarized in Table III. As seen, the K_m values are identical within experimental error for all mutants except for those that are impaired in R6G transport, but v_{max} values display considerable variation representing differential effects of the point mutations on the rate of substrate transport.

Visualization of R6G accumulation in whole cells

When compared to the liquid drug resistance results of R6G, one has to stress that some mutants displayed better resistance than wild type Pdr5, but did not transport R6G in the *in vitro* transport assay. In order to investigate this disparity, we visualized R6G accumulations in yeast cells in the presence of R6G using fluorescence microscopy. As demonstrated in Figures 6a and 6b cells lacking Pdr5 (Δ*pdr5*) clearly displayed an accumulation of the dye within the cells, while wild type cells efficiently transported R6G out of the cells as no R6G fluorescence could be detected within the cells (Figures 6c and 6d). Cells expressing the C199K mutation of Pdr5 (Walker A mutant) that are comparatively less efficient than the wild type cells in transporting R6G (Figure 5) displayed accumulation of the dye, but to a reduced extent as compared to the knockout strain (Figures 6e and 6f). In contrast, the HC-loop and the ABHC mutants, which displayed higher resistance towards R6G in the liquid drug assays (Figure 2), demonstrated accumulation of the drug within the cells while maintaining cell viability (Figures 6g-l). This strongly suggests that compensatory mechanisms apart from transport of the substrate outside the cell plays a significant role in the resistance towards the drug in these specific mutants and explain the disparity between the transport and liquid-drug assays..

Discussion

Asymmetry in NBS is a feature not exclusively observed in fungal ABC transporters. Rather a number of human ABC transporters display this degeneration as well. Our observations with Pdr5 after exchange of degenerate residues with consensus ones provides strong evidence that the degenerated site is indeed optimized to structurally and functionally support ATP hydrolysis occurring at the opposite end. It has been proposed for a number of asymmetric transporters such as CFTR along with fungal ABC transporters that the degenerated site might act as a platform for ATP hydrolysis at the consensus site (Basso et al, 2003; Ernst et al, 2008). This theory gains more support from our observations where, in an attempt of making the degenerate site capable of ATP hydrolysis, renders the protein completely non-functional in terms of ATP hydrolysis as well as substrate transport.

These observations also point in the direction of subtle inter and intra-domain communication necessary for the protein to fuel substrate transport with the energy of ATP hydrolysis. For an ABC transporter to function properly a number of structural elements have been proposed to play key roles in the 'chain of communication' necessary for optimal activity. Among these the D-loops are involved in *trans* interactions within the NBDs, especially the Asp residue from the consensus sequence has been shown to interact with the Ser residue of the Walker A in the opposite NBD (Zaitseva et al, 2005a). D-loops are also proposed to be the sensors and communicators in between the NBSs where they can communicate ATP binding and hydrolysis at one site to the other (Jones & George, 2012). The Q-loops Gln residue has been proposed to be important in coordinating the water molecule in the active site during ATP hydrolysis (Smith et al, 2002). The Q-loops have also been proposed to be essential for conformational coupling of movements in NBDs to the TMDs in Pgp (Urbatsch et al, 2000), interestingly in Mrp1 it was observed that the Q-loops did not play an essential role in inter domain communication (Yang et al, 2011). As seen from the homology model of Pdr5 (Rutledge et al, 2011) based on the crystal structures of Sav1866 (Dawson & Locher, 2006) and mouse Pgp (Aller et al,

2009), it is plausible that the Q loops in Pdr5 might play a role in inter domain communication (Ananthaswamy et al, 2010). In addition to these are the coupling helices that are one of the most structurally distinct elements in this communication pathway. They are like the gatekeepers guarding the substrate binding pocket as well as the anchors of the TMDs fitting in the sockets of NBDs (Locher, 2009). The X-loops Glu residues are also potentially important in the communication pathway owing to their placement right near the substrate binding pocket as was first observed in the Sav1866 structure (Dawson & Locher, 2006), but not enough studies have been carried out on its precise role so far.

We believe that in our 'regenerated' Pdr5 it is this very communication within the NBDs and in turn from the NBDs to the TMDs, which is disrupted by vast changes in the degenerate NBS. This hypothesis is also supported by the recent study carried out on the D loops of Pdr5 by Furman *et al.* (Furman et al, 2013) where its role in intradomain signaling was studied. As seen from the observations individual mutations viz. Walker A, Walker B, H loop and C loop are tolerated. ATP hydrolysis is not greatly affected in these mutants and R6G transport is also evident, although with varying degrees compared to the wild type. But as these mutations are combined viz. HC loop, AHC loop and ABHC loop, it leads to firstly lack of R6G transport (HC loop) (Table III) and later drastic decrease in ATP hydrolysis (AHC and ABHC loops) (Table II and III). The HC loop mutant is particularly interesting because it displays lack of substrate transport for R6G despite near wild type levels of ATPase activity. This indicates that the two events of ATP hydrolysis and substrate transport are indeed uncoupled at least for R6G in this mutant. In our opinion the major effect of changes in the degenerate site due to amino acid alterations is the breakdown of communication between the two NBSs and the NBS(s) and TMD(s). This is much severe in the case of AHC loop and ABHC loop mutants and hence, hampers ATP hydrolysis even at the consensus NBS which was untouched in this study.

In our view Pdr5 like other yeast ABC transporters has evolved a structural architecture comprising of a degenerate NBS and the entire intra and inter domain communication involving D, Q and X loops are in place and optimized taking into account one consensus and one degenerate NBS. Our

study of mutating the residues involved in the degenerate site altered the communication between the two NBS and hence affected the ATP hydrolysis occurring at the consensus NBS. Taking into consideration biochemical evidence from asymmetric transporters does imply the necessity of a 'quiet' platform at the degenerate NBS where nucleotide exchange might occur, but much less frequently as compared to the consensus NBS. When we make this 'quiet' site more flexible by careful exchange of key residues, it seems to be tolerated up to an extent, in case of Pdr5 up to the C-loop. But further changes disrupt ATP hydrolysis completely.

In the liquid resistance assays (Fig. 2) it was observed that the completely regenerated Pdr5 was clearly at a disadvantage in providing resistance to the yeast cells when challenged with different drugs. The big exception was R6G where resistance was slightly better as compared to WT. This observation although primary, tells us that restoring all residues back to the consensus sequence does more harm to the protein than being beneficial. When compared to the liquid resistance assay results for R6G the AHC mutant is indeed worse than WT in imparting resistance. But the HC loop and ABHC loop mutants do display increased resistance towards R6G in the liquid resistance assay. This is contradictory to our observation in the R6G transport assays where these two mutants do not display any transport of rhodamine in membrane vesicles. To investigate this contradiction we employed microscopic techniques to directly observe R6G in whole cells. The Pdr5WT (Fig. 6c & 6d) and ΔPdr5 (Fig. 6a & 6b) were our positive and negative controls, respectively. As can be clearly observed the WT cells which can actively transport R6G outside show no accumulation of the dye within the cells, while the knock-out strain accumulates the dye in the absence of the transporter. The Walker A mutant, C199K (Fig. 6e & 6f), which is deficient in R6G transport, displays few cells, which accumulate the dye, while the HC (Fig. 6g & 6h) and ABHC (Fig. 6i & 6j) mutants show a large number of cells, which have accumulation of the dye inside the cells. DIC images of these cells also confirmed that these cells were alive. These observations point towards compensatory mechanisms, which come into

play only when a transport inefficient protein is present in the cell, as the knock-out and the WT strains do not display such behavior. We therefore can rule out the possibility of additional transporters being up-regulated in the HC and ABHC mutants to pump out the substrate that might lead to increased resistance towards R6G as seen in the liquid drug tests. However, further investigations, which are beyond the scope of this study are required to explain this observation at a protein level.

Here we have presented the first comprehensive study of systematically replacing each degenerate amino acid residue involved in ATP binding and hydrolysis in Pdr5 with its consensus counterpart. The completely regenerated Pdr5 protein was functionally severely impaired as seen with ATP hydrolysis and in-vitro transport experiments. This leads us to conclude that maintaining a degenerate ATP hydrolysis site seems essential for the optimal functioning of Pdr5 from an energetic and also evolutionary point of view. It is also plausible that for ABC transporters harboring a degenerate NBS that is incapable of hydrolyzing ATP could lead to high basal ATPase activity occurring at the consensus site. This in turn is a possible explanation as to why some ABC transporters have and continue to maintain a degenerate site. The trade-off between constant ATP hydrolysis at only one site instead of two leads to the protein being ready at all times to protect the cell against xenotoxic compounds without delay. This to our knowledge is a significant deviation from ABC transporters having both NBS capable of ATP hydrolysis and displaying substrate stimulation and validates further investigation.

Materials and Methods

Liquid drug assay

Ketoconazole, fluconazole and rhodamine 6g (R6G) were obtained from Sigma-Aldrich and cycloheximide was obtained from Fluka. All drug stock solutions were prepared in dimethyl sulfoxide (DMSO, Acros Organics) and further dilutions were carried out in sterile water. Assay was carried out in sterile 96 well microtiter plates (Falcon) with 20 µl drug, 180 µl YPD medium and 50 µl of OD_{600} 0.2 yeast culture. Plates were incubated at 30 ^{o}C for 48 hours and OD_{600} was measured with an elisa plate reader (Fluostar-Optima).

Yeast Strains and Plasmid Mutagenesis

Yeast strains were cultured in YPD medium containing 10g/l yeast extract, 20g/l peptone and 2% glucose. The following *S. cerevisiae* strains were used in this study: YALF-A1 (*MATa; ura3-52 trp 1-1 leu 2-3, his 3-11, 15 ade 2-1 PDR 1-3*), YHW-A5 (*MATa; ura3-52 trp 1-1 leu 2-3, his 3-11, 15 ade 2-1 PDR 1-3 pdr5Δ::TRP1*), and YRE1001 (*MATa; ura3-52 trp 1-1 leu 2-3, his 3-11, 15 ade 2-1 PDR 1-3 pdr5pdr5promΔ::TRP1*). Details about plasmid and strain construction can be found in (Ernst et al, 2008) and supplementary table S1. Site-directed mutagenesis of *pdr5* was performed on plasmid pRE5 with the QuickChange II XL site-directed mutagenesis kit (Stratagene).

Isolation of Plasma Membranes

Cells were grown in YPD medium at 30 ^{o}C. At OD_{600} of 1.5, the nitrogen source was replenished by addition of a 10th volume of 5x YP (50 g/liter yeast extract; 100 g/liter tryptone/peptone). Cells were harvested at OD_{600} of 3.5. The isolation of plasma membranes was performed as described elsewhere (Ernst et al, 2008; Kolaczkowski et al, 1996).

Rhodamine 6G Transport Assay

Active R6G transport was recorded according to the protocol developed by Kolaczkowski *et al.*, using a Fluorolog III fluorescence spectrometer (Horiba)

(Decottignies et al, 1994). Isolated plasma membranes (30 μg of total protein content) were re-suspended in 1 ml of transport buffer (50 mM Hepes pH 7.0, 10 mM $MgCl_2$, 150 nM R6G and 10 mM azide) and incubated at 35 ^{o}C. Transport was initiated by addition of 10 mM ATP.

ATPase activity Assays

Oligomycin (OM) sensitive ATPase activity of plasma membrane fractions was measured by a colorimetric assay performed in 96-well microtiter plates (Decottignies et al, 1994; Goffeau & Dufour, 1988; Wada et al, 2002). Isolated plasma membranes (0.1 or 0.2 μg per well) were incubated with 4 mM ATP, 5 mM $MgCl_2$ in 300 mM Tris-glycine buffer (pH 9.0) in a final volume of 25 μl. To reduce background, 0.2 mM ammonium molybdate, 50 mM KNO_3, and 10 mM NaN_3, respectively were added (Dufour et al, 1988; Goffeau & Dufour, 1988). In a control reaction, OM (20 μg/ml) was added to the assay to determine the OM-sensitive ATPase activity. After incubation at 30 ^{o}C for 20 minutes, the reaction was stopped by addition of 175 μl of ice-cold 40 mM H_2SO_4. The amount of released inorganic phosphate was determined by a colorimetric assay, using Na_2HPO_4 as standard (Zaitseva et al, 2004).

Acknowledgements

We thank Katerina Krikoni, Marianne Kluth and Martha Swiatek for important support at various stages of the project. We are indebted to Robert Ernst, University of Frankfurt, and Karl Kuchler, Medical University of Vienna for important contributions at an early stage of the project and many fruitful and stimulating discussions. We also thank Peter Zentis and Stephanie Weidtkamp-Peters for invaluable support in the LSM measurements. This work was funded by the DFG (grant Schm1279/5-3) and the EU (EDICT (European Drug Initiative on Channels and Transporters) FP7 Theme [Health-2007-2.1.1.-5]) to L.S..

Author Contribution

R.G, P.K and L.S designed research. R.G and P.K performed research. R.G, P.K, N.H and L.S analyzed data and wrote the manuscript.

Conflict of Interest

The authors declare no conflict of interest.

References

Aller SG, Yu J, Ward A, Weng Y, Chittaboina S, Zhuo R, Harrell PM, Trinh YT, Zhang Q, Urbatsch IL, Chang G (2009) Structure of P-glycoprotein reveals a molecular basis for poly-specific drug binding. *Science* **323:** 1718-1722

Ananthaswamy N, Rutledge R, Sauna ZE, Ambudkar SV, Dine E, Nelson E, Xia D, Golin J (2010) The signaling interface of the yeast multidrug transporter Pdr5 adopts a cis conformation, and there are functional overlap and equivalence of the deviant and canonical Q-loop residues. *Biochemistry* **49:** 4440-4449

Basso C, Vergani P, Nairn AC, Gadsby DC (2003) Prolonged nonhydrolytic interaction of nucleotide with CFTR's NH2-terminal nucleotide binding domain and its role in channel gating. *J Gen Physiol* **122:** 333-348

Chen J, Sharma S, Quiocho FA, Davidson AL (2001) Trapping the transition state of an ATP-binding cassette transporter: evidence for a concerted mechanism of maltose transport. *Proc Natl Acad Sci U S A* **98:** 1525-1530

Csanady L, Mihalyi C, Szollosi A, Torocsik B, Vergani P (2013) Conformational changes in the catalytically inactive nucleotide-binding site of CFTR. *J Gen Physiol* **142:** 61-73

Dawson RJ, Locher KP (2006) Structure of a bacterial multidrug ABC transporter. *Nature* **443:** 180-185

Decottignies A, Kolaczkowski M, Balzi E, Goffeau A (1994) Solubilization and characterization of the overexpressed PDR5 multidrug resistance nucleotide triphosphatase of yeast. *J Biol Chem* **269:** 12797-12803

Dufour JP, Amory A, Goffeau A (1988) Plasma membrane ATPase from the yeast Schizosaccharomyces pombe. *Methods Enzymol* **157:** 513-528

Erkens GB, Majsnerowska M, ter Beek J, Slotboom DJ (2012) Energy coupling factor-type ABC transporters for vitamin uptake in prokaryotes. *Biochemistry* **51:** 4390-4396

Ernst R, Klemm R, Schmitt L, Kuchler K (2005) Yeast ATP-binding cassette transporters: cellular cleaning pumps. *Methods Enzymol* **400:** 460-484

Ernst R, Kueppers P, Klein CM, Schwarzmueller T, Kuchler K, Schmitt L (2008) A mutation of the H-loop selectively affects rhodamine transport by the yeast multidrug ABC transporter Pdr5. *Proc Natl Acad Sci U S A* **105:** 5069-5074

Furman C, Mehla J, Ananthaswamy N, Arya N, Kulesh B, Kovach I, Ambudkar SV, Golin J (2013) The deviant ATP-binding site of the multidrug

efflux pump Pdr5 plays an active role in the transport cycle. *J Biol Chem* **288:** 30420-30431

Goffeau A, Dufour JP (1988) Plasma membrane ATPase from the yeast Saccharomyces cerevisiae. *Methods Enzymol* **157:** 528-533

Golin J, Ambudkar SV, May L (2007) The yeast Pdr5p multidrug transporter: how does it recognize so many substrates? *Biochem Biophys Res Commun* **356:** 1-5

Hanekop N, Zaitseva J, Jenewein S, Holland IB, Schmitt L (2006) Molecular insights into the mechanism of ATP-hydrolysis by the NBD of the ABC-transporter HlyB. *FEBS Lett* **580:** 1036-1041

Hinz A, Tampe R (2012) ABC transporters and immunity: mechanism of self-defense. *Biochemistry* **51:** 4981-4989

Jones PM, George AM (2012) Role of the D-loops in allosteric control of ATP hydrolysis in an ABC transporter. *J Phys Chem A* **116:** 3004-3013

Klein C, Kuchler K, Valachovic M (2011) ABC proteins in yeast and fungal pathogens. *Essays Biochem* **50:** 101-119

Kolaczkowski M, van der Rest M, Cybularz-Kolaczkowska A, Soumillion JP, Konings WN, Goffeau A (1996) Anticancer drugs, ionophoric peptides, and steroids as substrates of the yeast multidrug transporter Pdr5p. *J Biol Chem* **271:** 31543-31548

Lamping E, Baret PV, Holmes AR, Monk BC, Goffeau A, Cannon RD (2010) Fungal PDR transporters: Phylogeny, topology, motifs and function. *Fungal Genet Biol* **47:** 127-142

Linton KJ (2007) Structure and function of ABC transporters. *Physiology (Bethesda)* **22:** 122-130

Locher KP (2009) Review. Structure and mechanism of ATP-binding cassette transporters. *Philos Trans R Soc Lond B Biol Sci* **364:** 239-245

Oldham ML, Chen J (2011) Snapshots of the maltose transporter during ATP hydrolysis. *Proc Natl Acad Sci U S A* **108:** 15152-15156

Prasad R, Goffeau A (2012) Yeast ATP-binding cassette transporters conferring multidrug resistance. *Annu Rev Microbiol* **66:** 39-63

Rutledge RM, Esser L, Ma J, Xia D (2011) Toward understanding the mechanism of action of the yeast multidrug resistance transporter Pdr5p: a molecular modeling study. *J Struct Biol* **173:** 333-344

Serrano R (1988) H+-ATPase from plasma membranes of Saccharomyces cerevisiae and Avena sativa roots: purification and reconstitution. *Methods Enzymol* **157:** 533-544

Shapiro AB, Ling V (1998) The mechanism of ATP-dependent multidrug transport by P-glycoprotein. *Acta Physiol Scand Suppl* **643:** 227-234

Sharom FJ (2011) The P-glycoprotein multidrug transporter. *Essays Biochem* **50:** 161-178

Smith PC, Karpowich N, Millen L, Moody JE, Rosen J, Thomas PJ, Hunt JF (2002) ATP binding to the motor domain from an ABC transporter drives formation of a nucleotide sandwich dimer. *Mol Cell* **10:** 139-149

Urbatsch IL, Gimi K, Wilke-Mounts S, Senior AE (2000) Investigation of the role of glutamine-471 and glutamine-1114 in the two catalytic sites of P-glycoprotein. *Biochemistry* **39:** 11921-11927

Vetter IR, Wittinghofer A (1999) Nucleoside triphosphate-binding proteins: different scaffolds to achieve phosphoryl transfer. *Q Rev Biophys* **32:** 1-56

Wada S, Niimi M, Niimi K, Holmes AR, Monk BC, Cannon RD, Uehara Y (2002) Candida glabrata ATP-binding cassette transporters Cdr1p and Pdh1p expressed in a Saccharomyces cerevisiae strain deficient in membrane transporters show phosphorylation-dependent pumping properties. *J Biol Chem* **277:** 46809-46821

Yang R, Hou YX, Campbell CA, Palaniyandi K, Zhao Q, Bordner AJ, Chang XB (2011) Glutamine residues in Q-loops of multidrug resistance protein MRP1 contribute to ATP binding via interaction with metal cofactor. *Biochim Biophys Acta* **1808:** 1790-1796

Zaitseva J, Holland IB, Schmitt L (2004) The role of CAPS buffer in expanding the crystallization space of the nucleotide-binding domain of the ABC transporter haemolysin B from Escherichia coli. *Acta Crystallogr D Biol Crystallogr* **60:** 1076-1084

Zaitseva J, Jenewein S, Jumpertz T, Holland IB, Schmitt L (2005a) H662 is the linchpin of ATP hydrolysis in the nucleotide-binding domain of the ABC transporter HlyB. *EMBO J* **24:** 1901-1910

Zaitseva J, Jenewein S, Oswald C, Jumpertz T, Holland IB, Schmitt L (2005b) A molecular understanding of the catalytic cycle of the nucleotide-binding domain of the ABC transporter HlyB. *Biochem Soc Trans* **33:** 990-995

Table legends

Table I List of mutations generated and used in this study.

Table II Kinetics of ATPase activity of Pdr5 mutants. K_M and V_{max} values derived from Michaelis-Menten analysis of the OM-sensitive ATPase data for wild type Pdr5 and the different mutants.

Table III Kinetics of in-vitro R6G transport activity of Pdr5 mutants.
K_M values calculated from Michaelis-Menten analysis of the transport rates with varying R6G concentration for wild type Pdr5 and the different mutants. V_{max} values were calculated by measuring the relative percent of R6G transported at the end of 700s.

Figure legends

Figure 1 Schematic architecture of NBS

(A) Canonical NBS of ABC transporters. (B) NBS1 and NBS2 of Pdr5.

Figure 2 Liquid drug resistance assay

Growth curves of Pdr5 mutants were analyzed after 48 hours of incubation at 30°C with (**A**) Cycloheximide (CHX), (**B**) Fluconazole (FA) (**C**) Ketoconazole (KA) and (**D**) Rhodamine 6G (R6G). Color coding is as follows: red- Pdr5WT, black- ΔPdr5, orange- Walker A, green- Walker B, purple- H loop, blue- C loop, brown- HC loop, asparagus- AHC loop and magenta- ABHC loop.

Figure 3 Expression levels of Pdr5 mutants

(**Upper panel**) Coomassie Blue stained SDS Page of plasma membrane preparations of *S. cerevisiae* cells expressing wild type Pdr5 (Pdr5), no Pdr5 (Δ), or the different NBD mutations. 15 µg total protein amount were applied per lane. Molecular masses of marker proteins are indicated at the left. Bands corresponding to Pdr5 and the plasma membrane ATPase Pma1 are indicated. (**Lower panel**) Detection of Pdr5 variants by Western blot analysis employing a polyclonal α-Pdr5 antibody.

Figure 4 OM-sensitive ATPase activity of Pdr5 mutants.

The assay was performed with 0.1 or 0.2 µg protein and incubation at 30°C for 20 min. The released inorganic phosphate was detected by the malachite green assay for P_i determination. (See Materials and Methods for assay details)

Figure 5 *In vitro* R6G transport activity of Pdr5 mutants

Reaction mixture contained 20 µg protein, 300 nM R6G, 10mM $MgCl_2$, 10 mM NaN_3 and 10 mM ATP. Reaction was initiated by addition of ATP and decrease in fluorescence intensity monitored using a Spectrofluorometer (Horiba – Fluorolog III). Color-coding of mutants is the same as in figure 2.

Figure 6 *In vivo* accumulation of R6G within selective Pdr5 mutants.

Saccharomyces cerevisiae cells from the liquid drug assay microtiter plates after 48 hours of incubation at 30^{o}C were observed for R6G accumulation using a Zeiss LSM 780 microscope. Upper panel (a, c, e, g, i) displays DIC images while lower panel (b, d, f, h, j) display the corresponding fluorescent images. Bright fluorescence indicates rhodamine accumulation within cells. The final R6G concentration in the cells was 10.6 µg/ml. Bar represents length of 10 µm.

Table 1.

Mutation	Abbreviation	Alteration	Motif	Domain
P195S		Pro in Walker A	Walker A	NBD 1
C199K	Walker A	Cys in Walker A	Walker A	NBD 1
N334E	Walker B	Asn in Walker B	Walker B	NBD 1
Y367H	H-loop	Tyr in H-loop	H-loop	NBD 1
N1011S, V1012G, E1013G	C-loop	Asn, Val and Glu in C-loop	C-loop	NBD 2
Y367H, N1011S, V1012G, E1013G	HC-loop	Tyr in H-loop Asn, Val and Glu in C-loop	H-loop C-loop	NBD1/2
C199K Y367H N1011S, V1012G, E1013G	AHC	Cys in Walker A Tyr in H-loop Asn, Val and Glu in C-loop	Walker A H-loop C-loop	NBD 1/2
P195S C199K N334E Y367H N1011S, V1012G, E1013G	ABHC	Pro in Walker A Cys in Walker A Asn in Walker B Tyr in H-loop Asn, Val and Glu in C-loop	Walker A Walker B H-loop C-loop	NBD 1/2

Table 2.

Mutant	K_m [mM]	V_{max} [µmol/min*mg]
Pdr5 WT	1.71 ± 0.71	1.33 ± 0.23
Walker A	1.06 ± 0.27	1.50 ± 0.13
Walker B	1.97 ± 0.50	1.15 ± 0.13
H-loop	4.08 ± 1.49	2.09 ± 0.46
C-loop	1.36 ± 0.46	1.33 ± 0.17
HC-loop	1.04 ± 0.23	1.37 ± 0.10
AHC	1.19 ± 0.75	0.48 ± 0.97
ABHC	1.80 ± 0.50	0.20 ± 0.03

Table 3.

Mutant	K_m [nM]	V_{max} [Relative transport of R6G %]
Pdr5 WT	20.1 ± 2.9	83.52 ± 5.7
Walker A	25.3 ± 6.6	23.62 ± 2.7
Walker B	21.4 ± 3.3	61.44 ± 5.8
H-loop	18.7 ± 3.4	71.52 ± 9.7
C-loop	20.2 ± 7.5	36.40 ± 5.6
HC-loop	No transport	3.74 ± 0.80
AHC	No transport	2.33 ± 0.67
ABHC	No transport	0.68 ± 0.13

Figures

Figure 1

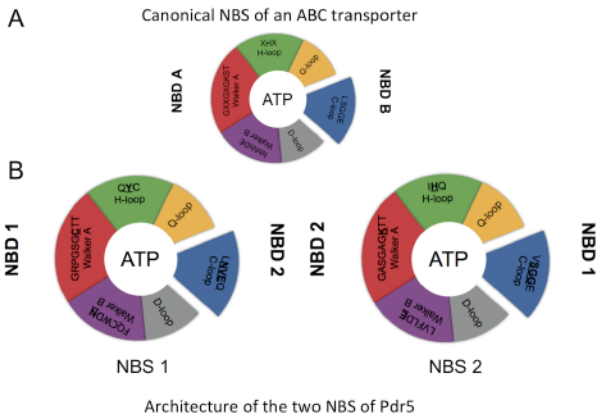

Architecture of the two NBS of Pdr5

Figure 2

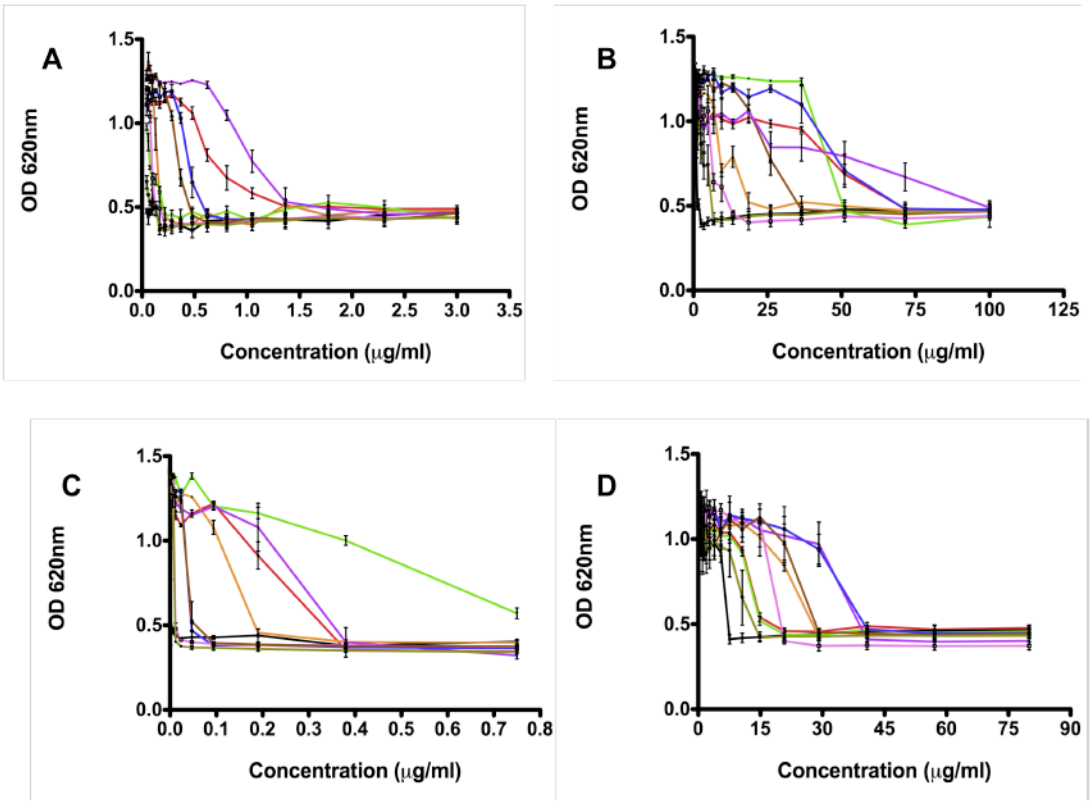
A
OD 620nm
1.5
1.0
0.5
0.0
0.0 0.5 1.0 1.5 2.0 2.5 3.0 3.5
Concentration (μg/ml)
B
OD 620nm
1.5
1.0
0.5
0.0
0 25 50 75 100 125
Concentration (μg/ml)
C
OD 620nm
1.5
1.0
0.5
0.0
0.0 0.1 0.2 0.3 0.4 0.5 0.6 0.7 0.8
Concentration (μg/ml)
D
OD 620nm
1.5
1.0
0.5
0.0
0 15 30 45 60 75 90
Concentration (μg/ml)

Figure 3

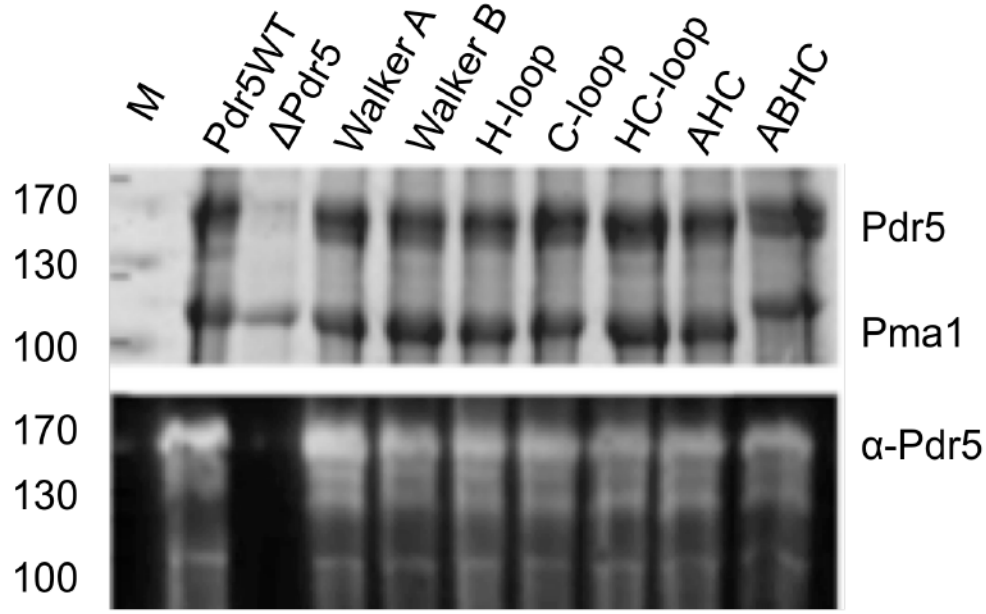
M
Pdr5WT
ΔPdr5
Walker A
Walker B
H-loop
C-loop
HC-loop
AHC
ABHC
170
130
100
Pdr5
Pma1
170
130
100
α-Pdr5

Figure 4

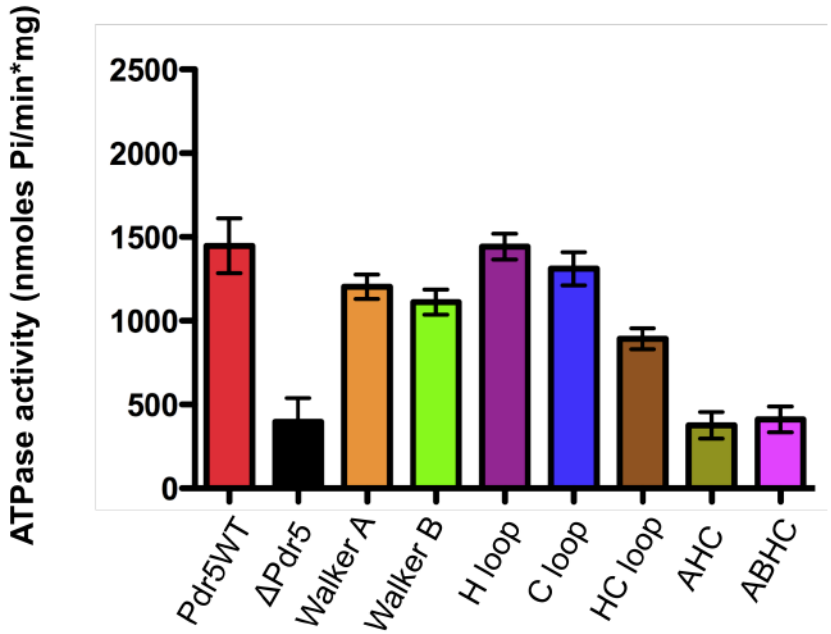
ATPase activity (nmoles Pi/min*mg)
2500
2000
1500
1000
500
0
Pdr5WT
ΔPdr5
Walker A
Walker B
H loop
C loop
HC loop
AHC
ABHC

Figure 5

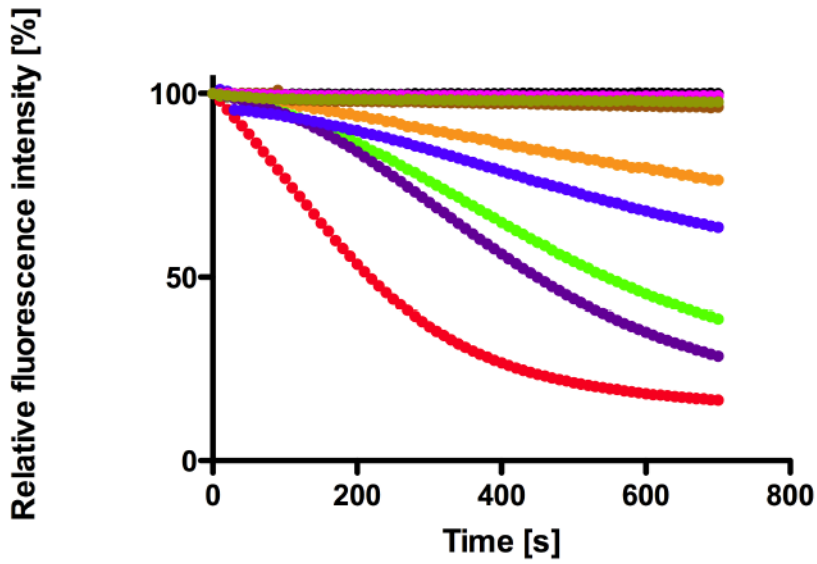
Relative fluorescence intensity [%]
100
50
0
0
200
400
600
800
Time [s]

Figure 6

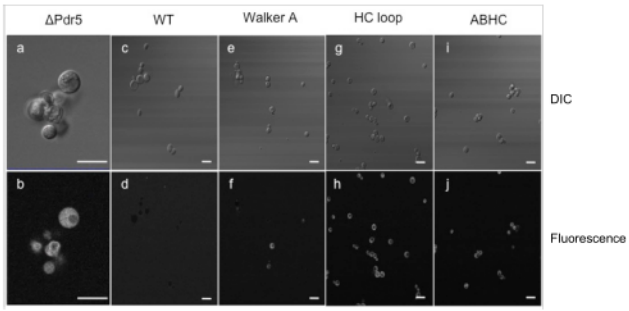

Supplementary Data

Table S1.

List of primers used for introducing point mutations in Pdr5 gene on pRE5 plasmid

Mutation	Direction	Sequence, 5' to 3'
P195S	S	GCTAGTCGTTTTAGGTAGATCAGGCTCTGGCAAAAC
	AS	GTTTTGCCAGAGCCTGATCTACCTAAAACGACTAGC
C199K	S	CGTTTTAGGTAGACCAGGCTCTGGCAAAACTACTTTATTAAAATCCATCTCTTC
	AS	GAAGAGATGGATTTTAATAAAGTAGTTTTGCCAGAGC CTGGTCTACCTAAAACG
N334E	S	GATCCAAATTTCAATGCTGGGATGAAGCTACAAGGG GTTTGGATTC
	AS	GAATCCAAACCCCTTGTAGCTTCATCCCAGCATTGAA ATTTGGATC
Y367H	S	CTGCCACAGTGGCCATCCATCAATGTTCTCAAGATG
	AS	CATCTTGAGAACATTGATGGATGGCCACTGTGGCAG
N1011S	S	GTTGTTGGTGTTGCTGGTGAAGGTTTATCTGTTGAAC AAAGAAAAAGATTAACCATTG
	AS	CAATGGTTAATCTTTTTCTTTGTTCAACAGATAAACCT TCACCAGCAACACCAACAAC
V1012G	S	GTTGCTGGTGAAGGTTTAAACGGTGAACAAAGAAAA AGATTAACC
	AS	GGTTAATCTTTTTCTTTGTTCACCGTTTAAACCTTCAC CAGCAAC
E1013G	S	GTTGCTGGTGAAGGTTTAAACGTTGGTCAAAGAAAAA GATTAACCATTGGTG
	AS	CACCAATGGTTAATCTTTTTCTTTGACCAACGTTTAAA CCTTCACCAGCAAC

Proportionate work on this publication: 60%

Journal to which submitted: EMBO Reports

Impact factor: 7.189

Publication II

A stochastic coupling of ATP hydrolysis and substrate transport in the yeast ABC transporter Pdr5

Rakeshkumar P. Gupta[1], Nils Hanekop[1], Stefanie Weidtkamp-Peters[2] and Lutz Schmitt[1,#]

[1]Institute of Biochemistry and [2]Center for Advanced Imaging (CAi), Heinrich-Heine-Universität, Universitätsstr 1, 40225 Düsseldorf, Germany

Submitted to Proceedings of the National Academy of Sciences of the United States of America

The ABC transporter Pdr5 is a key element of the pleiotropic drug resistance (PDR) network, which represents the first line of defense against toxic compounds in Saccharomyces cerevisiae. Like its human counterpart P-gylcoprotein (P-gp, MDR1 or ABCB1), Pdr5 transports a large variety of structurally unrelated, hydrophobic compounds including antibiotics, azoles, anticancer drugs, detergents, ionophores, steroids and fluorescent dyes such as rhodamine 6g (R6G) at the expense of ATP. Currently, it is assumed that ABC transporters involved in PDR or multidrug resistance (MDR) expel their substrates from the inner leaflet of the cellular membrane thereby actively preventing cell entrance. The coupling of ATP hydrolysis to substrate transport for Pdr5 like many other MDR/PDR ABC transporters is currently unknown. The exception is P-gp, for which an ATP / substrate stoichiometry of 0.3-1.0 has been reported. Here, we report a Pdr5- and ATP-dependent visualization of R6G transport in inside-out plasma membrane vesicle preparations by laser scanning fluorescence spectrometry. Furthermore, we determined the amount of ATP hydrolyzed per R6G molecule transported. Our results suggest a stochastic coupling ratio of ATP and R6G. This supports the fact that Pdr5 is a strictly uncoupled ABC transporter and that the efficiency of transport solely depends on the apparent substrate concentration accessible to Pdr5 for translocation.

ABC transporter | multidrug resistance | membrane transport

Introduction

Pdr5 is a 170-kDa plasma membrane protein from *S. cerevisiae* (1-3) and belongs to the ATP binding cassette (ABC) superfamily of proteins (4, 5). This class of primary active membrane proteins utilize the energy of ATP binding and / or hydrolysis to translocate substrates across cellular membranes. In concert with other ABC transporters (6, 7) and secondary active transporters of the major facilitator family (8, 9), Pdr5 forms the 'pleiotropic drug resistance (PDR) network', which represents the first line of defense against the deleterious action of xenobiotics (4). This process is of crucial importance for the survival of yeast cells when challenged with these toxic compounds.

Pdr5 bears functional homology with its human counterpart, P-glycoprotein (P-gp or MDR1, ABCB1) (10), which has been extensively studied for its implication as one important source of multidrug resistance in cancer treatment (11-13). On the other hand, Pdr5 serves as a model system for ABC transporters present in human pathogenic yeasts such as *Candida albicans* or *C. galbrata* (8, 14, 15). Understanding the mechanism of action of these ABC transporters is therefore vital in developing specific drug targets to overcome resistance to chemotherapy or fungicides.

The vectorial transport of substrates by ABC transporters is energized by binding and / or hydrolysis of ATP in the nucleotide binding domains (NBDs). Based on structural and functional studies, it is now commonly accepted that binding of ATP induces a dimerization of the NBDs, which is transmitted to the transmembrane domains (TMDs) (16, 17). This transmission, which likely occurs through the four coupling helices (18) of MDR ABC exporters, results in a conformational change that switches these exporters from an 'inward-facing' to an 'outward-facing' conformation. In the 'inward-facing' conformation, the substrate-binding site is accessible from the cytosol or the inner leaflet of the cell membrane, while it is exposed to the extracellular space in the 'outward-facing' conformation (5). Subsequent to this conformational switch and the resulting substrate transport and release, ATP hydrolysis in the NBDs resets the transporter to the ground state by switching back to the 'inward-facing' conformation.

For P-gp, a three-stage model of ATPase activity has been elaborated (19). The first stage represents the 'basal ATPase activity' of the transporter that is also present in the absence of substrates. Increase of the concentration of substrate beyond a certain threshold results in an increase of ATPase activity. This stage is called the 'substrate-stimulated' or 'stimulated ATPase activity' of the transporter. The threshold and the fold of stimulation depend strictly on the substrate. Finally, further increase in substrate concentration results in inhibition of ATPase activity of the transporter due to binding of the substrate to the substrate-binding site of the outward-facing conformation of P-gp. This binding locks the transporters in one conformation, inhibits resetting of the system and consequently inhibits ATPase activity (20-23).

Despite the homology in function, Pdr5 displays a different substrate-dependent ATPase cycle (24, 25). So far, substrates either do not influence the basal ATPase activity of the transporter, approximately 28 ATP s^{-1} (24), over the whole concentration range or even have not the capability of inhibiting the transporter's ATPase activity beyond a certain threshold of concentration. Substrates capable of inhibiting ATPase activity are for example R6G, rhodamine 123 or ketoconazole, while compounds such as cycloheximide or fluconazole do not influence the basal activity of Pdr5 (24-28). However and in striking contrast to P-gp, no substrate-induced stimulation of ATPase activity has

Significance

Pdr5 is an ATP binding cassette transporter from *Saccharomyces cerevisiae* and is involved in providing protection to the cell by extruding toxic compounds to the extracellular surface. Pdr5 utilizes ATP as an energy source for substrate transport. In this study we investigate the ATP and substrate dependent stochastic coupling for rhodamine 6g. We found this stoichiometric ratio to be 0.3. Pdr5 being an uncoupled transporter we discovered this ratio to be directly proportional to the concentration of available substrate until the substrate itself becomes inhibitory. In addition we show rhodamine 6g transport in a single membrane vesicle using laser scanning confocal microscopy.

Reserved for Publication Footnotes

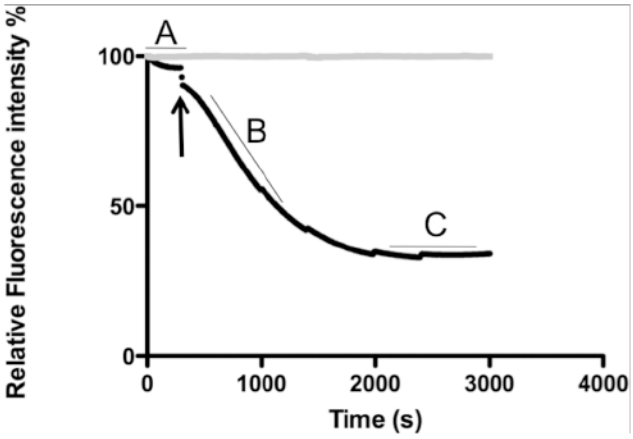

Fig. 1. Representative graph displaying a typical R6G transport assay. Concentration of R6G in transport buffer (300nM), 30 µg/ml plasma membrane vesicles (see Materials and Methods section for details) Part A: equilibration phase without added energy source (0-290s), part B: phase of rapid decrease in fluorescence upon addition of 10mM ATP (330-2000s) and part C: saturation phase where active transport of R6G in the vesicle reaches its maximum (2000-3000s). The arrow represents the time point of addition of ATP. Black trace: membrane vesicles containing Pdr5, grey trace: control experiment using membrane vesicles lacking Pdr5.

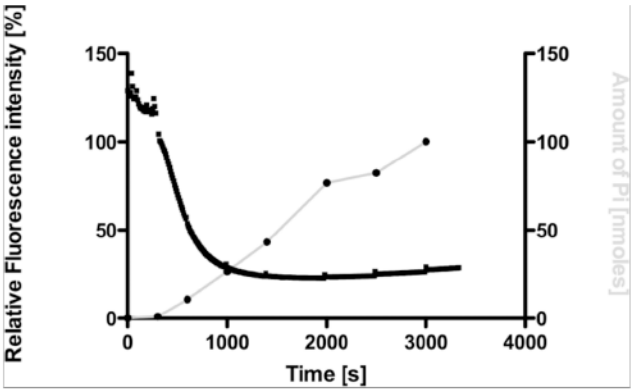

Fig. 2. Graph displaying R6G transport corresponding to a decrease in relative fluorescence intensity with time (left Y-axis) and increase in the amount of liberated P_i being released due to ATP hydrolysis (right Y-axis). Experimental details are given in the Materials and Methods section.

Table 1.

Rhodamine 6G [nM]	Moles R6G transported per mole of ATP hydrolyzed
75	0.002 ± 0.0
150	0.008 ± 0.001
300	0.034 ± 0.002
600	0.370 ± 0.018
1000	0.174 ± 0.028
1500	0.138 ± 0.032
2000	0.134 ± 0.002

Table representing the amount of moles of R6G being transported per mole of ATP being hydrolyzed at different R6G concentrations.

been observed so far. This suggests that Pdr5 possesses an uncoupled ATPase activity. Here, the transporter constantly binds

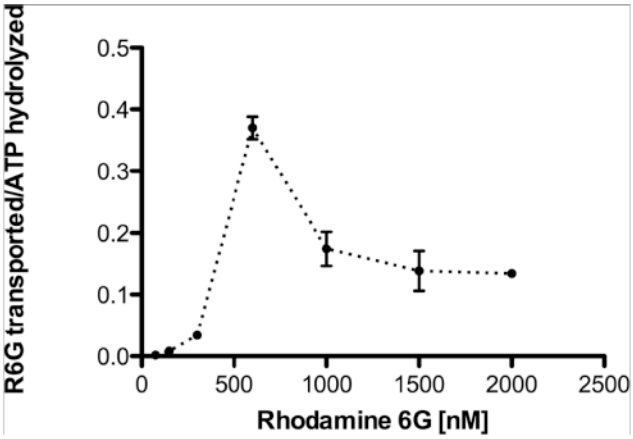

Fig. 3. Graphical representation of substrate concentration dependent stochastic coupling of R6G transport to ATP hydrolysis. Mean values of at least three independent experiments are shown and the error bars represent the standard deviation.

and hydrolysis ATP independent of the presence or absence of substrates (5).

Despite these mechanistic and structural insights, the stoichiometry of ATP hydrolysis to substrate transport of ABC transporters has been investigated only for a number of different substrates of P-gp (29, 30), a bacterial glycine betaine import system (OpuA from *L.* lactis) (31), a vitamin B_{12} uptake system $BtuC_2D_2$-F (32) and the maltose transporter system from *E. coli* $MalFGK_2$ (33). In the case of P-gp, the coupling ratios reported vary from 0.3-1.0 moles of substrate transported per mole of ATP hydrolyzed (29, 30), while a stoichiometry of 2 was determined for OpuA (31). For $BtuC_2D_2$-F an apparent stoichiometry of about 100 ATP per vitamin B_{12} was reported (32) while for the maltose system 1.4 moles of ATP per mole of maltose transported was calculated, although this number went up to 17 in some experiments of the same study (33). These different values of stoichiometry imply mechanistic differences in the coupling of ATPase activity and substrate transport.

Attempts to determine the substrate / ATP stoichiometry have not been carried out for Pdr5 or any other yeast ABC transporter. On the other hand, Pdr5 is a validate model system for yeast MDR or PDR ABC transporters, because its homologous overexpression is established, functional studies have deciphered the substrate spectrum of the transporter as well as crucial amino acids involved in binding and hydrolysis of ATP as well as communication between NBD and TMD (25, 28, 34-37) and a homology model was recently proposed (38). For example, Kolaczkowski *et. al* (39) established a membrane based R6G transport assay, which has been proven as essential in the past to determine the functionality of Pdr5 in crude membrane preparations (28, 40). This method allows the visualization of Pdr5 mediated R6G transport in inside-out membrane vesicles in the presence of ATP as energy source in real time.

We visualized real time R6G transport in a single membrane vesicle immobilized on a cover slide with the aid of laser scanning confocal microscopy. In addition we used the approach developed by Kolaczkowski *et al.* (28) to visualize Pdr5 mediated R6G transport and measured the amount of ATP that is hydrolyzed during the transport of R6G. A quantitative analysis allowed us to calculate the stoichiometry of the number of moles of R6G transported per mole of ATP hydrolyzed. Strikingly, we did not obtain a constant stoichiometry. Rather, an increase in the concentration of the substrate R6G resulted in an increase in mole R6G transported per mole ATP hydrolyzed. We refer to this scenario as a stochastic coupling of ATP hydrolysis and substrate

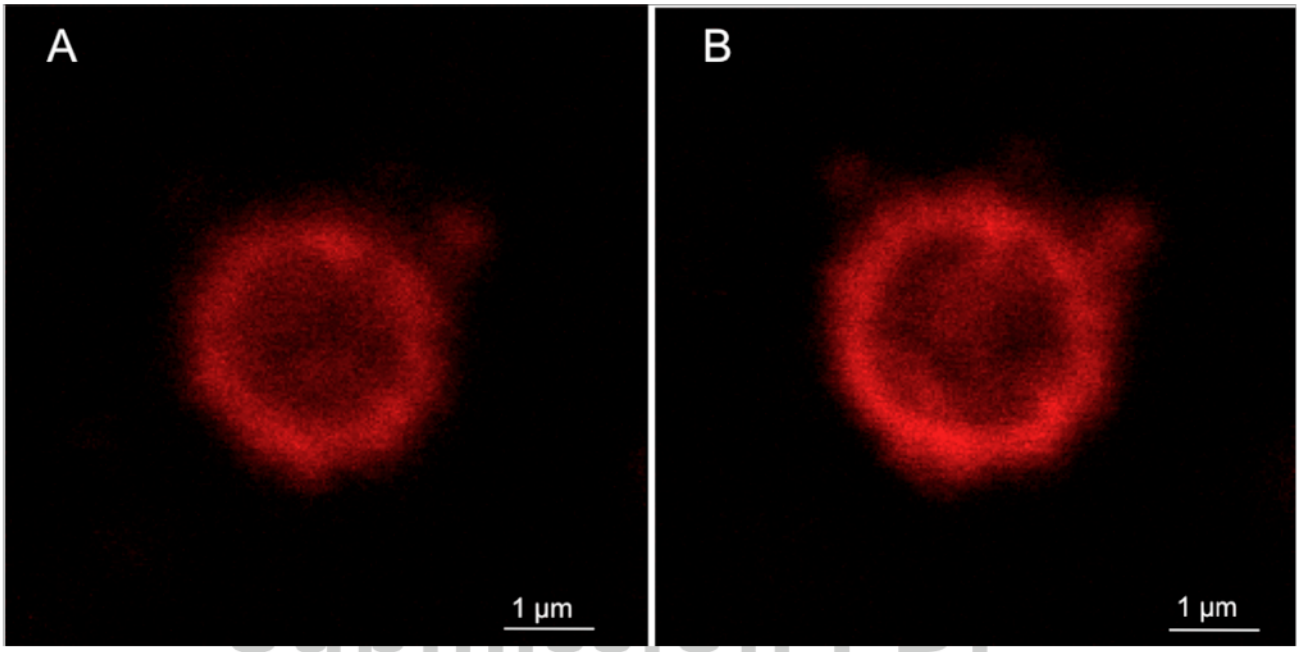

Fig. 4. Image displaying Pdr5 WT membrane vesicle before the addition of ATP (A) and after the addition of ATP (B). A corresponding movie of the experiment can be found in Supplementary Information (Movie S1).

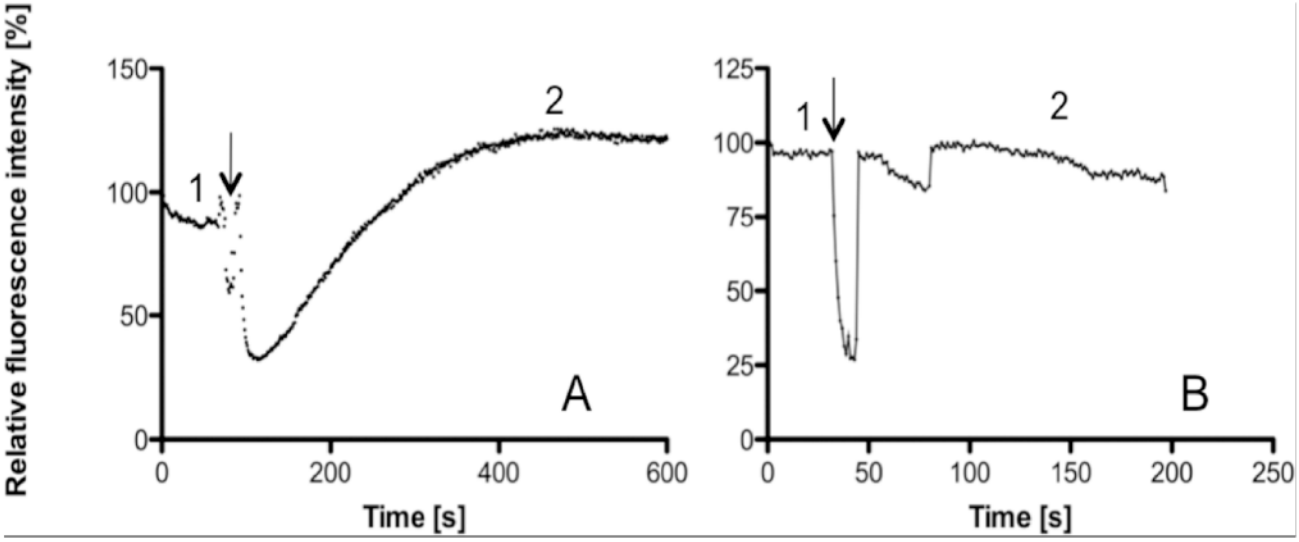

Fig. 5. Traces of fluorescence intensities over time during observation of R6G transport in a single membrane vesicle. Phase 1 is the equilibration phase without ATP addition. An arrow represents the addition of either 20mM ATP (A) or buffer (B). Phase 2 displays rise in fluorescence intensity due to Pdr5 mediated active transport in (A), while the intensity remains more or less constant in (B).

transport. As expected, further increase in R6G concentration beyond a certain threshold resulted in a subsequent decrease of the stoichiometry. These experimental results directly support the proposal that Pdr5 is a strictly uncoupled ABC transporter (5), i.e. that substrate transport occurs based on the probability that a substrate is present, while Pdr5 constantly undergoes cycles of ATP hydrolysis thereby constantly switching between the 'inward'- and 'outward-facing' conformation. Furthermore, these data suggest a new mode of action of fungal MDR / PDR ABC transporters clearly different from the mode of action of bacterial ABC import systems such as OpuA (31) or the maltose importer (33).

Results

Real-time R6G transport

R6G transport is one of the most reliable assays to analyze the functionality of Pdr5 (28). The only requirement for this assay is the presence of a structurally intact Pdr5 molecule embedded in the inside-out membrane vesicle that is capable of hydrolyzing ATP and using this as an energy source to transport the dye to the inner leaflet and eventually to the lumen of the vesicle. A typical R6G transport assay is depicted in Figure 1. The reaction mixture comprising of membrane vesicles in buffer is equilibrated for 290 s (part A), after which addition of 10mM ATP initiates the reaction as indicated by an arrow in Figure 1. The drop in fluorescence intensity (330s-1500s) is an indication of the dye being trans-

ported from the outside/outer leaflet to the inner leaflet/lumen of the vesicle (part B). The plateau (part C) of the transport assay represents saturation of the membrane vesicles with the dye, as well as the state where the amount of dye entering the vesicle and the amount of dye being released due to passive diffusion are in balance representing a macroscopic state of equilibrium.

Quantification of R6G transport and stoichiometry determination

R6G possesses a maximal fluorescence in the monomeric state while dimers or higher oligomers are non-fluorescent (47). For the calculation of stoichiometry of R6G transport we measured the amount of inorganic P_i that is generated by hydrolysis of ATP using the malachite green assay. This was performed while the R6G transport assay was in action by aliquoting samples from the reaction mixture. Figure 2 represents the amount of free Pi derived from the hydrolysis of ATP by Pdr5 that was measured and its co-relation with transport activity of Pdr5. A representative method of calculation is described in the Materials and Methods section for 300nM R6G.

The results of this simple and rather robust method are summarized in Table 1 for different concentrations of R6G. As seen from the stoichiometry calculations the mole-to-mole efficiency of transport is maximal at 600nM of R6G. The decrease of transport efficiency at higher concentrations coincides with the inhibitory effects of R6G on ATPase activity of Pdr5 (25) where a K_i of 600nM was reported (see discussion for further details). Figure 3 summarizes the data in Table 1 to represent the probabilistic nature of substrate transport by Pdr5. Pdr5 is an uncoupled transporter in the sense that it displays no substrate stimulated ATPase activity but maintains a high basal activity of ATP hydrolysis (24-28). As seen in Figure 3 optimal coupling of substrate transport with ATP hydrolysis occurs at a concentration of 600nM R6G. As the substrate becomes inhibitory to the transporter at higher concentrations, ATP hydrolysis is inhibited due to the transporter being locked in the outward conformation. Hence, even though Pdr5 is uncoupled in terms of substrate stimulation but is still mechanistically vulnerable to substrate inhibition that affects ATP hydrolysis.

Visualization of Rhodamine 6G transport in real-time

The data obtained from spectrofluorometric analysis of R6G transport provided valuable information for the determination of the transported R6G / ATP stoichiometry. Nevertheless, it is an average of all the membrane vesicles in the reaction mixture and the transport reactions taking place within them. On the other hand, we were curious to monitor R6G transport in a single membrane vesicle to actually visualize the process of active R6G transport in real time. For this purpose, membrane vesicles were immobilized on cover slides (as described in the Materials and Methods section) and used for Laser Scanning Confocal Microscopy (LSM). Measurements were performed at a concentration of 300nM R6G. Figure 4A shows the accumulation of R6G in the membranes of the vesicle. After this equilibration phase, 20mM ATP was added to energize the system and to observe active transport. Figure 4B represents the accumulation of R6G inside the vesicle lumen upon addition of ATP due to active transport by Pdr5 after 400s. To quantify these data, a compilation of mean fluorescence intensities of the vesicle over time is presented in Figure 5. The point of ATP addition represents a drop in intensity, because of dilution, which recovers due to active R6G transport mediated by Pdr5 and reaches well above the intensity observed in the first 100s. As a control a similar setup was used but buffer was added instead of ATP (Figure 4B). The fluctuations in intensity in the control are minimal and do not represent any Pdr5 mediated transport activity. Supplementary movie 1 shows the entire process over 600s with the initial resting membrane vesicle, addition of ATP and increase in fluorescence inside the vesicle over time.

Discussion

Stoichiometric coupling of substrate transport and ATP hydrolysis is an important read-out for the transporter functionality. A number of studies concerning this have been carried out on Pgp in the past employing various techniques. The values calculated for Pgp with different substrates range from 0.3-1.0 moles of substrate transported per mole of ATP hydrolyzed (29, 30, 48), while for other proteins viz. OpuA (31), $MalFGK_2$ (33), $BtuC_2D_2$-F (32) transporter these ratios vary considerably. Pdr5 being studied as a functional homolog of Pgp residing in yeast has certain similarities as well as differences with Pgp. Wild type Pdr5 has a degenerate nucleotide binding site (NBS) which has been proposed to play only a supporting role for ATP hydrolysis at the second NBS (25). Moreover Pdr5 has so far not displayed any substrate stimulated ATPase activity with any of the substrates tested so far (24-28). Pdr5 has been investigated to a great extent with regards to its biochemical functions but the aspect of stoichiometry had not been investigated so far. Our approach to this problem was rather simple which involved direct measurement of the amount of ATP that is hydrolyzed while R6G is being transported to the lumen of the vesicles (Figure 2). The number that we arrived at is 0.3 moles of R6G transported per mole of ATP being hydrolyzed (Table 1). In other words about 3 molecules of ATP are needed to transport 1 molecule of R6G. The stoichiometric ratio of 0.3 was determined at a concentration of 600nM R6G. Below this concentration the ratio was even lower indicating sub-saturation conditions, while the lower ratios observed above 600nM indicate over-saturation of the transporter with its substrate and may represent inhibition of transporter activity. As per our control measurements are concerned, we checked for inner-filter effects to see the sensitivity of our experimental setup to detect high concentrations of R6G in use (Supplementary Figure 1). The obtained data tells us that R6G up to concentrations of 5000 nM could be measured during transport using our set up without losing sensitivity due to detector over saturation. On the other hand the main counter-argument with transport measurements is that the substrate can diffuse or 'flip outside' the vesicle passively. The litmus test for an active transporter to be functional is to actively pump much more substrate inside the vesicle than what is passively diffusing out to give an overall decrease in fluorescence intensity. We tried to measure the threshold concentration of R6G at which we can theoretically visualize transport (assuming no substrate inhibition). In principle, 5371 nM of R6G would represent the upper limit beyond which using our experimental conditions transport can no longer be visualized (Supplementary Figure 2). However, owing to substrate inhibition of Pdr5 by R6G practically one can only measure transport up to 2000nM. When we compare the substrate dependent stoichiometry of Pdr5 with those ABC transporters for which a substrate / ATP stoichiometry has been reported (29-33, 48), a striking difference becomes apparent. Pdr5 has been shown to be an uncoupled ABC transporter (24, 25), which so far has not shown any substrate stimulated ATPase activity. This is in stark contrast to other ABC transporters, for which a strict coupling between substrate transport and ATP hydrolysis has been observed. This would mean that the stoichiometry that we calculated is merely a probalistic or stochastic event that occurs when the active transporter encounters a substrate i.e R6G, while ATP is constantly being hydrolyzed. This probability is directly proportional to the substrate concentration available. As shown in Table 1 and Figure 3, higher substrate concentrations result in higher stoichiometric ratios. This holds true until the substrate itself becomes inhibitory to the transporter activity, either by locking the substrate in the outward facing conformation or interfering directly with ATP hydrolysis. With the current setup we cannot distinguish between these two outcomes. This is to our knowledge a novel finding in the mechanistic understanding of uncoupled ABC transporters.

The second part of our work involved real time visualization of R6G transport in a single inside-out membrane vesicle. Figure 4 and Figure 5 summarize our findings. R6G was actively transported in the vesicle when ATP was added, while the control with buffer displayed no increase in fluorescence intensity inside the vesicle (Figure 5A and 5B). These results are in complete agreement with our data obtained with the fluorescence spectrofluorometer. The decrease in fluorescence intensity observed here are the combined events of transport happening in all the membrane vesicles present in the reaction mixture at the time. When we look at a single membrane vesicle, the relative increase in fluorescence intensity may appear small on addition of ATP. But when thousands of these events take place at the same time, it would result in a read out as seen with the spectrofluorometer. A closer look at the membrane vesicle tells us that the membrane itself appears to be too thick for a monolayer (Figure 4A). To analyze the lamillarity of our membrane vesicles, we carried out some fluorescence correlation spectroscopy (FCS) as well as Stochastic Optical Reconstruction Microscopy (STORM) measurements. Our initial observations suggest that the vesicles are multilamellar. Due to resolution limits it is very difficult to precisely calculate the concentration of R6G in the membrane leaflets (inner and outer) and get a definite answer as to whether Pdr5 can pump against a concentration gradient and if so what is the limit for this activity. We are presently trying to investigate these further using new approaches.

In summary, this is the first report of substrate dependent stoichiometry of an uncoupled ABC transporter as well as real time visualization of substrate transport in a membrane vesicle system for Pdr5. Thus, this work shall prove useful in better understanding differences in the mechanisms of substrate transport of uncoupled and coupled ABC transporters.

Materials and Methods

Growth media and Chemicals

S. cerevisiae cells were grown in YPD medium (10g/l Yeast extract, 20g/l Peptone/Tryptone and 20g/l Glucose). All chemicals were purchased from Carl Roth. All other chemicals were purchased from Sigma unless otherwise stated. Protease inhibitor tablets were obtained from Roche. Bradford's reagent was purchased from Thermo Scientific.

Yeast strains

The following yeast strains were used in this study YALF-A1 (*MATa ura3-52 trp 1-1 leu 2-3 his 3-11 15 ade 2-1 PDR 1-3*), YHW-A5 (*MATa ura3-52 trp 1-1 leu 2-3 his 3-11 15 ade 2-1 PDR 1-3 pdr5$^{\triangle}$::TRP1*).

Culturing of yeast cells and isolation of plasma membranes

Cells were grown in YPD medium at 30° C. At OD_{600} of 1.5, the nitrogen source was replenished by addition of a 10^{th} volume of 5X YP (50 g/liter yeast extract; 100 g/liter tryptone/peptone). Cells were harvested at OD_{600} of 3.5. The isolation of plasma membranes was performed as described (25).

R6G Transport Assay

Active R6G transport was recorded according to the protocol developed by Kolaczkowski *et al.*, using a Fluorolog III fluorescence spectrometer (Horiba) (28, 41). Isolated plasma membranes (30 µg of total protein content) were re-suspended in 1ml of transport buffer (50 mM Hepes pH 7.0, 10 mM $MgCl_2$, varying concentrations of R6G and 10 mM azide) and incubated at 35° C. Transport was initiated by addition of 10mM ATP. The excitation wavelength was 529nm and emission wavelength was 553nm.

ATPase activity Assays

Oligomycin (OM) sensitive ATPase activity of plasma membrane fractions was measured by a colorimetric assay performed in 96-well microtiter plates (41-43). Aliquots from the reaction mixture in which R6G transport is measured were taken at regular intervals and liberation of free P_i as a result of ATP hydrolysis was measured. To reduce background, 0.2 mM ammonium molybdate, 50 mM KNO_3, and 10 mM NaN_3, respectively were added (42, 44). In a control reaction, OM (20 µg/ml) was added to the assay to determine the OM-sensitive ATPase activity. After incubation at 30° C for 20 min, the reaction was stopped by addition of 175 µl of ice-cold 40 mM H_2SO_4. The amount of released P_i was determined by a colorimetric assay, using Na_2HPO_4 as standard (45).

Immobilization of membrane vesicles on cover slides

A slightly modified protocol to the one described by Cha *et al.* (46) was used to prepare cover slides for immobilization of membrane vesicles. Clean glass slides were thoroughly washed and dried with dry nitrogen. This was followed by activation of the surface by placing them in plasma cleaner under vacuum for 12 min. Subsequently, slides were incubated in 5M ethanolamine in DMSO for 12 hours and washed again. This was followed by incubation of the slides with 2mM NHS-PEG in chloroform and 0.5% triethylamine for 1 hour followed by intensive washing. The final step of derivatisation of the surface was achieved by incubating the slides in 100mM disuccinimidyl carbonate (DSC) and 100mM dimethyl amino pyridine (DMAP) in acetonitrile for 6 hours. Washing and drying of the slides for further use again followed this.

Real-time visualization of R6G transport in inside-out membrane vesicles

Imaging of vesicles was performed on an Olympus FV1000 confocal laser scanning microscope (Olympus GmbH, Hamburg, Germany) equipped with a 60x water immersion objective, NA 1.2. R6G fluorescence was excited at 515 nm using an argon laser at an output power of 5%. The fluorescence signal was detected between 530 and 630 nm using a spectral detector.

Determination of the stoichiometry of moles of R6G transported per moles of ATP hydrolyzed.

The following equations were used for determining the stoichiometry of R6G transport.

X = C – B (equation 1)

Y = (X*(pmoles of R6G in assay)) / A (equation 2)

Stoichiometry = Y / Z (equation 3)

Here A refers to fluorescence of R6G in counts per second (CPS) at t=0, B and C indicate the fluorescence in counts per second (CPS) at 290 s and 1000 s, respectively. 290 s corresponds to the time point at which R6G transport was initiated by the addition of ATP and Mg^{2+}. The difference between 0s and 290s is the amount of R6G that may have been transported in the absence of added ATP or passively diffused. Z corresponds to the amount of ATP hydrolyzed in the transport assay, which was determined as described as described above (ATPase activity assay).

A representative calculation is described for stoichiometry determination with 300nM R6G.

1. Amount of ATP hydrolyzed in 1000s = 4.95 ± 0.06 nmoles (equals Z).
2. Total amount of R6G in the transport assay = 300 pmoles.
3. CPS of 300 pmoles of R6G = 10286380.73 (equals A).
4. CPS at 290s = 8467576.686 (equals B).
5. CPS at 1000s = 2568851.641 (equals C).
6. According to equation 1, X equals to 5898725.045.
7. According to equation 2, Y equals to 172.03 pmoles of R6G that was actively transported in 1000 s.
8. Based on these values, equation 3 equals to 0.034.
9. Therefore, **0.034** ± **0.002** moles of R6G were transported per mole of ATP hydrolyzed.

Acknowledgements.

We thank Markus Richert and Stefan Marawske for support in preparing cover slides for immobilization of the membrane vesicles. We also thank Patrick J. Bakkes for stimulating discussions. This work was funded through the Heinrich Heine University Düsseldorf, the EU (European Drug Initiative on Channels and Transporters, EDICT) FP7 theme (Health-2007-2.1.1.-5). Microscopy facilities were provided by Center for Advanced Imaging (CAi) of Heinrich Heine Universität Düsseldorf.

1. Balzi E & Goffeau A (1994) Genetics and biochemistry of yeast multidrug resistance. *Biochim Biophys Acta* 1187(2):152-162.
2. Bissinger PH & Kuchler K (1994) Molecular cloning and expression of the Saccharomyces cerevisiae STS1 gene product. A yeast ABC transporter conferring mycotoxin resistance. *J Biol Chem* 269(6):4180-4186.
3. Hirata D, Yano K, Miyahara K, & Miyakawa T (1994) Saccharomyces cerevisiae YDR1, which encodes a member of the ATP-binding cassette (ABC) superfamily, is required for multidrug resistance. *Curr Genet* 26(4):285-294.
4. Ernst R, Klemm R, Schmitt L, & Kuchler K (2005) Yeast ABC-transporters - Cellular cleaning pumps. *Methods Enzymol.* 400:460-484.
5. Gupta RP, Kueppers P, Schmitt L, & Ernst R (2011) The multidrug transporter Pdr5: a molecular diode? *Biol Chem* 392(1-2):53-60.
6. Balzi E & Goffeau A (1995) Yeast multidrug-resistance - the pdr network *Journal of Bioenergetics and Biomembranes* 27(N1):71-76.
7. Bauer BE, Wolfger H, & Kuchler K (1999) Inventory and function of yeast ABC proteins: about sex, stress, pleiotropic drug and heavy metal resistance. *Biochim Biophys Acta* 1461(2):217-236.
8. Cannon RD, *et al.* (2009) Efflux-mediated antifungal drug resistance. *Clin Microbiol Rev* 22(2):291-321, Table of Contents.
9. Monk BC & Goffeau A (2008) Outwitting multidrug resistance to antifungals. *Science* 321(5887):367-369.
10. Juliano RL & Ling V (1976) A surface glycoprotein modulating drug permeability in Chinese hamster ovary cell mutants. *Biochimica et biophysica acta* 455(1):152-162.
11. Callaghan R (2010) Multidrug efflux pumps: the big issues. *FEBS J* 277(3):529.
12. Seeger MA & van Veen HW (2009) Molecular basis of multidrug transport by ABC transporters. *Biochim Biophys Acta* 1794(5):725-737.
13. Szakacs G, Paterson JK, Ludwig JA, Booth-Genthe C, & Gottesman MM (2006) Targeting multidrug resistance in cancer. *Nat Rev Drug Discov* 5(3):219-234.
14. Fitzpatrick DA, Logue ME, Stajich JE, & Butler G (2006) A fungal phylogeny based on 42 complete genomes derived from supertree and combined gene analysis. *BMC Evol Biol* 6:99.

15. Lamping E, *et al.* (2010) Fungal PDR transporters: Phylogeny, topology, motifs and function. *Fungal Genet Biol* 47(2):127-142.
16. Locher KP (2009) Review. Structure and mechanism of ATP-binding cassette transporters. *Philos Trans R Soc Lond B Biol Sci* 364(1514):239-245.
17. Davidson AL, Dassa E, Orelle C, & Chen J (2008) Structure, function, and evolution of bacterial ATP-binding cassette systems. *Microbiol Mol Biol Rev* 72(2):317-364, table of contents.
18. Dawson RJ & Locher KP (2006) Structure of a bacterial multidrug ABC transporter. *Nature* 443(7108):180-185.
19. Al-Shawi MK & Omote H (2005) The remarkable transport mechanism of P-glycoprotein: a multidrug transporter. *J Bioenerg Biomembr* 37(6):489-496.
20. Al-Shawi MK, Polar MK, Omote H, & Figler RA (2003) Transition state analysis of the coupling of drug transport to ATP hydrolysis by P-glycoprotein. *J Biol Chem* 278(52):52629-52640.
21. Crowley E & Callaghan R (2010) Multidrug efflux pumps: drug binding--gates or cavity? *FEBS J* 277(3):530-539.
22. Davidson AL, Laghaeian SS, & Mannering DE (1996) The maltose transport system of Escherichia coli displays positive cooperativity in ATP hydrolysis. *J Biol Chem* 271(9):4858-4863.
23. Gerber S, Comellas-Bigler M, Goetz BA, & Locher KP (2008) Structural basis of trans-inhibition in a molybdate/tungstate ABC transporter. *Science* 321(5886):246-250.
24. Decottignies A, *et al.* (1995) Identification and characterization of SNQ2, a new multidrug ATP binding cassette transporter of the yeast plasma membrane. *J Biol Chem* 270(30):18150-18157.
25. Ernst R, *et al.* (2008) A mutation of the H-loop selectively affects rhodamine transport by the yeast multidrug ABC transporter Pdr5. *Proc Natl Acad Sci U S A* 105(13):5069-5074.
26. Conseil G, *et al.* (2000) Prenyl-flavonoids as potent inhibitors of the Pdr5p multidrug ABC transporter from Saccharomyces cerevisiae. *Biochemistry* 39(23):6910-6917.
27. Conseil G, Perez-Victoria JM, Renoir JM, Goffeau A, & Di Pietro A (2003) Potent competitive inhibition of drug binding to the Saccharomyces cerevisiae ABC exporter Pdr5p by the hydrophobic estradiol-derivative RU49953. *Biochim Biophys Acta* 1614(2):131-134.
28. Kolaczkowski M, *et al.* (1996) Anticancer drugs, ionophoric peptides, and steroids as substrates of the yeast multidrug transporter Pdr5p. *J Biol Chem* 271(49):31543-31548.
29. Ambudkar SV, Cardarelli CO, Pashinsky I, & Stein WD (1997) Relation between the turnover number for vinblastine transport and for vinblastine-stimulated ATP hydrolysis by human P-glycoprotein. *J Biol Chem* 272(34):21160-21166.
30. Shapiro AB & Ling V (1998) Stoichiometry of coupling of rhodamine 123 transport to ATP hydrolysis by P-glycoprotein. *Eur J Biochem* 254(1):189-193.
31. Patzlaff JS, van der Heide T, & Poolman B (2003) The ATP/substrate stoichiometry of the ATP-binding cassette (ABC) transporter OpuA. *J Biol Chem* 278(32):29546-29551.
32. Borths EL, Poolman B, Hvorup RN, Locher KP, & Rees DC (2005) In vitro functional characterization of BtuCD-F, the Escherichia coli ABC transporter for vitamin B12 uptake. *Biochemistry* 44(49):16301-16309.
33. Davidson AL & Nikaido H (1990) Overproduction, solubilization, and reconstitution of the maltose transport system from Escherichia coli. *J Biol Chem* 265(8):4254-4260.
34. Ananthaswamy N, *et al.* (2010) The signaling interface of the yeast multidrug transporter Pdr5 adopts a cis conformation, and there are functional overlap and equivalence of the deviant and canonical Q-loop residues. *Biochemistry* 49(21):4440-4449.
35. Egner R, Bauer BE, & Kuchler K (2000) The transmembrane domain 10 of the yeast Pdr5p ABC antifungal efflux pump determines both substrate specificity and inhibitor susceptibility. *Mol Microbiol* 35(5):1255-1263.
36. Sauna ZE, *et al.* (2008) Mutations define cross-talk between the N-terminal nucleotide-binding domain and transmembrane helix-2 of the yeast multidrug transporter Pdr5: possible conservation of a signaling interface for coupling ATP hydrolysis to drug transport. *J Biol Chem* 283(50):35010-35022.
37. Kueppers P, Gupta RP, Stindt J, Smits SH, & Schmitt L (2013) Functional impact of a single mutation within the transmembrane domain of the multidrug ABC transporter Pdr5. *Biochemistry* 52(13):2184-2195.
38. Rutledge RM, Esser L, Ma J, & Xia D (2011) Toward understanding the mechanism of action of the yeast multidrug resistance transporter Pdr5p: a molecular modeling study. *J Struct Biol* 173(2):333-344.
39. Kolaczkowski M, Kolaczowska A, Luczynski J, Witek S, & Goffeau A (1998) In vivo characterization of the drug resistance profile of the major ABC transporters and other components of the yeast pleiotropic drug resistance network. *Microb Drug Resist* 4(3):143-158.
40. Egner R, Rosenthal FE, Kralli A, Sanglard D, & Kuchler K (1998) Genetic separation of FK506 susceptibility and drug transport in the yeast Pdr5 ATP-binding cassette multidrug resistance transporter. *Mol Biol Cell* 9(2):523-543.
41. Decottignies A, Kolaczkowski M, Balzi E, & Goffeau A (1994) Solubilization and characterization of the overexpressed PDR5 multidrug resistance nucleotide triphosphatase of yeast. *J Biol Chem* 269(17):12797-12803.
42. Goffeau A & Dufour JP (1988) Plasma membrane ATPase from the yeast Saccharomyces cerevisiae. *Methods Enzymol* 157:528-533.
43. Wada S, *et al.* (2002) Candida glabrata ATP-binding cassette transporters Cdr1p and Pdh1p expressed in a Saccharomyces cerevisiae strain deficient in membrane transporters show phosphorylation-dependent pumping properties. *J Biol Chem* 277(48):46809-46821.
44. Dufour JP, Amory A, & Goffeau A (1988) Plasma membrane ATPase from the yeast Schizosaccharomyces pombe. *Methods Enzymol* 157:513-528.
45. Zaitseva J, Holland IB, & Schmitt L (2004) The role of CAPS buffer in expanding the crystallization space of the nucleotide-binding domain of the ABC transporter haemolysin B from Escherichia coli. *Acta Crystallogr D Biol Crystallogr* 60(Pt 6):1076-1084.
46. Cha T, Guo A, Jun Y, Pei D, & Zhu XY (2004) Immobilization of oriented protein molecules on poly(ethylene glycol)-coated Si(111). *Proteomics* 4(7):1965-1976.
47. Toptygin D PBZ, Brand L (1997) Resolution of absorption spectra of rhodamine 6G aggregates in aqueous solution using the law of mass action. *Chemical Physics Letters* 277:430-435.
48. Eytan GD, Regev R, & Assaraf YG (1996) Functional reconstitution of P-glycoprotein reveals an apparent near stoichiometric drug transport to ATP hydrolysis. *J Biol Chem* 271(6):3172-3178.

Supplementary information

Supplementary Figure 1

Graph representing the control for inner filter effects for visualization of R6G transport at high concentrations.

Supplementary Figure 2

Determination of the upper limit of R6G, at which transport can be visualized under the given experimental conditions. Y-intercept represents the relative decrease in fluorescence intensity 2500s after addition of ATP. X-intercept represents the concentration of R6G beyond which transport can no longer be visualized in the given experimental setup.

Supplementary Movie 1

The movie is a time series of images captured every second for 600s and then compiled together. In the initial 100s the membrane is in resting state and R6G is seen in the lipid bilayer. ATP addition results in momentary decrease in intensity due to dilution. This recovers over time and reaches well above the initial baseline due to Pdr5 mediated active transport of R6G inside the vesicle. The scale is the same as shown in Figure 4.

Supplementary Figure 1

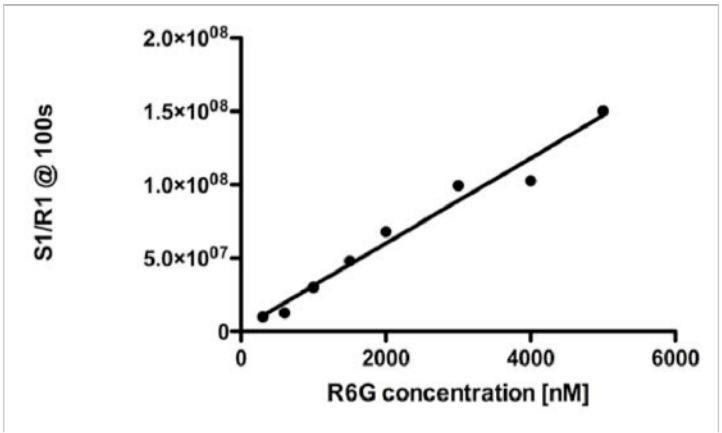

Supplementary Figure 2

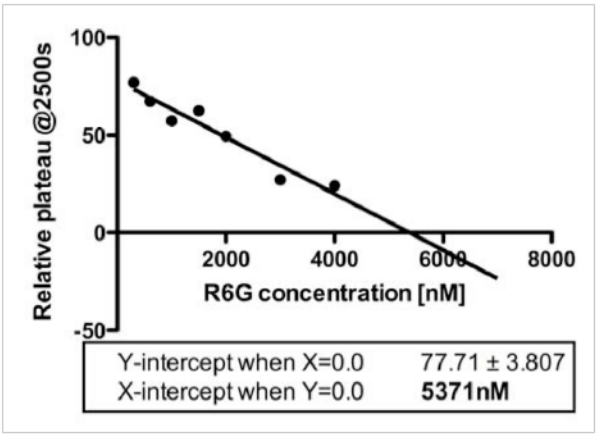

Proportionate work on the manuscript: 90%

Journal to which submitted: Proceedings of the National Academy of Sciences (PNAS)

Impact factor: 9.737

Publication III

BIOCHEMISTRY
including biophysical chemistry & molecular biology

Article

pubs.acs.org/biochemistry

Functional Impact of a Single Mutation within the Transmembrane Domain of the Multidrug ABC Transporter Pdr5

Petra Kueppers, Rakeshkumar P. Gupta, Jan Stindt,† Sander H. J. Smits, and Lutz Schmitt*

Institute of Biochemistry, Heinrich Heine University Duesseldorf, Universitaetsstrasse 1, 40225 Duesseldorf, Germany

Supporting Information

ABSTRACT: The pleiotropic drug resistance network in budding yeast presents a first line of defense against xenobiotics, which is formed by primary and secondary active membrane transporters. Among these transporters, the ABC transporter Pdr5 is a key component, because it confers resistance against a broad spectrum of such cytotoxic agents. Furthermore, it represents a model system for homologous transporters from pathogenic fungi and has been intensively studied in the past. In addition to other mutational studies, the S1360F mutation of Pdr5 was found to modulate substrate specificity and resistance. Notably, in the S1360F background, the resistance against the immunosuppressant FK506 is drastically increased. We present a detailed analysis of this mutation that is located in the predicted cytosolic part of transmembrane helix 11. Our data demonstrate that kinetic and thermodynamic parameters of the S1360F mutant are similar to those of the wild-type protein, except for FK506-inhibited ATPase activity and the degree of competitive inhibition. In summary, our results indicate that the S1360F mutation within the transmembrane domain interferes drastically with the ability of the nucleotide-binding domains to hydrolyze ATP by interfering with interdomain crosstalk.

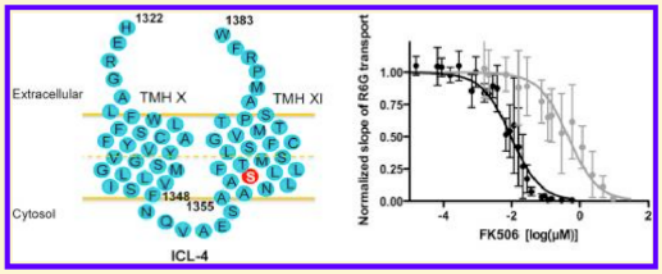

The occurrence of multidrug resistance (MDR) phenotypes is currently a major threat in medicine. Upon the treatment of cancer, bacterial infections, or fungal infections, the prolonged (or repetitive) challenge with sublethal doses of chemotherapeutics, antibiotics, or antifungal drugs, respectively, selects for more resistant cells.[1] One reason for such acquired MDR is the overexpression of plasma membrane-embedded MDR efflux pumps that actively expel a large number of cytotoxic compounds into the extracellular space.[2,3]

Drug resistance in fungi is regulated and executed by the pleiotropic drug resistance (PDR) network. Here, a battery of PDR efflux pumps under the control of PDR transcription factors acts as a first line of defense against a variety of xenobiotic compounds.[4] One of the best-studied and most abundant PDR ABC transporters in *Saccharomyces cerevisiae* is Pdr5. The remarkable degree of sequence conservation between Pdr5 and ABC transporters of clinically relevant fungi, such as *Candida albicans* and *Candida glabrata*,[5,6] makes Pdr5 a valuable model system for understanding the mechanism of multidrug transport and its inhibition in fungi.

Pdr5 consists of two nucleotide-binding domains (NBDs) and two transmembrane domains (TMDs), which represent the basic architecture of all ABC transporters.[7,8] In contrast with their general topology (TMD−NBD−TMD−NBD), a common feature of Pdr5 and its fungal homologues is an inverse arrangement of these four modules (NBD−TMD−NBD−TMD). It is now generally accepted that substrate translocation by Pdr5 and other ABC exporters is achieved by two alternating conformations that can be accessed from the inside of the cell (inward-facing conformation) or from the outside (outward-facing conformation).[9,10] Ongoing binding, hydrolysis, and product release by the NBDs provide the energetic input necessary for active transport.

The understanding of how a single protein can recognize and transport thousands of structurally and functionally diverse substrates is crucial for devising a strategy for inhibiting MDR transporters and ultimately overcoming MDR phenotypes. Numerous studies approached this by mutational analysis,[11−13] photoaffinity labeling,[14,15] cross-linking,[16−18] or substrate screens for Pdr5 and its mammalian homologue P-glycoprotein (P-gp).[19,20] The results pointed toward a polyspecific and shallow binding site. In the case of human P-gp, at least two distinct binding sites were identified (the so-called H- and R-sites). Together with these studies, the published crystal structure of mouse P-gp[21] established that transmembrane helices 5 and 6 and transmembrane helices 11 and 12 play an important role in substrate recognition.[18,22−24] In addition to the structure of mouse P-gp, the crystal structure of the putative bacterial MDR ABC transporter Sav1866 has been widely used to generate homology models of MDR ABC transporters, for which structural information is not yet available. This also includes a recently published homology model of Pdr5.[25] Nevertheless, comprehensive models that explain the dynamic processes of substrate selection, energy allocation, and transport are only starting to emerge.

Received: November 23, 2012
Revised: March 6, 2013
Published: March 6, 2013

The occurrence of MDR phenotypes during invasive fungal infections like candidiasis or aspergillosis in immunocompromised patients[26] calls out for the identification and development of specific inhibitors of PDR efflux pumps. Theoretically, an inhibition of the drug transport activity can be achieved by competition at the stage of drug binding, by noncompetitive pump inactivation, or by the stabilization of a specific conformation locking the transporter in a nontransport competent state. Competition with drug binding was observed, for example, with second-generation inhibitors or modulators of human P-gp,[3] while third-generation inhibitors such as tariquidar seem to block P-gp function by binding to a site distinct from the actual drug binding site.[27]

A number of mostly cytotoxic or invasive agents[3] have been shown to reverse the hyper-resistance conferred by MDR ABC efflux pumps such as the immunosuppressants cyclosporin A,[28] FK506,[11] ionophore antibiotics, enniatins,[29,30] or curcuminoids.[31,32] Here, the nature of the compounds defines the exact mode of action. For instance, the immunosuppressant FK506 affects the calcineurin pathway[33,34] and inhibits Pdr5-mediated transport of several drugs.[11,35] Notably, the concise mode of transport inhibition remains unknown. In this context, the question of whether the chemosensitizer FK506 is a substrate of Pdr5 affecting drug transport by direct competition or a regulator/inhibitor acting at a site remote from the substrate binding site is still controversial. Previous studies of the impact of different substrates by Egner and co-workers identified a transmembrane mutation in Pdr5 (S1360F) that altered the substrate specificity proposing that position 1360 in Pdr5 imposes selectivity on drug recognition.[11,36]

In this study, we focus in detail on the S1360F mutation of the MDR-ABC exporter Pdr5 from *S. cerevisiae* and examine the complex interplay of substrate binding and transport modulation by FK506 in whole yeast cells and in highly enriched plasma membrane preparations. Furthermore, a detailed characterization of Pdr5 and the S1360F transmembrane mutation with respect to transport and ATPase activity in the presence and absence of the immunosuppressant FK506 and its mode of inhibition is presented. The derived data shed further light on the modulatory effect of FK506 on the interaction with Pdr5, suggesting an as yet unknown sensory function of the S1360F mutation in the crosstalk between the sites of ATP hydrolysis (NBD) and those of substrate recognition and translocation (TMD).

EXPERIMENTAL PROCEDURES

Chemicals and Yeast Strains. All chemicals were purchased from Sigma Aldrich. Stock solutions of ketoconazole (KA), fluconazole (FA), and oligomycin (OM) were prepared in dimethyl sulfoxide, and FK506 and rhodamine 6G (R6G) were dissolved in ethanol. [^{3}H]FK506 (185 GBq/mmol) and [γ-^{32}P]-8-azido-ATP (320−360 GBq/mmol) were purchased from Hartmann Analytic. Yeast was cultivated in either rich medium (YPD) or synthetic medium supplemented with appropriate auxotrophic components. In this study, *S. cerevisiae* strains *N14HISPdr5* (*MATa, ura3-52, trp1-1, leu2-3, 112 his3-11, 15, ade2-1,* Pdr1-3, N-terminal 14-histidine tag), *YHW-A5* (*MATa, ura3-52, trp1-1, leu2-3, 112, his3-11, 15, ade2-1,* Pdr1-3, *pdr5Δ::TRP1*), and *YRE1001* (*MATa, ura3-52, trp1-1, leu2-3, 112, his3-11, 15, ade2-1,* Pdr1-3, *pdr5, pdr5promΔ::TRP1*) were used. Cloning and overexpression of the S1360F mutant were performed via site-directed mutagenesis of Pdr5 on plasmid pRE5[12] using the QuikChange II XL site-directed mutagenesis kit (Stratagene).

Liquid Drug Resistance Assay. The microdilution method was performed to determine the minimal inhibitory concentration (MIC).[37] Exponentially growing cells from a liquid YPD culture were diluted to an OD_{600} of 0.25 and used for inoculation of YPD with a constant concentration of drug and serial dilutions of FK506. Plates were incubated for 48 h at 30 °C.[11,36]

Isolation of *S. cerevisiae* Plasma Membranes. Yeast cell cultivation and isolation of plasma membranes were performed as described previously.[12,38] Cells were cultivated in YPD at 25 °C overnight with an additional supply of nitrogen and harvested at an OD_{600} of 3.5.

Sodium dodecyl sulfate−polyacrylamide gel electrophoresis (SDS−PAGE) and Western blot analysis for quality controls were performed as described previously.[12] For Western blot detection, proteins were resolved by SDS−PAGE on a 7% gel and transferred via semidry blotting to methanol-activated PVDF membranes. Whatman filters as well as the methanol-activated PVDF membranes were prepared as described previously for blotting. Membranes were incubated for at least 30 min in blocking buffer containing 3% BSA. Antiserum dilutions in blocking solutions were 1:20000 for polyclonal α-Pdr5 and 1:1000 for α-penta HIS (Qiagen) antibodies. Goat anti-rabbit (Sigma Aldrich) and goat anti-mouse (Pierce) horseradish peroxidase conjugates were used as secondary antibodies. Anti-rabbit antibodies were used at a 1:10000 dilution in TBST [20 mM Tris-HCl (pH 8.0), 250 mM NaCl, and 0.1% (w/v) Tween 20] and anti-mouse antibodies at a 1:20000 dilution in TBS buffer (TBST without Tween 20) containing 10% fat-free dry powdered milk.

R6G Transport in Whole Cells and in Isolated Plasma Membranes. Whole cell drug extrusion was measured using the method of Kolaczkowski et al.[38] with the following modifications. Equal amounts of yeast cells of exponentially growing cultures (OD_{600} = 1) were de-energized by supplementation of 5 mM 2-deoxy-D-glucose and incubated with 5 μM R6G, with or without 25 μM FK506. Identical results were obtained with 20 mM 2-deoxy-D-glucose. Therefore, all experiments were performed at a concentration of 5 mM. Cells were collected by centrifugation, washed twice with 50 mM Hepes (pH 7.0), and resuspended in this buffer. R6G efflux was initiated by addition of 20 mM glucose. Fluorescence intensities were recorded by a Fluorolog III fluorescence spectrometer (Horiba) at an excitation wavelength of 529 nm and an emission wavelength of 553 nm. Active R6G transport was performed as described previously[12] by resuspending isolated plasma membranes (20 μg) in 1 mL of transport buffer [50 mM Hepes (pH 7.0), 5 mM $MgCl_2$, 0−450 nM R6G, and 10 mM azide] and incubation at 35 °C with or without increasing amounts of FK506 prior to the initiation of transport by the addition of 10 mM ATP. Kinetic analysis of R6G fluorescence quenching was performed using Prism (version 5, GraphPad). The IC_{50} values were determined at a constant R6G concentration of 300 nM and analyzed by nonlinear regression using the general dose−response equation (eq 1):

$$Y = B_{min} + \frac{B_{max} - B_{min}}{1 + 10^{[drug] - \log IC_{50}}} \quad (1)$$

where Y represents the residual slope of the R6G fluorescence quenching, B_{min} the minimal slope, B_{max} the maximal slope, and [drug] the FK506 concentration.

Whole Cell Transport Assay of Radioactively Labeled FK506. Cellular transport studies were established according to accumulation assays in whole yeast cells as described previously[39] with minor modifications. Whole yeast cells were harvested from midlog phase (OD_{600} = 1) and de-energized in YP2D medium (5 mM 2-deoxy-D-glucose in YP) as a 5% cell suspension including different concentrations of [^{3}H]FK506 and FK506 in a ratio of 1:250 (total drug concentration of 0.025−40 μM) for 2 h at 30 °C to allow accumulation. Cells were collected and washed briefly four times with YP2D medium by centrifugation. One-third of the sample was separated as an internal control. The remaining cells were resuspended in YP after centrifugation and split equally, and the reaction was started by the addition of either 20 mM glucose or 5 mM 2-deoxy-D-glucose instead of glucose to take passive diffusion into account. After different times of incubation at 30 °C and while being gently shaken, the samples were rapidly harvested by centrifugation. The supernatant and the resuspended pellet in YP medium were measured upon addition of 2 mL of scintillation solution in a Beckman liquid scintillation counter (LS 3801).

Notably, in these experiments, the final concentration of FK506 was 25 μM. This is 450 times higher than the concentration required to inhibit 50% of the ATPase activity in the in vitro measurements that utilize plasma membrane preparations highly enriched in Pdr5. In intact yeast cells, however, other cellular organelles such as the vacuole effectively reduced the concentration of de facto available FK506, whose high hydrophobicity enhances this effect.

ATPase Activity Assays. Pdr5-specific ATPase activity was determined via ATPase activity measurements in the presence and absence of 20 μg/mL oligomycin. The ATPase activity measurements were taken in the presence of 4 mM ATP. Oligomycin is a specific inhibitor of the Pdr5-mediated ATPase activity.[40] The inhibitory effect of increased drug concentrations such as R6G on Pdr5-specific ATPase activity of plasma membrane fractions was measured by a colorimetric assay and performed in microtiter plates[40−42] in the presence of serial drug dilutions. K_i values were determined by fitting the data to a steady state kinetic model using a modified equation of the nonpartitioning model (eq 2) described for human P-glycoprotein (Pg-p, ABCB1):[12]

$$v = 100\left(\frac{1 - [\text{drug}]}{K_i + [\text{drug}]}\right) \quad (2)$$

Binding of [γ-^{32}P]-8-Azido-ATP to Pdr5. Photoaffinity labeling of Pdr5 was based on previously published methods.[23,43−45] Plasma membrane preparations (2.5 μg) were incubated in reaction buffer [50 mM Hepes (pH 7.0), 10 mM NaN_3, 50 mM KNO_3, 0.2 mM ammonium molybdate, and 10 mM $MgCl_2$] containing 2−10 μM [γ-^{32}P]-8-azido-ATP in a total volume of 30 μL on ice for 10 min under subdued light. Samples were cross-linked by UV illumination at 254 nm via a Stratalinker 1800 cross-linker for 8 min. The reaction was stopped by supplementation of 20 μM dithiothreitol prior to protein precipitation with 7.5% (w/v) TCA and 0.015% (w/v) sodium deoxycholate to remove excess nucleotides. The dry precipitate was resuspended in SDS sample buffer, and protein bands were separated by 7% SDS−PAGE. Photolabeling was detected by autoradiography upon exposure of the samples to Kodak Biomax Films MS/XAR at −20 °C for at least 24 h. The radioactivity incorporated was quantified by densitometry using Fujifilm MultiGauge version 3. The interaction with nonlabeled nucleotides was investigated with 5 μM [γ-^{32}P]-8-azido-ATP in the presence of increasing concentrations of ATP (0.005−4 mM) or ADP (0.01−4 mM). The analysis was performed according to nonlinear regression using the general dose−response curve described in eq 1. In this case, Y represents the extent of bound [γ-^{32}P]-8-azido-ATP, B_{min} and B_{max} stand for the corresponding minimum and maximum, respectively, and [drug] is the added ATP and ADP concentration.

Analysis of the Mode of Inhibition of FK506. R6G transport in Pdr5 wild type (WT)- or Pdr5 S1360F-containing plasma membrane vesicles was analyzed as described (see R6G Transport in Whole Cells and in Isolated Plasma Membranes). The following concentrations were used: 300, 200, 150, 75, 50, and 25 nM R6G in the presence of 0, 2, 5, 7.5, and 10 nM FK506 (Pdr5 WT) and 0, 250, 500, 750, and 1000 nM FK506 (Pdr5 S1360F). Linear slopes of the initial transport rates were determined for the 110−500 s time window and plotted as 1/slope versus 1/[R6G] (Figure 8). K_i values were determined according to the method of Dixon[46] and are summarized in Table 1.

Table 1. Summary of the Kinetic and Thermodynamic Properties of Pdr5 WT and the S1360F Mutant

	Pdr5 WT	Pdr5 S1360F
$K_{m,R6G}$ (transport) (nM)	21 ± 3	20 ± 3
$IC_{50,FK506}$ (R6G transport) (nM)	10 ± 0.1	450 ± 80
$K_{i,R6G}$ (ATPase) (μM)	0.63 ± 0.07	1.82 ± 0.17
$K_{i,FK506}$ (ATPase) (μM)	0.05 ± 0.007	4.91 ± 0.36
$IC_{50,ATP}$ (binding) (μM)	48 ± 7	51 ± 5
$IC_{50,ADP}$ (binding) (mM)	0.30 ± 0.06	0.38 ± 0.07
K_i (R6G transport by FK506) (nM)	30 ± 11	739 ± 147

RESULTS

Functional Characterization of Pdr5. Pdr5-mediated resistance toward several drugs, including steroids or azole derivatives, can be inhibited by the macrocyclic lactone FK506.[35] The S1360F mutation of Pdr5, however, represents an exception. It sustains drug resistance in the presence of the immunosuppressant FK506, an effect that was first described by Egner et al.[11] According to a hydrophobicity analysis, residue 1360 is located in the intracellular part of putative transmembrane helix 11 (TMH 11) of Pdr5 (Figure 1A). This prediction is in agreement with the homology structure of Pdr5.[25] TMH 11 follows the fourth intracellular loop (ICL-4) corresponding to the second intracellular coupling helix, which interacts in trans with the X-loop of the second NBD in the crystal structure of Sav1866[47] and in the homology model of Pdr5. Additionally, TMH 11 seems to form an amphipathic α-helix (Figure 1B), in which the hydrophobic face is positioned toward the lipid bilayer. In such an alignment, the side chain of amino acid 1360 would point into the putative substrate transport pathway and a serine to phenylalanine mutation would influence the hydrophobic−hydrophilic balance. Sequence comparison with other fungal ABC transporters (Figure 1C) suggested that position 1360 is weakly conserved in fungal MDR pumps of the ABC family. With the exception of Snq2 and Cdr4, all drug exporters possess either a serine at position 1360 or a conservative exchange against threonine. In contrast, fungal ABC transporters specific for Cd^{2+} (Ycf1), bile acids (Bpt1 or Ybt1), sterol transport (Aus1), or the export of the a-

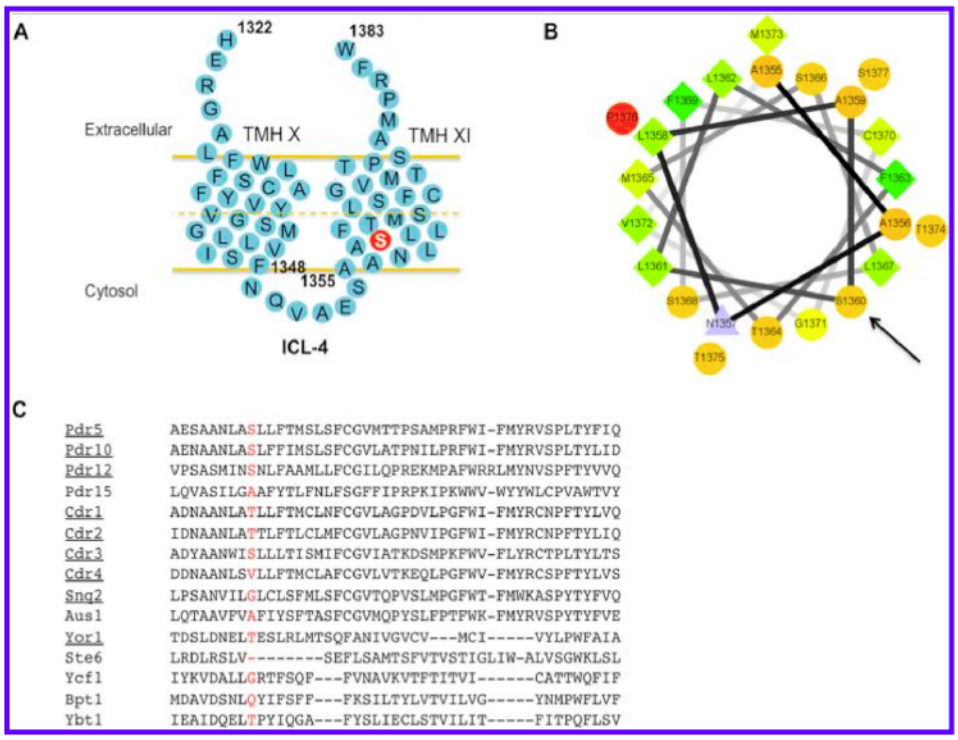

Figure 1. In silico analysis of amino acids 1322−1383 of Pdr5. (A) Predicted membrane topology of residues 1322−1383 of Pdr5 harboring putative TMH 10 and TMH 11. According to this model, residue 1360 (colored red) is localized in TMH 11. (B) Helical wheel projection of residues 1355−1377 forming TMH 11. Green and yellow diamonds represent hydrophobic residues and orange circles hydrophilic residues; the magenta triangle represents a polar, noncharged residue and the red circle a proline residue. (C) Sequence alignment of putative TMH 11 of Pdr5 with different fungal ABC transporters. Residue 1360 of Pdr5 and the other fungal ABC transporters is colored red. Fungal MDR ABC transporters are underlined.

factor (Ste6) do not contain a serine or threonine residue at the corresponding position. Our observation supports the earlier notion that the region around residue 1360 is involved in drug recognition and transport.[36,48]

For a detailed functional analysis of FK506 and its interactions with Pdr5, we focused on the S1360F mutation and generated it by site-directed mutagenesis and a subsequent homologous recombination into *S. cerevisiae* strain Δ*pdr5*Δ*pdr5prom*.[12] This strain contains a mutated transcription factor *PDR1-3*, which confers constitutive expression of Pdr5. In highly enriched plasma membrane preparations of cells expressing Pdr5 WT or the S1360F mutant, similar amounts of Pdr5 were detected (Figure 2). Here, Pdr5 and the plasma membrane ATPase Pma1 appear as distinct bands in a Coomassie Blue-stained SDS−PAGE gel (Figure 2A). In PDR5 deletion strain Δ*pdr5*, no Pdr5 signal could be detected. This result was supported by Western blots using either a polyclonal anti-Pdr5 or an anti-His tag antibody (Figure 2B). This knockout strain served as a negative control in all subsequent experiments.

R6G Transport Activity of Pdr5. Real-time R6G efflux measurements in the absence or presence of the immunosuppressant FK506 were performed to analyze the transport activity of Pdr5 WT and the S1360F mutant. Drug susceptibility assays either on drug agar plates[36] or in liquid cultures (Figure S1 of the Supporting Information) in the presence of FK506 demonstrated a hypersusceptibility to the fluorescent dye R6G in Pdr5 WT-expressing cells, but not in yeast cells expressing the S1360F mutant. Real-time efflux transport assays (Figure 3) were performed as described in Experimental Procedures. Here, R6G efflux was monitored by a concentration-dependent disintegration of R6G excimers,

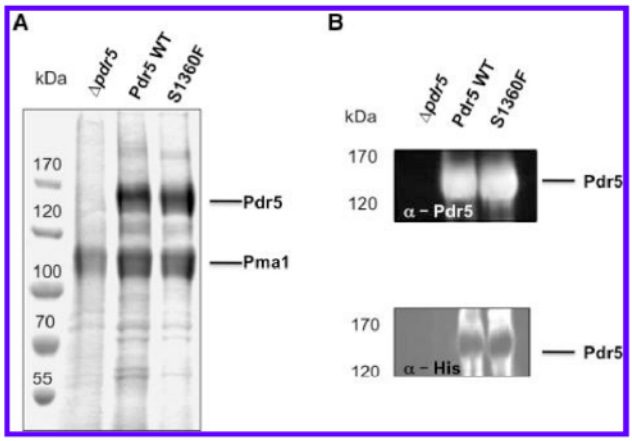

Figure 2. Expression of Pdr5 variants. (A) Coomassie Blue-stained SDS−PAGE of plasma membrane preparations of *S. cerevisiae* cells expressing no Pdr5 (Δpdr5), WT Pdr5 (Pdr5 WT), or the S1360F mutant (S1360F). Fifteen micrograms of total protein was applied per lane. Molecular masses of marker proteins are indicated at the left. Bands corresponding to Pdr5 and the plasma membrane ATPase Pma1 are indicated. (B) Western blot detection of Pdr5 variants using a polyclonal α-Pdr5 antibody (top) or a α-penta His antibody (bottom).

which results in an increase in fluorescence. In parallel, we performed two control experiments. First, H_2O was added instead of glucose to exclude diffusion effects that would increase the fluorescence. Second, deletion strain Δ*pdr5* was used to demonstrate Pdr5-dependent R6G efflux. As shown in Figure 3A, the observed changes in fluorescence intensities detected for Δpdr5 cells and the H_2O controls were minimal and therefore negligible, compared to those derived from

dx.doi.org/10.1021/bi3015778 | *Biochemistry* 2013, 52, 2184−2195

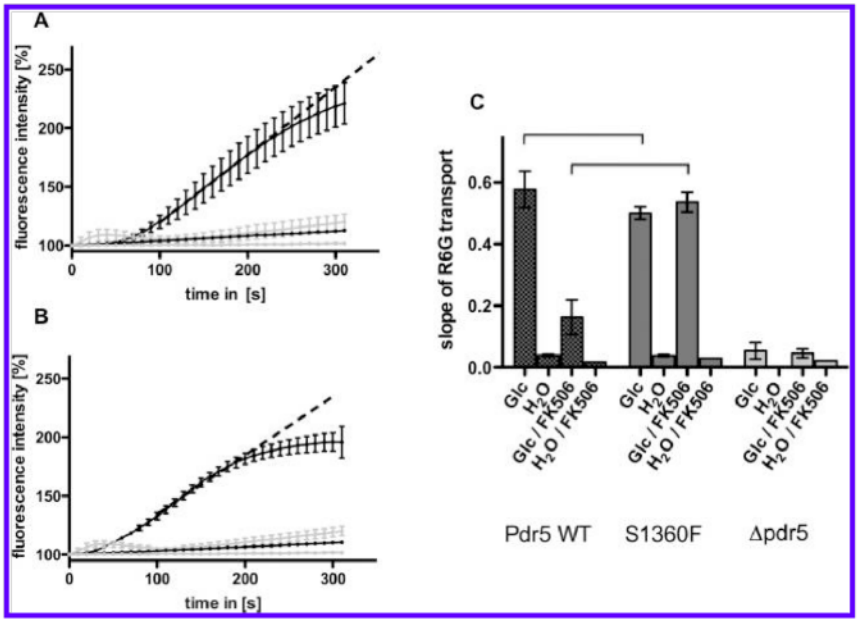

Figure 3. Whole cell drug transport. Cells were preloaded with 5 μM R6G with or without 25 μM FK506 under de-energizing conditions for 2.5 h. Twenty microliters of 1 M glucose (Glc) was added to re-energize the cells or 20 μL of H_2O as negative control at time zero. (A) Representative slope of increasing R6G fluorescence due to the export from Pdr5 WT-expressing cells after addition of glucose (■) or H_2O (□). (B) Representative slope of increasing R6G fluorescence due to the export from Pdr5 S1360F-expressing cells after addition of glucose (■) or H_2O (□). Cells lacking the *Pdr5* gene (Δ*pdr5*) were used as a negative control. Filled gray circles represent the data from the experiment conducted after energization with glucose and empty gray circles the data after addition of H_2O. (C) Rates corresponding to the slope of the linear region (dashed black line in panel A or B) of the fluorescence intensity trace. Mean values of at least three independent experiments are shown, and the error bars represent the SD.

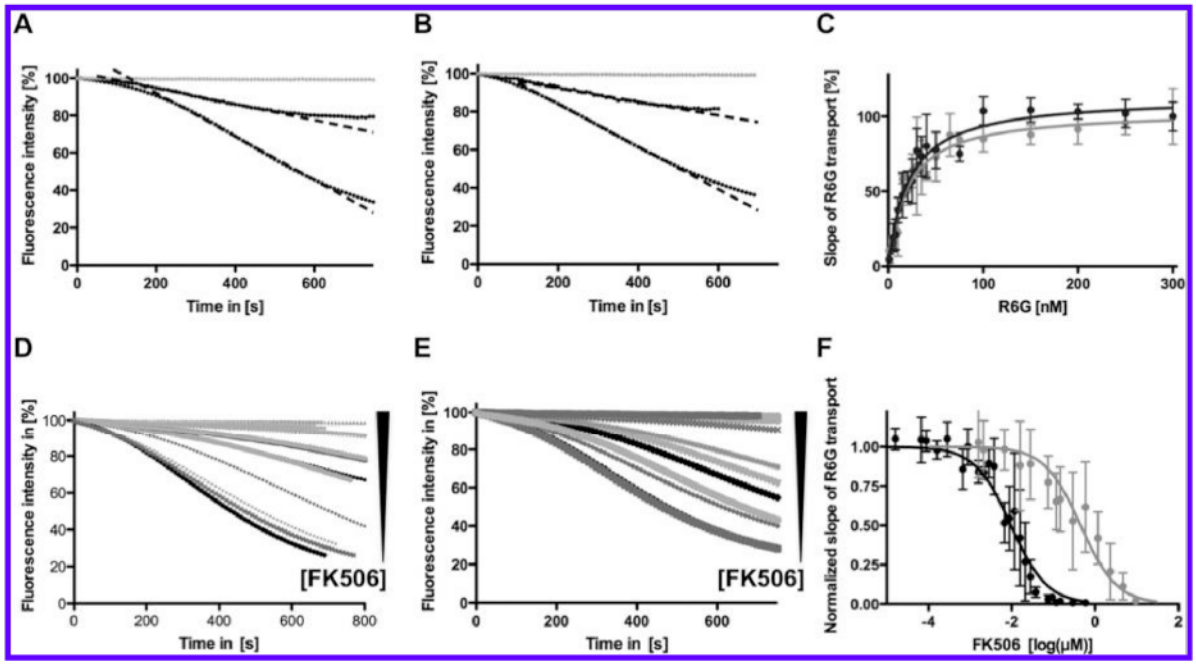

Figure 4. Kinetic characterization and inhibition of Pdr5-mediated R6G transport. (A–C) Plasma membrane preparations were incubated with different concentrations of R6G until a stable fluorescence signal was reached [roughly 300 s (trace not shown)], and the fluorescence intensity was normalized to 100%. At time zero, ATP was added. (A) Representative slopes of R6G quenching mediated by Pdr5 WT or S1360F (B) at 10 nM (top dashed line) and 300 nM R6G (bottom dashed line) as well as the negative control of plasma membrane preparations expressing no Pdr5 (gray lines) are shown. (C) Determination of K_m values for Pdr5 WT and the S1360F mutants. The rates corresponding to the linear part of the slopes for each R6G concentration were analyzed by nonlinear regression. The mean values ± SD of at least three independent experiments are plotted. (D–F) Plasma membrane preparations containing Pdr5 WT (D) or the S1360F mutant (E) were incubated with different FK506 concentrations (0–9.4 μM) in 300 nM R6G containing transport buffer prior to the addition of ATP (time zero). The recorded fluorescence intensity at time zero was normalized to 100%. (F) Analysis of the inhibitory effect of FK506 by nonlinear regression according to the general dose–response equation of R6G fluorescence quenching rates (eq 1). The derived IC_{50} values correspond to a 50% inhibition of the Pdr5-mediated R6G transport. The mean values ± SD of three to seven independent experiments are shown.

dx.doi.org/10.1021/bi3015778 | *Biochemistry* 2013, 52, 2184–2195

glucose-activated cells expressing either Pdr5 WT or the S1360F mutant (Figure 3A,B). This demonstrated that the observed R6G transport is Pdr5-dependent. To explore the impact of FK506, we determined the R6G transport rates of Pdr5 WT, the S1360F mutant, and the deletion strain in the presence and absence of FK506 under energized and de-energized conditions (Figure 3C). Transport rates in Pdr5 WT-expressing cells, which were preloaded with R6G, were reduced to 25% in the presence of FK506 as compared to the rates obtained in the absence of the immunosuppressant. An identical FK506 concentration did not affect the S1360F-mediated R6G export rate (Figure 3B,C).

To get a closer look at the mechanistic features of transport modulation by Pdr5 WT and the S1360F mutant and to test whether only structural features in the substrate-binding pocket caused the observed effect in the S1360F background, Pdr5-dependent transport of the fluorescent dye R6G was measured in isolated plasma membranes (see Experimental Procedures). Transport measurements were initiated by the addition of ATP/Mg^{2+} in the absence and presence of FK506. Here, the activation of the efflux pumps resulted in an R6G concentration-dependent formation of nonfluorescent excimers either by the redistribution of R6G within the two leaflets of the lipid bilayer in the plasma membranes or by the accumulation of R6G in inside-out plasma membrane vesicles.[38]

A comparison of the R6G transport efficiencies of Pdr5 WT and the S1360F mutant is presented in panels A and B of Figure 4 (for further details of data analysis, see Experimental Procedures). Control membranes of the deletion strain displayed no decrease in fluorescence intensity after addition of ATP. Analysis of the transport rates revealed identical Michaelis−Menten kinetics for both the wild type and the S1360F mutant (Table 1), although cells expressing the S1360F mutant exhibited an increased susceptibility to R6G compared to cells expressing Pdr5 WT in liquid cultures (data not shown) and on drug agar plates.[36] Both K_m values, for Pdr5 WT and the S1360F mutant, are in the low nanomolar range: K_m(Pdr5 WT) = 21 ± 3 nM, and K_m(S1360F) = 20 ± 3 nM (Figure 4C and Table 1). Thus, the introduction of the S1360F mutation had no apparent effect on R6G transport, suggesting that a mutation at position 1360 does not directly affect transport of this particular substrate.

As shown above, R6G transport kinetics are identical for Pdr5 WT and the S1360F mutant. However, the data derived from whole cell transport and resistance assays (Figure 3 and Figure S1 of the Supporting Information) demonstrated the abrogation of the inhibitory effect of FK506 on Pdr5-mediated R6G efflux in the background of the S1360F mutant. Therefore, we investigated R6G transport efficiencies of both the wild type and the S1360F mutant, in plasma membrane preparations in the presence of different FK506 concentrations. Already low concentrations of FK506 (0.075 μM) completely abolished R6G transport in Pdr5 WT-containing plasma membranes. In striking contrast, membranes containing Pdr5 S1360F still displayed around 40% transport activity compared to the fluorescence quenching rates in the absence of FK506. Determination of the IC_{50} values according to eq 1 revealed an almost 50-fold difference between Pdr5 WT (IC_{50} = 10 ± 0.1 nM) and the S1360F mutant (IC_{50} = 450 ± 80 nM) (Figure 4F and Table 1). Compared to whole cell transport measurements, efflux data obtained for plasma membrane preparations demonstrated that FK506 also influenced the transport efficiency of the S1360F mutant. Hence, the FK506 concentration used in the whole cell assay was not sufficient to cause an effect on the ability of the S1360F mutant to export R6G. Nevertheless, the derived transport data in plasma membrane preparations (Figure 4E,F) clearly displayed an involvement of FK506 in R6G transport modulation in the S1360F background. Most importantly, both transport assays confirmed that S1360F and Pdr5 WT display identical R6G transport parameters in the absence of FK506. Taken together, these results raised the question about the function of the S1360F mutation in FK506 transport modulation.

Cellular Transport of Radiolabeled FK506. Egner et al. suggested that FK506 might be a substrate of Pdr5.[36] Consistent with this interpretation, drug resistance assays performed in liquid cultures indicated no susceptibility of Pdr5 WT and the S1360F mutant to concentrations of FK506 of up to 100 μM (Figure S1A of the Supporting Information). To monitor whether FK506 is actively extruded by Pdr5, the cellular transport of FK506 was investigated by incubating yeast cells with ^{3}H-labeled FK506 (100 nM at a total FK506 concentration of 25 μM) under de-energizing conditions. The amount of radioactivity in the extracellular medium as well as accumulated in cells prior to glucose supplementation was determined. In parallel, the assay was performed with 2-deoxyglucose instead of glucose. Deletion strain Δ*pdr5* served again as a negative control. As shown in Figure 5, the amount of radioactivity detected in the extracellular medium for Pdr5 WT and the S1360F mutant cells was >30% higher than in the deletion strain. Under de-energized conditions, the radioactivity measured for both Pdr5 strains was even more than 2 times lower, whereas the radioactivity obtained for the deletion strain was only slightly reduced. In summary, these data demonstrated that Pdr5 actively exports FK506 and that FK506 is indeed a substrate of Pdr5.

Furthermore, the time dependencies of FK506 transport by Pdr5 WT and the S1360F mutant were determined to address the question of whether the observed inhibitory effect of FK506 on Pdr5-mediated R6G transport (Figures 3 and 4) might be due to changes in the overall transport efficiency. For this purpose, the efficiencies of transport of FK506 by Pdr5 WT and the S1360F mutant were compared at 25 μM FK506 (final concentration containing 100 nM ^{3}H-labeled FK506). This corresponds to the inhibitory conditions of R6G transport in whole yeast cells (see above). The time courses for Pdr5 WT- and S1360F-overexpressing cells were identical (Figure 5B, ii). Moreover, the application of drug at lower and higher concentrations led to comparable results for the time dependence of FK506 transport of both strains (Figure 5B, i−iv). The same held true for the slopes of Pdr5 WT- and S1360F-mediated FK506 transport. In addition, the susceptibility assays in liquid cultures with increasing FK506 concentrations revealed identical resistance patterns of both strains (Figure S1A of the Supporting Information). Taken together, these results demonstrated that Pdr5 WT and the S1360F mutant transport FK506 in a similar if not identical manner.

Pdr5-Specific ATPase Activity in the Presence of Drugs. The reported transport studies (Figures 3−5) prompted us to perform a thorough comparison of ATPase activities of Pdr5 WT and S1360F in the hope of obtaining a better mechanistic understanding of this mutation. Hence, the substrate-induced effects on the Pdr5-specific ATPase activity in the presence of R6G or FK506 were analyzed (Figure 6). Pdr5 WT[12] as well as the S1360F mutant displayed a high basal

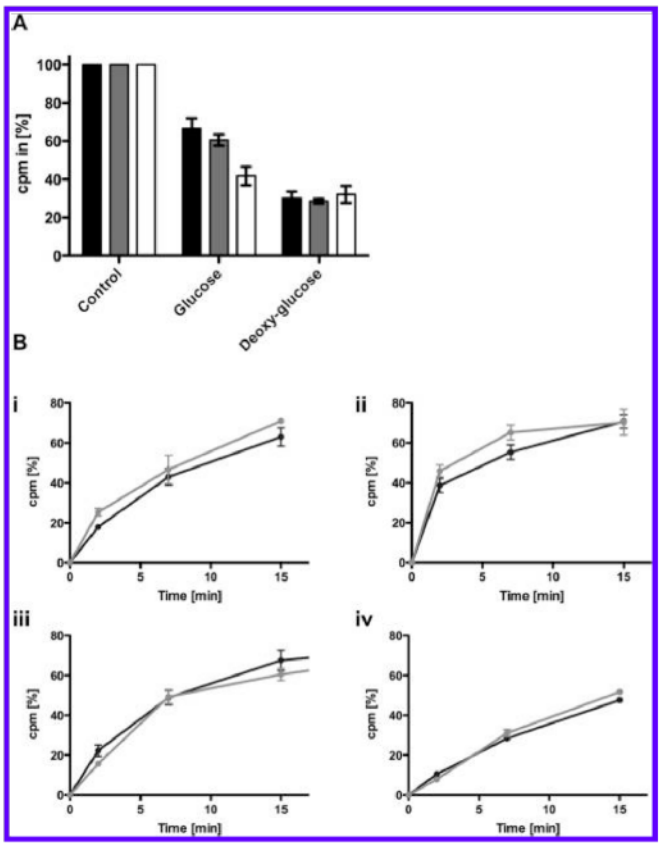

Figure 5. Cellular [^{3}H]FK506 transport. (A) Radioactive FK506 transport in yeast. Cells were incubated with 25 μM FK506 (100 nM [^{3}H]FK506) under de-energizing conditions for 2 h at 30 °C while being constantly shaken. One-third of the cells served as an internal control, and the radioactivity measured was set to 100%. The remaining two-thirds were split equally for transport measurements, and the reaction was started by the addition of 20 mM glucose or 5 mM 2-deoxyglucose as a negative control. The radioactivity in the supernatant was detected after incubation for 15 min at 30 °C and displayed for Pdr5 WT (black bars) or Pdr5 S1360F (gray bars) cells. Yeast cells expressing no Pdr5 (white bars) were used as a negative control in both experiments. The mean values ± SD of at least three independent experiments are shown. (B) Time dependencies of FK506 transport into the media by yeast cells overexpressing Pdr5 WT (gray circles) or S1360F (black circles). Cells were incubated with different FK506 concentrations under de-energizing conditions: (i) 0.25, (ii) 2.5, (iii) 25, and (iv) 40 μM FK506 (as described in Experimental Procedures). The amounts of radioactive FK506 detected in the media after incubation for various times prior to glucose addition were plotted as the fractions of total [^{3}H]FK506. The mean values ± SD of an average of four independent experiments are shown.

ATPase activity with an optimum around pH 9.5 with highly similar kinetics (data not shown). Pdr5, in contrast to many other ABC transporters, is a strictly uncoupled ABC transporter; i.e., its steady state ATPase activity cannot be stimulated by substrates.[12,49] In a previous study, we demonstrated that drugs can be categorized as inhibitory or noninhibitory drugs with respect to their capacity to inhibit ATPase activity at high substrate concentrations.[12] Indeed, in the presence of high concentrations of R6G, the ATPase activity of both Pdr5 variants could be inhibited, but a 2−3-fold higher concentration of R6G was required in the case of the S1360F mutant (Figure 6A). However, analysis of the FK506-mediated inhibition of the basal ATPase activity of both Pdr5 WT and the S1360F mutant revealed even more striking differences. To achieve 50% inhibition of the basal ATPase activity, 4.9 ± 0.4 μM FK506 was required in the case of the S1360F mutant, while 50% inhibition of Pdr5 WT ATPase was achieved when using only 0.05 ± 0.007 μM FK506. Thus, an almost 100-fold difference in the functional response of the S1360F mutant was observed (Figure 6B and Table 1).

Nucleotide Binding Properties. Drug translocation and transport modulation require an intense crosstalk between the TMDs and the allocation of energy in the NBDs.[23] An obvious prerequisite for energy allocation and coupling is the binding and hydrolysis of ATP as well as the subsequent release of ADP at the NBDs. In Pdr5, the S1360F mutation located in the TMD might induce alterations in the affinity of the NBDs for nucleotides in Pdr5 as described, for example, for mutations in P-gp.[23,50,51] Therefore, we analyzed the impact of the S1360F mutation on the nucleotide binding properties of Pdr5 WT and the S1360F mutation employing the photoactive nucleotide analogue [γ-^{32}P]-8-azido-ATP in the presence of increasing concentrations of nonlabeled ATP and ADP (Figure 7). The assay was performed at 4 °C to prevent ATP hydrolysis (see Experimental Procedures). Additional competition studies using varying ATP and ADP concentrations were performed with saturating concentrations of [γ-^{32}P]-8-azido-ATP (5 μM). An analysis of the dose-dependent displacement of [γ-^{32}P]-8-azido-ATP binding by ATP revealed similar potencies for Pdr5 WT (IC_{50} = 48 ± 7 μM) and the S1360F mutant (IC_{50} = 51 ± 5 μM), indicating identical binding affinities of ATP for both proteins within experimental error (Figure 7A and Table 1). Additionally, competition studies using ADP to displace the nucleotide analogue also showed no significant differences of the IC_{50} values within experimental error (IC_{50} values of 0.30 ± 0.06 mM for Pdr5 WT and 0.38 ± 0.07 mM for the S1360F mutant). In summary, the binding affinities of Pdr5 WT and the S1360F mutant for both ATP and ADP are identical, indicating that nucleotide binding is not affected by this mutation. Furthermore, the affinity of ATP for Pdr5 WT and the S1360F mutant (Figure S2 of the Supporting Information) was not influenced by increasing concentrations of FK506. These findings are in line with the results of Golin et al.[44] for clotrimazole, suggesting that the FK506-mediated inhibition of ATPase activity is not due to a direct competition between the nucleotide and FK506.

Inhibition Analysis of Pdr5 WT and the S1360F Mutant. All of the investigations presented so far revealed no obvious differences between Pdr5 WT and the S1360F mutation with respect to R6G transport or ATPase activity in the absence of FK506. In clear contrast, in the presence of FK506, R6G transport, binding of nucleotides, and the ATPase activity of Pdr5 WT and the S1360F mutant displayed profound differences (Table 1). To analyze the impact of the serine to phenylalanine mutation further, we determined the type of inhibition of FK506 for Pdr5 WT and the S1360F mutation (Figure 8). As a control, we used the well-known competitive inhibitor oligomycin.[38] The IC_{50} value determined under our experimental conditions (see Experimental Procedures) was identical within experimental error to that reported by Kolaczkowski (data not shown).[38] Lineweaver−Burk analysis of R6G transport inhibition by increasing concentrations of FK506 revealed enhanced apparent K_m values, implying that FK506 is a competitive inhibitor of both Pdr5 WT and the S1360F mutant (Figure 8). In other words, FK506 binds to the same substrate-binding site as R6G. However, the

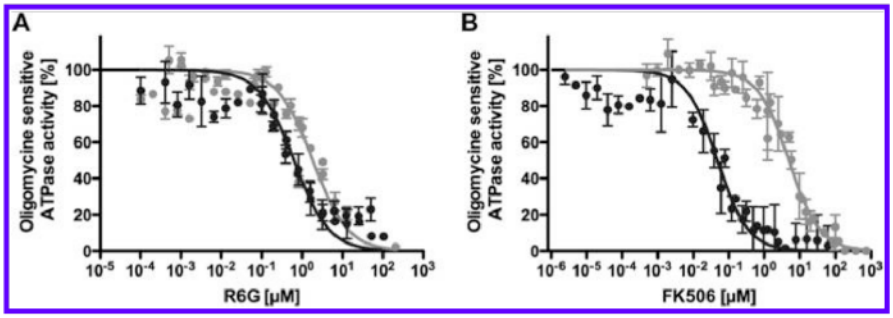

Figure 6. Concentration-dependent inhibition of Pdr5-specific ATPase activity by R6G and FK506. (A) R6G-mediated inhibition of Pdr5-specific ATPase activity of the wild type (black circles) or S1360F mutant (gray circles). (B) FK506-mediated inhibition of Pdr5-specific ATPase activity of the wild type (black circles) or S1360F mutant (gray circles). The mean values ± SD of three to seven independent experiments are shown. In both cases, the ATPase activity without added substrate was set to 100% and nonlinear regression of the data was performed according to eq 2.

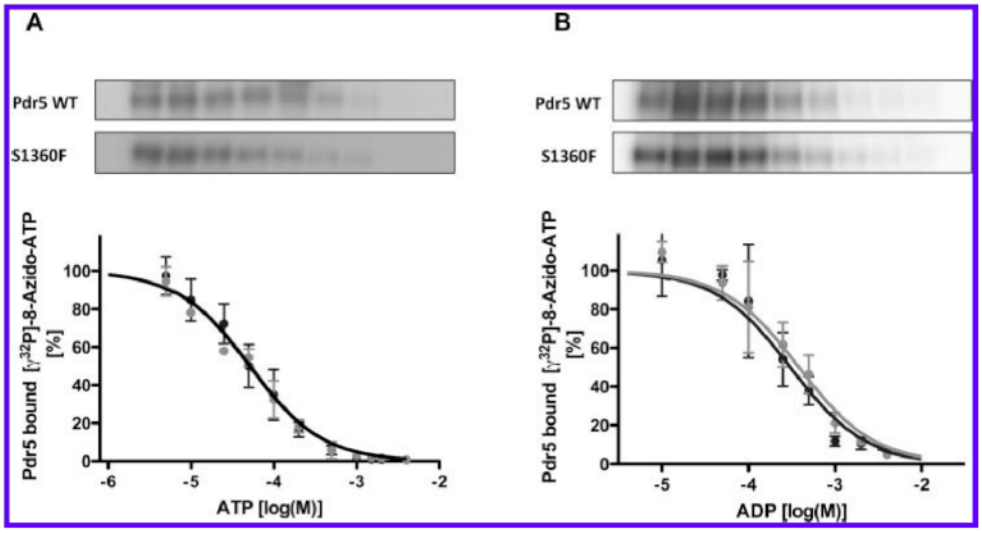

Figure 7. Nucleotide binding properties of Pdr5 and S1360F. Isolated plasma membranes of Pdr5 WT or the S1360F mutant were labeled with 5 μM [γ-^{32}P]-8-azido-ATP in the presence of nonlabeled nucleotides under nonhydrolyzing conditions as described in Experimental Procedures. (A) Displacement of [γ-^{32}P]-8-azido-ATP by increasing concentrations of ATP. The top panel shows two representative autoradiograms of Pdr5 WT or the S1360F mutant. The amount of radioactivity in the autoradiograms was analyzed by densitometry, and the extent of nucleotide binding in the absence of any nonlabeled nucleotide was set to 100%. The degree of labeling was analyzed by nonlinear regression using the general dose–response curve (eq 1). (B) Autoradiogram and analysis of the photolabeling of [γ-^{32}P]-8-azido-ATP in the presence of increasing concentrations of nonradioactive ADP for Pdr5 WT and the S1360F mutant (top). The densitometric analysis of the autoradiograms was plotted vs ATP concentration. Labeling was analyzed by nonlinear regression using the general dose–response curve (eq 1). Mean values ± SD of four independent experiments are shown for ATP or ADP displacement.

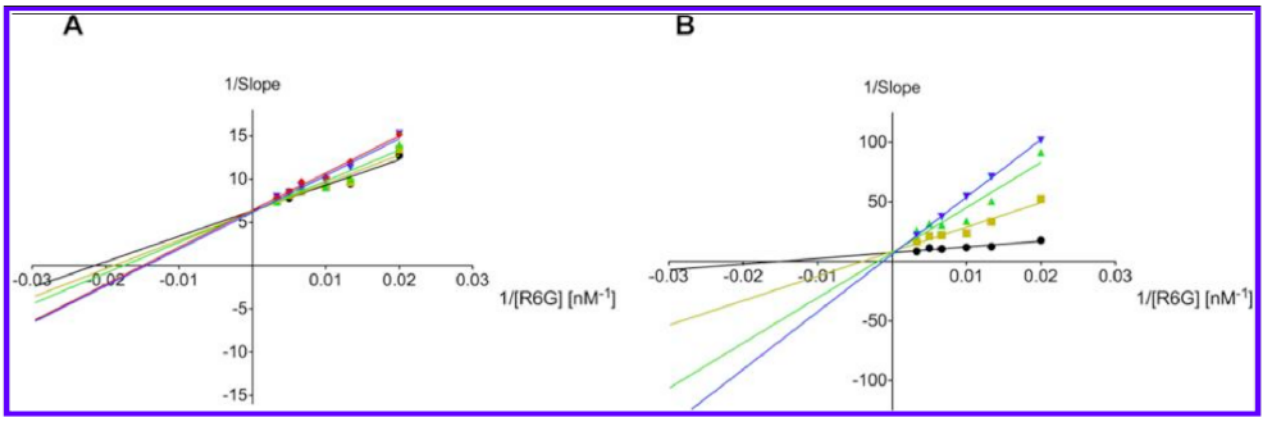

Figure 8. Inhibition of R6G transport by FK506. (A) Lineweaver–Burk analysis of R6G transport of Pdr5 WT in the presence of 0 (black), 2 (orange), 5 (green), 7.5 (blue), and 10 nM FK506 (red). (B) Lineweaver–Burk analysis of R6G transport of the S160F mutant in the presence of 0 (black), 250 (blue), 500 (green), and 750 nM FK506 (orange). Linear regression was performed using Prism version 5.0.

K_i of inhibition by FK506 increased 20-fold in the S1360F background (Table 1). This indicates that a single amino acid substitution substantially changed the nature of the substrate-binding site that R6G and FK506 occupy within Pdr5.

dx.doi.org/10.1021/bi3015778 | *Biochemistry* 2013, 52, 2184–2195

DISCUSSION

Pdr5 is the most abundant ABC transporter in yeast representing a relevant model system for fungal MDR ABC transporters. In this study, we focused on a detailed investigation of a certain mutation, S1360F, and its functional consequences for Pdr5. This missense mutation is located in putative transmembrane segment 11 (Figure 1), inside a region that displays a certain degree of conservation among fungal MDR ABC transporters from *S. cerevisiae* and *C. albicans* (Figure 1C). A specific role of the S1360F mutation in modulating antifungal resistance has been reported previously.[36,37] Substitutions of serine 1360 with different amino acids resulted in different phenotypes.[36] Interestingly, Pdr5 contains several unrelated binding sites as described by Golin et al.[52] that recognize, for instance, azoles or fluorescent dyes such as rhodamine.

In the yeast strain background used in this study, Pdr5 WT and the S1360F mutant are overexpressed to similar levels (Figure 2), allowing a quantitative comparison of the transport results (Figures 3−5), nucleotide binding, and ATPase activity measurements reported in this study. This permits a closer look at the functionality of Pdr5 WT and the S1360F mutant during the catalytic transport cycle. In addition to cell growth inhibition studies, the R6G transport data mediated by Pdr5 in vivo, especially the analysis of real-time R6G transport in vitro, demonstrated a large effect of FK506 on Pdr5's R6G transport rates (Figure 4D−F and Table 1). However, we demonstrated that the S1360F mutant displayed transport properties similar to those of Pdr5 WT in the absence of FK506. The analysis of the R6G quenching rates at different R6G concentrations revealed identical Michaelis−Menten kinetics for Pdr5 WT and the S1360F mutant with K_m values of ~20 nM (Figure 4A−C). This suggests that S1360F does not directly participate in R6G binding. On the other hand, K_i values for FK506-mediated R6G transport inhibition of both, Pdr5 WT and the S1360F mutant differed significantly, indicating that S1360F is involved in binding of this compound (Table 1). This observation is in contrast to, for example, the transmembrane mutation S558Y in putative transmembrane helix 2 within TMD 1 of Pdr5. Here, the mutation induced a hypersensitive towards cycloheximide without affecting ATPase activity.[45] Hence, one could argue that allosteric interactions caused by the binding of FK506 are responsible for the altered R6G transport in the S1360F mutant. Such communications between multiple binding and regulatory sites have been shown, for example, for human P-gp.[51,53]

The fact that FK506 is a substrate of Pdr5 is particularly important, because the underlying mechanism of the inhibitory effect of FK506 on MDR ABC transporters is still unclear. It was reported that FK506 serves as a substrate for human P-gp.[54] Yeast cell growth inhibition studies pointed toward a similar function for Pdr5,[36] and we could show that FK506 is indeed exported by Pdr5 in an ATP-dependent fashion (Figure 5). Subsequently, the evaluation of FK506 transport characteristics of yeast cells expressing either Pdr5 WT or the S1360F mutant revealed no significant differences (Figure 5B). This is supported by the observation of identical FK506 resistance patterns in liquid drug cultures (Figure S1 of the Supporting Information) and on drug agar plates.[36] Thus, the observed loss of the inhibitory effect in the S1360F mutant is apparently not caused by changes in any FK506 transport properties.

According to the generally accepted alternating access model,[55] the process of substrate recognition and transport by the TMDs is intimately connected with the catalytic cycle of the NBDs.[56] Thus, we determined whether the mutation causes any changes in the substrate-mediated inhibition of Pdr5-specific ATPase activity to investigate the functional relevance of the S1360F mutant involved in the catalytic translocation process. Although both Pdr5 proteins (WT and S1360F) displayed almost identical K_m and v_{max} values for basal ATPase activity (data not shown), a substantial shift in the FK506-mediated inhibition of the S1360F-derived ATPase activity was observed (Figure 6B and Table 1). The K_i values differed almost 100-fold. As energy allocation in the NBDs is thought to be tightly coupled to the corresponding conformational changes in the TMDs for substrate translocation, one could expect that drastic changes in ATPase activity in the presence of a substrate are reflected in its transport properties.[12] However, in the case of FK506, such an effect was not detected. Pdr5 as well as the S1360F mutant displayed similar FK506 transport properties and susceptibilities (Figure 5B and Figure S1 of the Supporting Information), although the FK506 concentrations used exceeded the inhibitory drug concentration for Pdr5-specific ATPase activity. This observation was made on the basis of the experimental setup. While ATPase activities are measured in isolated plasma membrane preparations, radiolabeled FK506 transport is measured in whole cells, requiring much higher drug concentrations to overcome the protection barriers of the cells as well as to saturate the intracellular membranous compartments (e.g., the vacuole) that drastically lower the concentration of effectively available FK506.

In addition, displacement studies of [γ-^{32}P]-8-azido-ATP with ATP and ADP demonstrated identical nucleotide binding affinities for Pdr5 and the S1360F mutant under non-hydrolyzable conditions (Figure 7 and Table 1). Thus, changed binding affinities for these nucleotides cannot explain the observed shift in the FK506-mediated inhibition of ATPase activity between Pdr5 WT and the S1360F mutant.

However, the results obtained from liquid drug resistance assays (Figure S1 of the Supporting Information) as well as R6G transport measurements clearly demonstrated the ability of the S1360F mutation to overcome the inhibitory effect of FK506 in the presence of other substrates such as KA, FA, or R6G (Figure S1 of the Supporting Information). Moreover, the shifts in IC_{50} values to higher concentrations, as observed in both FK506-mediated ATPase and R6G transport inhibition, point to a specific role of this residue in FK506−PDR5 interactions (Figures 4F and 6B).

Further analysis revealed that FK506 is a competitive inhibitor of R6G transport in both Pdr5 WT and the S1360F mutant (Figure 8). This suggests that R6G and FK506 compete for the same binding site in Pdr5. Because R6G transport and ATPase inhibition are highly similar in the absence of FK506 for Pdr5 and the S1360F mutant (Figures 4C and 6A), these results delineate a sensory function of the S1360F mutation in FK506 transport modulation. The determined K_i of R6G transport inhibition by FK506 differed by a factor of 25 between Pdr5 WT and the S1360F mutant. The K_i of ATPase activity in the presence of FK506, however, displayed a 100-fold difference (Table 1). These significant differences lead to two conclusions. First, the affinity of Pdr5 for FK506 is increased in the S1360F background in the presence of R6G. Second and even more intriguing, the mutation actively modulates TMD−NBD communication with a pronounced effect on ATPase

activity. Because transmembrane helix 11, which harbors position 1360, is located downstream of the proposed second coupling helix observed in the crystal structure of Sav1866, such a scenario is plausible.

The identification of functionally relevant interaction partners such as amino acid residues or modulators represents an important step in elucidating the underlying mechanisms of MDR ABC transporters.[12,23,43,45] Work of Callaghan and co-workers supports the assumption that drug binding is communicated to the NBDs via distinct pathways, corroborated by an analysis of cysteine mutants in transmembrane helices 6 and 12 in P-gp.[23,43] In support of this, a modulatory communication between FK506 and the NBDs is conferred by serine 1360 and is evident by the different degree of inhibition of the ATPase activity and transport (Figures 6B and 8). In contrast to Pdr5 WT, the S1360F mutant senses the presence of FK506 differently, resulting in a stable ATPase activity as well as R6G transport, inhibition of which required larger amounts of FK506 (Figures 4F and 8). As stated above, serine 1360 is located at the interface of several potential binding sites within Pdr5,[36] of which at least three were postulated.[19,52] However, because the transport properties of Pdr5 WT and the S1360F mutant are identical (Figures 3C, 4C, and 5) and the analysis of nucleotide binding affinities showed no differences implying similar binding, hydrolysis, and release characteristics, we assume that besides thermodynamic substrate− and nucleotide−protein interactions the sensory effect of the S1360F mutation is caused by changed interprotein communications as proposed recently in the kinetic selection model.[13]

In summary, the data presented here show that a single amino acid exchange in one of the TMDs of Pdr5, S1360, has a drastic effect on substrate recognition and transport modulation by FK506. In terms of selection and transport of several substrates, this observed effect could be attributed to changes in the crosstalk of the TMDs with the NBDs and vice versa.

■ ASSOCIATED CONTENT

Supporting Information

Liquid drug resistance assays of Pdr5 WT and the S1306F mutant (Figure S1) and nucleotide binding in the absence or presence of FK506 of Pdr5 WT and the S1306F mutant (Figure S2). This material is available free of charge via the Internet at http://pubs.acs.org.

■ AUTHOR INFORMATION

Corresponding Author

*Institute of Biochemistry, Heinrich Heine University Duesseldorf, Universitaetsstr. 1, 40225 Duesseldorf, Germany. Phone: +49-211-81-10773. E-mail: lutz.schmitt@hhu.de.

Present Address

†J.S.: Clinic for Gasteroenterology, Hepatology and Infectiology, University Hospital Duesseldorf, Heinrich Heine University Duesseldorf, Moorenstr. 5, 40225 Duesseldorf, Germany.

Funding

This work was supported by the DFG (Grants Schm 1279/5-3 and SFB 575 Project A9) to L.S.

Notes

The authors declare no competing financial interest.

■ ACKNOWLEDGMENTS

We are indebted to Robert Ernst for essential support during the project and Karl Kuchler for stimulating discussions. We also thank Norman Nebendorf, Melanie Seidemann, Nils Hanekop, and Nacera Infed for initial support of the project and many discussions.

■ ABBREVIATIONS

ABC, ATP-binding cassette; FA, fluconazole; KA, ketoconazole; MDR, multidrug resistance; NBD, nucleotide-binding domain; OM, oligomycin; PDR, pleiotropic drug resistance; P-gp, P-glycoprotein; R6G, rhodamine 6G; SD, standard deviation; TMD, transmembrane domain.

■ REFERENCES

(1) Taubes, G. (2008) The bacteria fight back. *Science 321*, 356−361.

(2) Szakacs, G., Paterson, J. K., Ludwig, J. A., Booth-Genthe, C., and Gottesman, M. M. (2006) Targeting multidrug resistance in cancer. *Nat. Rev. Drug Discovery 5*, 219−234.

(3) Thomas, H., and Coley, H. M. (2003) Overcoming multidrug resistance in cancer: An update on the clinical strategy of inhibiting p-glycoprotein. *Cancer Control 10*, 159−165.

(4) Ernst, R., Klemm, R., Schmitt, L., and Kuchler, K. (2005) Yeast ATP-binding cassette transporters: Cellular cleaning pumps. *Methods Enzymol. 400*, 460−484.

(5) Cannon, R. D., Lamping, E., Holmes, A. R., Niimi, K., Baret, P. V., Keniya, M. V., Tanabe, K., Niimi, M., Goffeau, A., and Monk, B. C. (2009) Efflux-mediated antifungal drug resistance. *Clin. Microbiol. Rev. 22*, 291−321.

(6) Sanglard, D. (2002) Resistance of human fungal pathogens to antifungal drugs. *Curr. Opin. Microbiol. 5*, 379−385.

(7) Oswald, C., Holland, I. B., and Schmitt, L. (2006) The motor domains of ABC-transporters. What can structures tell us? *Naunyn-Schmiedeberg's Arch. Pharmacol. 372*, 385−399.

(8) Schmitt, L., and Tampe, R. (2002) Structure and mechanism of ABC transporters. *Curr. Opin. Struct. Biol. 12*, 754−760.

(9) Higgins, C. F., and Linton, K. J. (2004) The ATP switch model for ABC transporters. *Nat. Struct. Mol. Biol. 11*, 918−926.

(10) Crowley, E., and Callaghan, R. (2010) Multidrug efflux pumps: Drug binding—gates or cavity? *FEBS J. 277*, 530−539.

(11) Egner, R., Rosenthal, F. E., Kralli, A., Sanglard, D., and Kuchler, K. (1998) Genetic separation of FK506 susceptibility and drug transport in the yeast Pdr5 ATP-binding cassette multidrug resistance transporter. *Mol. Biol. Cell 9*, 523−543.

(12) Ernst, R., Kueppers, P., Klein, C. M., Schwarzmueller, T., Kuchler, K., and Schmitt, L. (2008) A mutation of the H-loop selectively affects rhodamine transport by the yeast multidrug ABC transporter Pdr5. *Proc. Natl. Acad. Sci. U.S.A. 105*, 5069−5074.

(13) Ernst, R., Kueppers, P., Stindt, J., Kuchler, K., and Schmitt, L. (2010) Multidrug efflux pumps: Substrate selection in ATP-binding cassette multidrug efflux pumps—first come, first served? *FEBS J. 277*, 540−549.

(14) Gottesman, M. M., Hrycyna, C. A., Schoenlein, P. V., Germann, U. A., and Pastan, I. (1995) Genetic analysis of the multidrug transporter. *Annu. Rev. Genet. 29*, 607−649.

(15) Kane, S. E. (1996) *Multidrug resistance of cancer cells*, Vol. *28*, pp 181−252, Academic Press, San Diego.

(16) Loo, T. W., Bartlett, M. C., and Clarke, D. M. (2004) Disulfide cross-linking analysis shows that transmembrane segments 5 and 8 of human P-glycoprotein are close together on the cytoplasmic side of the membrane. *J. Biol. Chem. 279*, 7692−7697.

(17) Loo, T. W., and Clarke, D. M. (1999) Determining the structure and mechanism of the human multidrug resistance P-glycoprotein using cysteine-scanning mutagenesis and thiol-modification techniques. *Biochim. Biophys. Acta 1461*, 315−325.

(18) Loo, T. W., and Clarke, D. M. (2000) The packing of the transmembrane segments of human multidrug resistance P-glyco-

protein is revealed by disulfide cross-linking analysis. *J. Biol. Chem. 275*, 5253−5256.
(19) Golin, J., Ambudkar, S. V., Gottesman, M. M., Habib, A. D., Sczepanski, J., Ziccardi, W., and May, L. (2003) Studies with novel Pdr5p substrates demonstrate a strong size dependence for xenobiotic efflux. *J. Biol. Chem. 278*, 5963−5969.
(20) Golin, J., Barkatt, A., Cronin, S., Eng, G., and May, L. (2000) Chemical specificity of the PDR5 multidrug resistance gene product of *Saccharomyces cerevisiae* based on studies with tri-n-alkyltin chlorides. *Antimicrob. Agents Chemother. 44*, 134−138.
(21) Aller, S. G., Yu, J., Ward, A., Weng, Y., Chittaboina, S., Zhuo, R., Harrell, P. M., Trinh, Y. T., Zhang, Q., Urbatsch, I. L., and Chang, G. (2009) Structure of P-glycoprotein reveals a molecular basis for poly-specific drug binding. *Science 323*, 1718−1722.
(22) Ueda, K., Taguchi, Y., and Morishima, M. (1997) How does P-glycoprotein recognize its substrates? *Semin. Cancer Biol. 8*, 151−159.
(23) Crowley, E., O'Mara, M. L., Reynolds, C., Tieleman, D. P., Storm, J., Kerr, I. D., and Callaghan, R. (2009) Transmembrane helix 12 modulates progression of the ATP catalytic cycle in ABCB1. *Biochemistry 48*, 6249−6258.
(24) Crowley, E., McDevitt, C. A., and Callaghan, R. (2010) Generating inhibitors of P-glycoprotein: Where to, now? *Methods Mol. Biol. 596*, 405−432.
(25) Rutledge, R. M., Esser, L., Ma, J., and Xia, D. (2011) Toward understanding the mechanism of action of the yeast multidrug resistance transporter Pdr5p: A molecular modeling study. *J. Struct. Biol. 173*, 333−344.
(26) Pfaller, M. A., and Diekema, D. J. (2007) Epidemiology of invasive candidiasis: A persistent public health problem. *Clin. Microbiol. Rev. 20*, 133−163.
(27) McDevitt, C. A., Crowley, E., Hobbs, G., Starr, K. J., Kerr, I. D., and Callaghan, R. (2008) Is ATP binding responsible for initiating drug translocation by the multidrug transporter ABCG2? *FEBS J. 275*, 4354−4362.
(28) Demeule, M., Wenger, R. M., and Beliveau, R. (1997) Molecular interactions of cyclosporin A with P-glycoprotein. Photolabeling with cyclosporin derivatives. *J. Biol. Chem. 272*, 6647−6652.
(29) Hiraga, K., Yamamoto, S., Fukuda, H., Hamanaka, N., and Oda, K. (2005) Enniatin has a new function as an inhibitor of Pdr5p, one of the ABC transporters in *Saccharomyces cerevisiae*. *Biochem. Biophys. Res. Commun. 328*, 1119−1125.
(30) Holmes, A. R., Lin, Y. H., Niimi, K., Lamping, E., Keniya, M., Niimi, M., Tanabe, K., Monk, B. C., and Cannon, R. D. (2008) ABC transporter Cdr1p contributes more than Cdr2p does to fluconazole efflux in fluconazole-resistant *Candida albicans* clinical isolates. *Antimicrob. Agents Chemother. 52*, 3851−3862.
(31) Chearwae, W., Anuchapreeda, S., Nandigama, K., Ambudkar, S. V., and Limtrakul, P. (2004) Biochemical mechanism of modulation of human P-glycoprotein (ABCB1) by curcumin I, II, and III purified from turmeric powder. *Biochem. Pharmacol. 68*, 2043−2052.
(32) Chearwae, W., Shukla, S., Limtrakul, P., and Ambudkar, S. V. (2006) Modulation of the function of the multidrug resistance-linked ATP-binding cassette transporter ABCG2 by the cancer chemo-preventive agent curcumin. *Mol. Cancer Ther. 5*, 1995−2006.
(33) Liu, J., Farmer, J. D., Jr., Lane, W. S., Friedman, J., Weissman, I., and Schreiber, S. L. (1991) Calcineurin is a common target of cyclophilin-cyclosporin A and FKBP-FK506 complexes. *Cell 66*, 807−815.
(34) Foor, F., Parent, S. A., Morin, N., Dahl, A. M., Ramadan, N., Chrebet, G., Bostian, K. A., and Nielsen, J. B. (1992) Calcineurin mediates inhibition by FK506 and cyclosporin of recovery from α-factor arrest in yeast. *Nature 360*, 682−684.
(35) Kralli, A., and Yamamoto, K. R. (1996) An FK506-sensitive transporter selectively decreases intracellular levels and potency of steroid hormones. *J. Biol. Chem. 271*, 17152−17156.
(36) Egner, R., Bauer, B. E., and Kuchler, K. (2000) The transmembrane domain 10 of the yeast Pdr5p ABC antifungal efflux pump determines both substrate specificity and inhibitor susceptibility. *Mol. Microbiol. 35*, 1255−1263.
(37) Sanglard, D., Kuchler, K., Ischer, F., Pagani, J. L., Monod, M., and Bille, J. (1995) Mechanisms of resistance to azole antifungal agents in *Candida albicans* isolates from AIDS patients involve specific multidrug transporters. *Antimicrob. Agents Chemother. 39*, 2378−2386.
(38) Kolaczkowski, M., van der Rest, M., Cybularz-Kolaczkowska, A., Soumillion, J. P., Konings, W. N., and Goffeau, A. (1996) Anticancer drugs, ionophoric peptides, and steroids as substrates of the yeast multidrug transporter Pdr5p. *J. Biol. Chem. 271*, 31543−31548.
(39) Mahe, Y., Lemoine, Y., and Kuchler, K. (1996) The ATP binding cassette transporters Pdr5 and Snq2 of *Saccharomyces cerevisiae* can mediate transport of steroids in vivo. *J. Biol. Chem. 271*, 25167−25172.
(40) Decottignies, A., Kolaczkowski, M., Balzi, E., and Goffeau, A. (1994) Solubilization and characterization of the overexpressed PDR5 multidrug resistance nucleotide triphosphatase of yeast. *J. Biol. Chem. 269*, 12797−12803.
(41) Goffeau, A., and Dufour, J. P. (1988) Plasma membrane ATPase from the yeast *Saccharomyces cerevisiae*. *Methods Enzymol. 157*, 528−533.
(42) Wada, S., Niimi, M., Niimi, K., Holmes, A. R., Monk, B. C., Cannon, R. D., and Uehara, Y. (2002) *Candida glabrata* ATP-binding cassette transporters Cdr1p and Pdh1p expressed in a *Saccharomyces cerevisiae* strain deficient in membrane transporters show phosphorylation-dependent pumping properties. *J. Biol. Chem. 277*, 46809−46821.
(43) Storm, J., O'Mara, M. L., Crowley, E. H., Peall, J., Tieleman, D. P., Kerr, I. D., and Callaghan, R. (2007) Residue G346 in transmembrane segment six is involved in inter-domain communication in P-glycoprotein. *Biochemistry 46*, 9899−9910.
(44) Golin, J., Kon, Z. N., Wu, C. P., Martello, J., Hanson, L., Supernavage, S., Ambudkar, S. V., and Sauna, Z. E. (2007) Complete inhibition of the Pdr5p multidrug efflux pump ATPase activity by its transport substrate clotrimazole suggests that GTP as well as ATP may be used as an energy source. *Biochemistry 46*, 13109−13119.
(45) Sauna, Z. E., Bohn, S. S., Rutledge, R., Dougherty, M. P., Cronin, S., May, L., Xia, D., Ambudkar, S. V., and Golin, J. (2008) Mutations define cross-talk between the N-terminal nucleotide-binding domain and transmembrane helix-2 of the yeast multidrug transporter Pdr5: Possible conservation of a signaling interface for coupling ATP hydrolysis to drug transport. *J. Biol. Chem. 283*, 35010−35022.
(46) Schuetzer-Muehlbauer, M., Willinger, B., Egner, R., Ecker, G., and Kuchler, K. (2003) Reversal of antifungal resistance mediated by ABC efflux pumps from *Candida albicans* functionally expressed in yeast. *Int. J. Antimicrob. Agents 22*, 291−300.
(47) Dawson, R. J., and Locher, K. P. (2006) Structure of a bacterial multidrug ABC transporter. *Nature 443*, 180−185.
(48) Saini, P., Prasad, T., Gaur, N. A., Shukla, S., Jha, S., Komath, S. S., Khan, L. A., Haq, Q. M., and Prasad, R. (2005) Alanine scanning of transmembrane helix 11 of Cdr1p ABC antifungal efflux pump of *Candida albicans*: Identification of amino acid residues critical for drug efflux. *J. Antimicrob. Chemother. 56*, 77−86.
(49) Shukla, S., Rai, V., Banerjee, D., and Prasad, R. (2006) Characterization of Cdr1p, a major multidrug efflux protein of *Candida albicans*: Purified protein is amenable to intrinsic fluorescence analysis. *Biochemistry 45*, 2425−2435.
(50) Song, J., and Melera, P. W. (2001) Further characterization of the sixth transmembrane domain of Pgp1 by site-directed mutagenesis. *Cancer Chemother. Pharmacol. 48*, 339−346.
(51) Martin, C., Berridge, G., Mistry, P., Higgins, C., Charlton, P., and Callaghan, R. (2000) Drug binding sites on P-glycoprotein are altered by ATP binding prior to nucleotide hydrolysis. *Biochemistry 39*, 11901−11906.
(52) Golin, J., Ambudkar, S. V., and May, L. (2007) The yeast Pdr5p multidrug transporter: How does it recognize so many substrates? *Biochem. Biophys. Res. Commun. 356*, 1−5.
(53) Martin, C., Berridge, G., Higgins, C. F., Mistry, P., Charlton, P., and Callaghan, R. (2000) Communication between multiple drug binding sites on P-glycoprotein. *Mol. Pharmacol. 58*, 624−632.

(54) Saeki, T., Ueda, K., Tanigawara, Y., Hori, R., and Komano, T. (1993) Human P-glycoprotein transports cyclosporin A and FK506. *J. Biol. Chem. 268*, 6077−6080.
(55) Jardetzky, O. (1966) Simple allosteric model for membrane pumps. *Nature 211*, 969−970.
(56) Linton, K. J. (2007) Structure and function of ABC transporters. *Physiology 22*, 122−130.

Supplementary Material

Figure S1:

Liquid drug resistance assay

Drug susceptibility of yeast cells expressing Pdr5 WT (black line), no Pdr5 (*ΔPdr5*, dashed grey line*)* and the S1360F mutant (grey line) towards different drugs. The microdilution method was performed as described in Experimental Procedures. (**A**) Susceptibility towards increasing FK506 concentrations. The optical density OD_{600} of each well on the microtiter plate was determined after incubation for 48h at 30°C and plotted against the corresponding FK506 concentration. (**B - D**) Drug resistance pattern towards different substrates in the presence of FK506. (**B**) Fluconazole (41,8 µM), (**C**) Ketoconazole (1,5 µM) and (**D**) R6G (15,7 µM) in the presence of increasing FK506 concentrations.

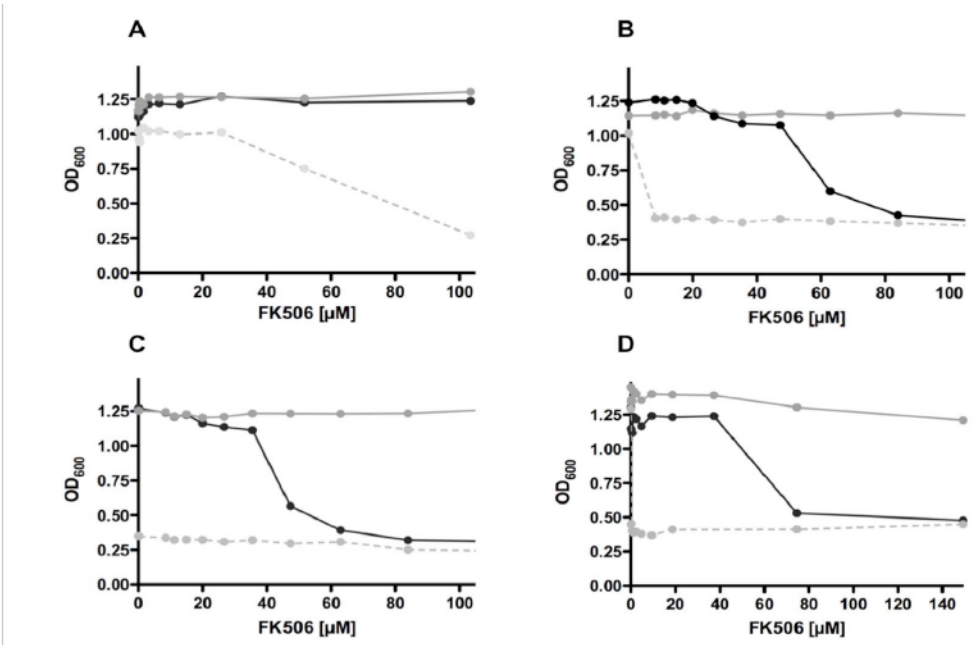

Figure S2:

FK506 does not interfere with ATP binding.

Isolated plasma membranes of Pdr5 WT (A) or the S1360F mutant (B) were labeled with 5 µM [α- or γ-^{32}P]-8-azido-ATP in the presence or the absence of non-labeled nucleotides and FK506 under non-hydrolyzing conditions as described in Experimental Procedures. The upper lanes show autoradiograms after cross-linking of γ-^{32}P- or α-^{32}P-8-azido-ATP to Pdr5 WT (A) and the S1360F mutant (B), while the lower panel displays a representative silver-stained SDS-PAGE analysis of one of the experiments of the upper panel. The positions of Pdr5 and Pma1 are indicated. Densitometric analysis of the autoradiograms and correlation to the amount of protein used in the individual experiments did not show any influence of FK506 on the binding of ATP.

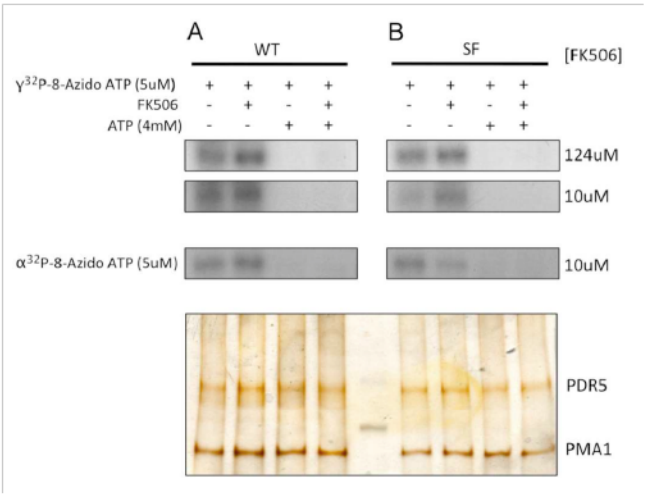

Proportionate work on the manuscript: 30%

Journal: Biochemistry

Impact factor: 3.377

Publication IV

Biol. Chem., Vol. 392, pp. 53–60, January/February 2011 • Copyright © by Walter de Gruyter • Berlin • New York. DOI 10.1515/BC.2011.011

Review

The multidrug transporter Pdr5: a molecular diode?

Rakeshkumar P. Gupta, Petra Kueppers, Lutz Schmitt* and Robert Ernst*,[a]

Institute of Biochemistry, Heinrich Heine University, Universitätsstr. 1, D-40225 Düsseldorf, Germany

*Corresponding authors
e-mail: lutz.schmitt@uni-duesseldorf.de; rernst@mpi-cbg.de

Abstract

A subset of the family of ATP-binding cassette (ABC) transporters has been in focus owing to their involvement in conferring multidrug resistance in cancer cells and among immune compromised individuals. *Saccharomyces cerevisiae* is protected against xenobiotics by similar machineries that are part of the pleitropic drug resistance (PDR) network. The ABC transporter Pdr5 is an important member of this PDR network in yeast and is involved in cellular detoxification by the efflux of a wide variety of drugs and substrates. In this review, we focus on the aspects of detergent effects and the degeneracy in conserved sequences that is observed in the nucleotide binding domains of Pdr5 and discuss their functional relevance.

Keywords: ABC transporter; kinetic substrate selection; molecular diode; multidrug resistance; P-glycoprotein (P-gp); Pdr5; transinhibition.

Introduction

ATP-binding cassette transporters (ABC transporters) are ubiquitous ATP-dependent transmembrane pumps, receptors or ion channels that are found in all three kingdoms of life and can be categorized in three distinct classes (for details see Davidson et al., 2008). Although highly diverse with regard to their individual transport substrates and their transport directionality, all members of this family are thought to share a common four-domain architecture, which consists of two transmembrane domains (TMDs) and two nucleotide binding domains (NBDs) or ABC domains (Schmitt and Tampé, 2002; Linton, 2007). The NBDs contain all diagnostic sequence motifs, the Walker A and B motifs, the H-loop as well as C-loop (LSGGQ motif), which is the hallmark of ABC transporters (Hanekop et al., 2006).

The NBDs can be regarded as molecular motors that transform chemical energy in mechanical work. Binding and hydrolysis of ATP (or other nucleotides) are coupled to conformational changes of the TMDs that bind and translocate the substrates. Analogously to the 'two side access' model proposed in 1966 for secondary transporters (Jardetzky, 1966), ABC transporters also continuously switch back and forth between two conformations that are accessible only from one side of the membrane at a time. In the case of ABC multidrug exporters, the inward-facing conformation (accessible from the cytosol or cytosolic membrane leaflet) is thought to have a higher affinity to the substrate than the outward-facing conformation from which the substrates are released to the surroundings (Figure 1A).

Because of their clinical importance, one of the most fascinating classes of ABC transporters is involved in the phenomenon of multidrug resistance (MDR) (Seeger and van Veen, 2009; Callaghan, 2010).

In the past decades, MDR and pleiotropic drug resistance (PDR), which are functionally similar, have become a major obstacle for the treatment of cancer, bacterial and fungal infections (Szakacs et al., 2006; Monk and Goffeau, 2008; Taubes, 2008). One of the principle mechanisms of PDR is related to membrane transport processes (Putman et al., 2000). Here, the efflux of a multiplicity of structurally unrelated cytotoxic compounds is dramatically increased owing to the (over)expression of membrane transporters such as ABC transporters. In the PDR network of *Saccharomyces cerevisiae*, secondary transporters of the MFS family (Monk and Goffeau, 2008; Cannon et al., 2009) and ABC exporters localized in the plasma membrane serve together as a first line of defense against cytotoxic compounds (Ernst et al., 2005). In this review, we will discuss possible mechanisms of substrate selection and directed transport, address an issue that one faces when studying MDR transporters in detergent solution, and elaborate on the putative role of transporter asymmetry and sequence degeneration.

Pdr5: our model

Pdr5 is one of the most extensively studied ABC transporters from *S. cerevisiae* and among the most abundant plasma membrane proteins, with a reported number of approximately 42 000 molecules per exponentially growing cell (Ghaemmaghami et al., 2003). The NBDs and TMDs of Pdr5 are fused in a 'reverse' manner, yielding a full-size transporter with $(NBD\text{-}TMD)_2$ topology. PDR5 was discovered as a gene responsible for cycloheximide, mycotoxin and cerulin resistance (Balzi et al., 1994; Bissinger and Kuchler, 1994; Hirata et al., 1994) and its gene product was later shown to

[a]Present address: Max Planck Institute for Molecular Cell Biology and Genetics, Pfotenhauerstrasse 108, D-01307 Dresden, Germany.

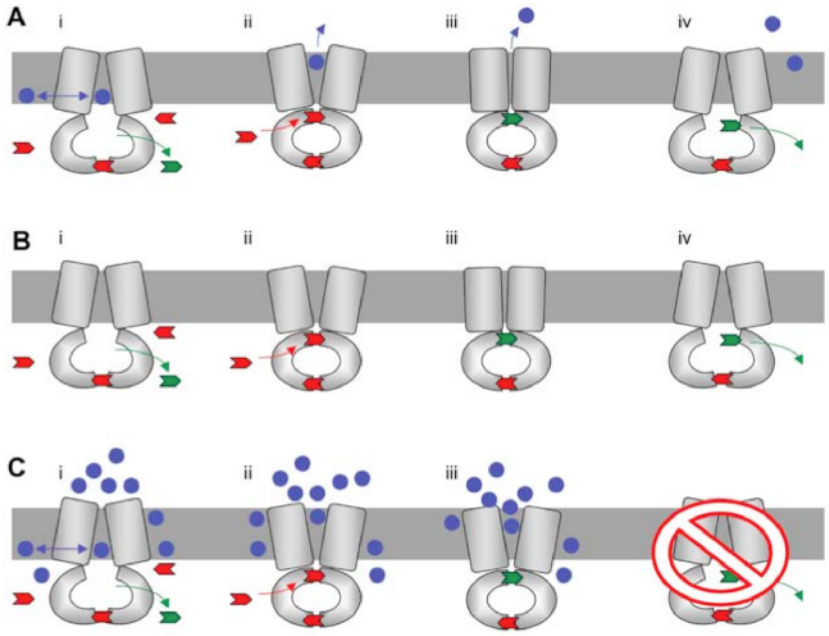

Figure 1 A transport model for Pdr5.
(A) A normal transport cycle. (i) In the resting state, one ATP molecule (red) is tightly bound to the NBD1 composite site. Exchange of nucleotides (red and green) at the NBD2 composite site occurs simultaneously with substrate (blue) binding at the inward-facing substrate binding region of the TMDs. The time of substrate equilibration with the transporter might impact on the substrate selection (Ernst et al., 2010). The second ATP molecule remains bound in the drawing because hydrolysis is drastically impaired and probably does not occur on the timescale of transport. (ii) Upon binding of ATP, the NBDs dimerizes tightly and the TMDs switch from the inward- to the outward-facing conformation. Substrate release might occur immediately. (iii) ATP hydrolysis at the NBD2 composite site and/or substrate release results in remodeling of the TMDs and the substrate affinity is reduced. We hypothesize that at the same time the volume of the outward-facing substrate binding region is reduced as illustrated by the movement of the TMDs. (iv) The destabilized NBD dimer dissociates and allows for nucleotide release from the NBD2 composite site. Simultaneously, the transporter flips back to the inward-facing conformation to start a new transport cycle. (B) Basal ATPase activity and a 'futile' transport cycle. Even in the absence of substrates, the transporter cycles through the substeps (i), (ii), (iii) and (iv). ATP hydrolysis is uncoupled from substrate transport. (C) Transinhibition of Pdr5. At very high concentrations of substrate (illustrated by circles) the transporter can still bind ATP (i) and switch from the inward- to the outward-facing conformation. (ii) The high extracellular substrate concentration results in a situation where substrate is bound to the outward-facing conformation at virtually all times (iii) and locks the transporter in this conformation. In the conformation, the transporter is incompetent to exchange nucleotides. Hence, the transporter cycle is blocked.

reside in the plasma membrane (Decottignies et al., 1994; Egner et al., 1998).

Phylogenetic studies demonstrated a very close relationship between PDR transporters in the non-pathogenic yeast *S. cerevisiae* and those found in infective *Candida* species such as CDR1–4 that are responsible for a dramatic increase in resistance towards antifungal drugs (Fitzpatrick et al., 2006; Cannon et al., 2009; Lamping et al., 2010).

A basal ATPase activity uncoupled from substrate transport

ABC transporters display three different ATPase activities: basal, substrate-stimulated and substrate-inhibited (Davidson et al., 1996; Al-Shawi et al., 2003; Gerber et al., 2008; Crowley and Callaghan, 2010). Even in the absence of added drugs, P-glycoprotein (P-gp), a major contributor to human MDR, exhibits a basal activity and hydrolyzes ATP (Figure 1B). The turnover of ATP can be stimulated several-fold by the addition of substrates (Al-Shawi and Omote, 2005; Dawson and Locher, 2007). However, a further increase of substrate concentration often inhibits the ATPase activity of the transporter (Figure 1C). Here, the lack of substrate release blocks ATP turnover by stabilizing a non-productive conformation of the transporter. This phenomenon is referred to as transinhibition and can be seen analogous to product inhibition of enzymes (Pall and Kelly, 1971; Gerber et al., 2008; Kadaba et al., 2008).

Pdr5 behaves different to P-gp. All drugs and artificial substrates presented to Pdr5 failed to substantially stimulate its ATPase activity beyond the high level of basal activity (approximately 28 $ATPs^{-1}$) (Decottignies et al., 1995; Ernst et al., 2008). Interestingly, the basal activity of Pdr5 has been proposed to affect the cellular level of ATP (Krasowska et al., 2010). Both a high basal ATPase activity and the lack of substrate stimulation are seemingly conserved among fungal homologs. A high basal activity was also observed for Cdr1 from *Candida albicans* and Cdr1 and Pdh1 of *Candida glabrata* (Nakamura et al., 2001; Wada et al., 2002; Shukla et

al., 2006). Only in the case of detergent solubilized Cdr1 from *C. albicans*, a minor stimulation by fluconazol and cycloheximide (1.2- and 1.4-fold, respectively) was reported (Shukla et al., 2006).

Basal and potentially futile ATP hydrolysis (Figure 1B) – is there really such a thing? Is it only because of contaminating natural substrates in the preparation or is it simply an artifact of detergent solubilization? The latter scenario was indeed described for the maltose import system from *Escherichia coli* (Davidson et al., 1996; Reich-Slotky et al., 2000). By contrast, Pdr5 in its natural plasma membrane environment exhibits high basal activity (Decottignies et al., 1994, 1995; Kolaczkowski et al., 1996; Conseil et al., 2000, 2003; Ernst et al., 2008). Therefore, the observed activity cannot be just an artifact due to detergent solubilization.

Could the activity of Pdr5 be due to the presence of natural substrates and thus rather reflect a substrate-stimulated than a basal activity? We consider this hypothesis as unlikely. In general, ATPase and transport activities of Pdr5 are studied *in vitro* after isolation of the plasma membrane. Given the proposed role of Pdr5 in the transport and homeostasis of lipids and lipid-like molecules (Decottignies et al., 1998; Schuller et al., 2007; Guan et al., 2010), the presence of natural substrates cannot be excluded *a priori*. However, once the transporter is energized and starts to pump, the distribution of those natural substrates would change over time. If the ATPase activity was controlled by an interaction of the natural substrate with the transporter, the observed ATPase activity should change over time as the available substrate is transported. This is not observed in our ongoing studies nor, to our knowledge, is it described in the literature. Notably, the passive flip-flop rate of lipids in a cellular membrane (John et al., 2002; Steck et al., 2002) is at least one order of magnitude lower than the rate of ATP hydrolysis reported for Pdr5 (28 s^{-1}) (Decottignies et al., 1995).

For these reasons, we propose that a high basal activity is a mode of operation in Pdr5 and its fungal homologs. As in the case of P-gp (Al-Shawi et al., 2003), the basal activity could be responsible to keep Pdr5 in a receptive conformation. The pronounced basal activity that is observed in fungal PDR pumps can represent an adaptation of a single cell organism that encounters much faster changing environments.

Substrate selection by P-gp and Pdr5

The prime example of MDR transporters is P-gp. The number of studies that address structure-function relationships reported is overwhelming (for a summary of characterized mutations please see http://www.nottingham.ac.uk/~mbzidk/P-gp%20Mutations.htm). Remarkably, all transmembrane helices have been implicated in drug transport (directly or indirectly) and even a silent single nucleotide polymorphism that did not result in an amino acid substitution was shown to alter the substrate spectrum (probably by influencing the overall folding kinetics of P-gp) (Kimchi-Sarfaty et al., 2007). Historically, at least two distinct substrate binding sites have been pharmacologically defined for P-gp, the so-called H-site (Hoechst 33342 binding site) and the R-site (Rhodamine 123 binding site; Shapiro and Ling, 1997). Later on, competition experiments suggested that P-gp could contain at least seven different drug-binding sites (Safa, 2004). More recently, the reported crystal structure of mouse P-gp along with biochemical data identified a large internal binding cavity that is capable of accommodating various, structurally unrelated compounds at the same time (Aller et al., 2009). However, because transporter-drug interactions are highly dynamic (Ernst et al., 2010) and the crystal structure is only of medium resolution, the mysteries of multidrug recognition and selection remains.

The substrate spectra of P-gp and Pdr5 are overlapping. However, the rules for selection differ. Many substrates of P-gp are positively charged and possess aromatic ring systems. They vary in their sizes (200–1900 kDa) and their lipid-water coefficients (300–20 000) (for a recent review see Eckford and Sharom, 2009). For Pdr5, Golin et al. demonstrated in a well-designed study that substrates are not primarily selected by their chemical nature but rather based on their volume (Golin et al., 2003) and proposed an important role of hydrogen bond acceptor groups within the substrate (Hanson et al., 2005). A similar, yet different mechanism of substrate selection was proposed for P-gp (Seelig and Gatlik-Landwojtowicz, 2005). Clearly, a detailed description of the molecular differences in substrate selection by fungal PDR transporters and mammalian MDR transporters might provide valuable insights and yield novel strategies in the treatment of pathogenic fungi.

The structure-function relationships of Pdr5 have been studied to a large extent by site-directed and random mutagenesis (Egner et al., 1998, 2000; Tutulan-Cunita et al., 2005; Ernst et al., 2008; Sauna et al., 2008; Ananthaswamy et al., 2010). Very surprisingly, we observed that the H1068A mutation (H-loop of NBD2) did not affect the steady-state ATPase activity but caused altered drug specificity towards Rhodamine 6G (Ernst et al., 2008, 2010). First of all, this was in striking contrast to reports of other ABC systems that demonstrated an essential role of this conserved residue for ATPase hydrolysis and substrate transport (Davidson and Sharma, 1997; Nikaido and Ames, 1999; Zaitseva et al., 2005; Ernst et al., 2006). Secondly, it raised the question of how the NBDs contribute to substrate selection and challenged the simplistic view of a strict division of labor by NBDs and TMDs. How can mutations of the motor domains result in altered substrate selection by the TMDs (Tutulan-Cunita et al., 2005; Ernst et al., 2008; Kumar et al., 2010)? Very strikingly, even the energy source in use, ATP, UTP or GTP, can modulate which drug is being transported efficiently (Kolaczkowski et al., 1996; Golin et al., 2007b; Ernst et al., 2008). Although the underlying molecular mechanism remains to be solved, a possible explanation has been provided and coined as 'kinetic substrate selection' model (Ernst et al., 2010). It proposes that the time Pdr5 spends in the inward- or outward-facing conformation, respectively, affects the substrate selection and explains how two substrates with identical affinities can be transported with different efficiencies.

In light of the strong size dependency of substrate selection (Golin et al., 2003) and transporter inhibition (Ernst et al., 2008), there is another intriguing possibility as an extension to existing models (Figure 1A). If there is an upper limit for the substrate size that can be accommodated by the transporter upon switching from the inward- to the outward-facing conformation (as implicated by Golin et al., 2003, 2007a) and if the size limit would be more restrictive for the switch back (as suggested, for example, by the transinhibitory activity of only rather sizeable transport substrates), then a MDR transporter might also act as a molecular diode. Sizeable substrates can only be transported from the inside to the outside, whereas a fraction of smaller substrates that fail to be released are simply transported back in. A prerequisite for this model is that the conformational changes of inward and outward switching must be asymmetric. Numerous studies that address the asymmetries of NBDs (Chen et al., 2004; Tombline et al., 2005; Siarheyeva et al., 2010) and their strict coupling to the TMDs (Sauna et al., 2008; Locher, 2009; Csanady et al., 2010) at minimum imply that this scenario is possible for MDR and other ABC exporters (also see below).

Recently, Gutmann et al. proposed that the inward and outward switching of P-gp is accompanied by a rotation of transmembrane helices, which might destabilize the interaction of a substrate with its ligand binding site (Gutmann et al., 2010). Although this model explains how a switch in affinity might be accomplished for a highly diverse population of substrates, it raises another question: what happens to compounds that bind with higher affinity to the outward facing conformation of the transporter? Are such compounds actively taken up by MDR efflux pumps?

Data mining of the drug activity dataset of >100 000 compounds across 60 human cancer cell lines (by the Developmental Therapeutics Program of the National Cancer Institute, USA) provides a great opportunity to identify compounds that selectively kill MDR cells. An *in silico* screening with 42 000 compounds identified only 22 compounds with MDR-selective activity and 15 additional drugs showing increased toxicity for P-gp expressing cells (Turk et al., 2009). The most intuitive mode of action, an active P-gp mediated uptake, could not be verified for any tested drug (Turk et al., 2009).

Therefore, in all likelihood, a 'molecular diode' mechanism is at work to prevent undesired uptake of cytotoxic compounds by multidrug exporters. Such a 'molecular diode' mechanism is not mutually exclusive to other transport models nor does it exclude the existence of high- and low-affinity binding sites as a basis for directed transport. However, it represents a previously unanticipated and intriguing mechanism to mediate vectorial transport based on the volume of a substrate and explains how undesired uptake of putatively toxic compounds might be prevented.

Pdr5 and detergents: a 'love-and-hate' relationship?

Around 16 years ago, Goffeau and coworkers reported the first isolation protocols of Pdr5 (Decottignies et al., 1994, 1995, 1998). Already then, it became evident that the ATPase activity of Pdr5 is drastically reduced in the detergent-solubilized state. Much has happened since then, including a first glimpse on the three-dimensional structure of Pdr5 through single particle electron microscopy analysis (Ferreira-Pereira et al., 2003). We systematically tested solubilization conditions for Pdr5 and, also in our hands, all of the >30 tested detergents had a great inhibitory effect on the steady-state ATPase activity. This was unlikely owing to delipidation (e.g., the loss of a specific protein-lipid interaction) because the biochemical properties of the chosen detergents were highly diverse. Why then do detergents inhibit Pdr5? Some studies have suggested that detergents could be actually substrates of Pdr5 (Tutulan-Cunita et al., 2005; Schuller et al., 2007) and/or P-gp (Li-Blatter et al., 2009). Because Pdr5 is inhibited by its own substrates (Decottignies et al., 1994; Kolaczkowski et al., 1996; Ernst et al., 2008), it is fair to question whether it is at all possible to yield complete ATPase active Pdr5 in detergent solution.

In support of the hypothesis that detergents are substrates of Pdr5, we performed more detailed studies. n-Dodecyl-β-maltopyranoside (DDM) and other maltoside-based detergents that differ only in the length of their aliphatic chains inhibited Pdr5-mediated Rhodamin6G transport at concentrations far below their critical micelle concentrations, indicative for competitive binding to the drug binding sites (data not shown). Only at higher concentrations, we observed an inhibition of the ATPase activity. Interestingly, these effects were fully reversible: both activities could be restored upon reduction of the detergent concentration. Therefore, DDM and other detergents of the maltoside series behave similar to other substrates of Pdr5. We hypothesize analogously to other substrates of Pdr5 that detergents are capable of locking the transporter in a transinhibited conformation presumably incompatible with efficient nucleotide exchange. The crystal structure of an analogously, detergent-induced conformation was solved and discussed for the putative bacterial multidrug transporter Sav1866 (Dawson and Locher, 2006). Thus, one might conclude that a functional analysis of Pdr5 in detergent solution might not be very informative.

Inherent degeneration: why?

A careful look at the sequences of Pdr5 and a comparison with the consensus sequences of the diagnostic motifs of ABC transporters (Table 1) reveals the asymmetry of Pdr5. Based on the crystal structures of isolated NBDs and full-length transporters complexed with ATP (Smith et al., 2002; Chen et al., 2003; Zaitseva et al., 2005; Procko et al., 2006;

Table 1 Comparison of the consensus sequence of ABC transporters and selected sequences of these conserved motifs in Pdr5.

	Walker A	Walker B	C-loop	H-loop
Consensus	GXXGXGKST	ΦΦΦΦDE	LSGGQ	H
NBD1	GRPGSGCTT	FQCWDNN	VSGGER	Y
NBD2	GASGAGKTT	LVFLDE	LNVEQR	H

Dawson et al., 2007; Oldham et al., 2007), it is generally accepted that an ATP molecule is sandwiched between the Walker A and B motifs of one NBD and the C-loop of the second NBD (first proposed by Jones and George, 1999). Bearing this in mind, NBD1 composite site of Pdr5 (constituted by the Walker A and B motifs of NBD1 and the C-loop of NBD2) shows a high degree of deviation from the consensus sequences. By contrast, the NBD2 composite site contains all canonical amino acids, including the histidine of the H-loop (Karpowich et al., 2001; Yuan et al., 2001; Austermuhle et al., 2004; Zaitseva et al., 2005). As a consequence, all amino acids that are required for ATP hydrolysis (for a review see Oswald et al., 2006) are found in the NBD2 composite site, whereas they are missing in the NBD1 composite site. This clearly implies an asymmetric function of the two NBDs and further suggests that the NBD1 composite site is catalytically inactive or active only at drastically reduced levels. This prediction was tested and goes hand in hand with mutational studies of Pdr5 and close fungal homologs (Holmes et al., 2006; Ernst et al., 2008).

Such degeneration is not a monopoly of Pdr5 or other fungal ABC transporters. In humans, CFTR and TAP, for example, display the same arrangement of degeneration and have verified to be functionally asymmetric (Basso et al., 2003; Chen et al., 2004). CFTR provides the unique possibility to study conformational transitions and activities of single CFTR molecules at high temporal resolution. Here, ATP has been shown to bind stably at NBD1 composite site for minutes (rendering this site virtually catalytically inactive) (Basso et al., 2003; Tsai et al., 2010), whereas gating of this chloride channel is tightly coupled to ATP-binding and hydrolysis at the NBD2 composite site (Csanady et al., 2010) that occurs on a much shorter time scale. In analogy to that and based on our mutational analysis, we propose that ATP-binding and hydrolysis at the NBD2 composite site in Pdr5 mediates drug transport (Figure 1A; Ernst et al., 2008). A stable interaction of ATP with the degenerate NBD1 composite site is crucially important to provide a platform for dimerization (Ernst et al., 2008) and to promote ATP hydrolysis at the consensus NBD2 composite site (similar to what was proposed for TAP; see Ernst et al., 2006; Procko et al., 2009).

With regard to degeneration, P-gp is strikingly different. Both NBDs are equipped with all catalytically important motifs and residues. Elegant studies on P-gp resulted in the proposal of the alternating site model (Senior and Gadsby, 1997; Gadsby et al., 1998; Sauna and Ambudkar, 2000) that has recently been refined (Jones et al., 2009). Here, ATP-binding, hydrolysis and release alternates between the two NBD composite sites with one nucleotide being occluded at all times (Tombline et al., 2005). The models proposed for ABC transporters with one degenerate site (Gadsby et al., 2006; Procko et al., 2009) might highlight a specialization of a common mechanism: ATP-binding and hydrolysis at one NBD is sufficient to induce the required conformational switches of the TMDs, but does not alternate between the two NBD composite sites (Figure 1).

There is a strict mechanical coupling between NBDs and TMDs (Dawson et al., 2006; Locher, 2009; Oancea et al., 2009) that can transmit asymmetric behavior of the NBDs to the TMDs. The relevant interface of Pdr5 has been investigated by Sauna et al. (2008) and revealed a functionally important interaction between transmembrane helix 2 and NBD1 through the intracellular loop 1. This interaction seems to be crucial to couple ATP-binding to drug translocation. The functional significance of asymmetry has been investigated by Kumar et al. (2010) by mutational analysis of the conserved and degenerated sequences of Cdr1 from *C. albicans*. The resulting phenotypes strongly point to an in-built degeneration of the NBD, which is non-interchangeable and absolutely necessary for function.

Analogously to the gating of CFTR, we propose that binding of ATP at the NBD2 composite site switches Pdr5 from the inward- to the outward-facing conformation and that subsequent hydrolysis of ATP is sufficient to induce the conformational changes that coincide with or follow drug release. Release of hydrolysis products requires a partial opening of the NBD dimer to reset Pdr5 in the inward-facing, receptive conformation. Thus, the movements of the NBD2 composite site along with its associated transmembrane helices (TMHs) during the transport are different from the movements of the NBD1 composite site and its associated TMHs. This concept is consistent with recent simulation studies using the Sav1866 crystal structure (Dawson et al., 2006; Aittoniemi et al., 2010). Here, the two functional and symmetric halves of Sav1866 behave asymmetrically with regard to the NBD dimer. Although the sequence and structures of the two NBDs are identical, the interactions at the dimer interface allow for sequential ATP hydrolysis and therefore asymmetric motions that are transmitted to the TMDs. It is probable that asymmetric movements could certainly be even more pronounced in an asymmetric system such as Pdr5. Clearly, the underlying molecular transport pathways and conformational rearrangements upon the switches between the extreme inward- and outward-facing conformations will be highly informative but remain to be elucidated.

Conclusions

Pdr5 is an ABC transporter involved in the fascinating PDR machinery. Although it displays characteristics common to all ABC transporters, some surprising features not intuitively expected have been discovered in the past. It will be more than interesting to unravel the commonalities and exceptions of Pdr5 to gain a more global view on how the selection and transport of a multiplicity of substrates can be accomplished by just one transport system.

Acknowledgments

We apologize to all colleagues whose work was not properly referenced owing to space limitations. Work in our laboratory was funded through the Heinrich Heine University Düsseldorf, the EU (European Drug Initiative on Channels and Transporters, EDICT)

FP7 Theme (Health-2007-2.1.1.-5) and the Deutsche Forschungsgemeinschaft (Schm1279/5-3 and SFB 575) to L.S.

References

Aittoniemi, J., de Wet, H., Ashcroft, F.M., and Sansom, M.S. (2010). Asymmetric switching in a homodimeric ABC transporter: a simulation study. PLoS Comput. Biol. *6*, e1000762.

Al-Shawi, M.K. and Omote, H. (2005). The remarkable transport mechanism of P-glycoprotein: a multidrug transporter. J. Bioenerg. Biomembr. *37*, 489–496.

Al-Shawi, M.K., Polar, M.K., Omote, H., and Figler, R.A. (2003). Transition state analysis of the coupling of drug transport to ATP hydrolysis by P-glycoprotein. J. Biol. Chem. *278*, 52629–52640.

Aller, S.G., Yu, J., Ward, A., Weng, Y., Chittaboina, S., Zhuo, R., Harrell, P.M., Trinh, Y.T., Zhang, Q., Urbatsch, I.L., et al. (2009). Structure of P-glycoprotein reveals a molecular basis for poly-specific drug binding. Science *323*, 1718–1722.

Ananthaswamy, N., Rutledge, R., Sauna, Z.E., Ambudkar, S.V., Dine, E., Nelson, E., Xia, D., and Golin, J. (2010). The signaling interface of the yeast multidrug transporter Pdr5 adopts a cis conformation, and there are functional overlap and equivalence of the deviant and canonical Q-loop residues. Biochemistry *49*, 4440–4449.

Austermuhle, M.I., Hall, J.A., Klug, C.S., and Davidson, A.L. (2004). Maltose-binding protein is open in the catalytic transition state for ATP hydrolysis during maltose transport. J. Biol. Chem. *279*, 28243–28250.

Balzi, E., Wang, M., Leterme, S., Van Dyck, L., and Goffeau, A. (1994). PDR5, a novel yeast multidrug resistance conferring transporter controlled by the transcription regulator PDR1. J. Biol. Chem. *269*, 2206–2214.

Basso, C., Vergani, P., Nairn, A.C., and Gadsby, D.C. (2003). Prolonged nonhydrolytic interaction of nucleotide with CFTR's NH_2-terminal nucleotide binding domain and its role in channel gating. J. Gen. Physiol. *122*, 333–348.

Bissinger, P.H. and Kuchler, K. (1994). Molecular cloning and expression of the *Saccharomyces cerevisiae* STS1 gene product. A yeast ABC transporter conferring mycotoxin resistance. J. Biol. Chem. *269*, 4180–4186.

Callaghan, R. (2010). Multidrug efflux pumps: the big issues. FEBS J. *277*, 529.

Cannon, R.D., Lamping, E., Holmes, A.R., Niimi, K., Baret, P.V., Keniya, M.V., Tanabe, K., Niimi, M., Goffeau, A., and Monk, B.C. (2009). Efflux-mediated antifungal drug resistance. Clin. Microbiol. Rev. *22*, 291–321.

Chen, J., Lu, G., Lin, J., Davidson, A.L., and Quiocho, F.A. (2003). A tweezers-like motion of the ATP-binding cassette dimer in an ABC transport cycle. Mol. Cell *12*, 651–661.

Chen, M., Abele, R., and Tampe, R. (2004). Functional non-equivalence of ATP-binding cassette signature motifs in the transporter associated with antigen processing (TAP). J. Biol. Chem. *279*, 46073–46081.

Conseil, G., Decottignies, A., Jault, J.M., Comte, G., Barron, D., Goffeau, A., and Di Pietro, A. (2000). Prenyl-flavonoids as potent inhibitors of the Pdr5p multidrug ABC transporter from *Saccharomyces cerevisiae*. Biochemistry *39*, 6910–6917.

Conseil, G., Perez-Victoria, J.M., Renoir, J.M., Goffeau, A., and Di Pietro, A. (2003). Potent competitive inhibition of drug binding to the *Saccharomyces cerevisiae* ABC exporter Pdr5p by the hydrophobic estradiol-derivative RU49953. Biochim. Biophys. Acta *1614*, 131–134.

Crowley, E. and Callaghan, R. (2010). Multidrug efflux pumps: drug binding-gates or cavity? FEBS J. *277*, 530–539.

Csanady, L., Vergani, P., and Gadsby, D.C. (2010). Strict coupling between CFTR's catalytic cycle and gating of its Cl- ion pore revealed by distributions of open channel burst durations. Proc. Natl. Acad. Sci. USA *107*, 1241–1246.

Davidson, A.L. and Sharma, S. (1997). Mutation of a single MalK subunit severely impairs maltose transport activity in *Escherichia coli*. J. Bacteriol. *179*, 5458–5464.

Davidson, A.L., Laghaeian, S.S., and Mannering, D.E. (1996). The maltose transport system of *Escherichia coli* displays positive cooperativity in ATP hydrolysis. J. Biol. Chem. *271*, 4858–4863.

Davidson, A.L., Dassa, E., Orelle, C., and Chen, J. (2008). Structure, function, and evolution of bacterial ATP-binding cassette systems. Microbiol. Mol. Biol. Rev. *72*, 317–364.

Dawson, R.J. and Locher, K.P. (2006). Structure of a bacterial multidrug ABC transporter. Nature *443*, 180–185.

Dawson, R.J. and Locher, K.P. (2007). Structure of the multidrug ABC transporter Sav1866 from *Staphylococcus aureus* in complex with AMP-PNP. FEBS Lett. *581*, 935–938.

Dawson, R.J., Hollenstein, K., and Locher, K.P. (2007). Uptake or extrusion: crystal structures of full ABC transporters suggest a common mechanism. Mol. Microbiol. *65*, 250–257.

Decottignies, A., Kolaczkowski, M., Balzi, E., and Goffeau, A. (1994). Solubilization and characterization of the overexpressed PDR5 multidrug resistance nucleotide triphosphatase of yeast. J. Biol. Chem. *269*, 12797–12803.

Decottignies, A., Lambert, L., Catty, P., Degand, H., Epping, E.A., Moye-Rowley, W.S., Balzi, E., and Goffeau, A. (1995). Identification and characterization of SNQ2, a new multidrug ATP binding cassette transporter of the yeast plasma membrane. J. Biol. Chem. *270*, 18150–18157.

Decottignies, A., Grant, A.M., Nichols, J.W., de Wet, H., McIntosh, D.B., and Goffeau, A. (1998). ATPase and multidrug transport activities of the overexpressed yeast ABC protein Yor1p. J. Biol. Chem. *273*, 12612–12622.

Eckford, P.D. and Sharom, F.J. (2009). ABC efflux pump-based resistance to chemotherapy drugs. Chem. Rev. *109*, 2989–3011.

Egner, R., Rosenthal, F.E., Kralli, A., Sanglard, D., and Kuchler, K. (1998). Genetic separation of FK506 susceptibility and drug transport in the yeast Pdr5 ATP-binding cassette multidrug resistance transporter. Mol. Biol. Cell *9*, 523–543.

Egner, R., Bauer, B.E., and Kuchler, K. (2000). The transmembrane domain 10 of the yeast Pdr5p ABC antifungal efflux pump determines both substrate specificity and inhibitor susceptibility. Mol. Microbiol. *35*, 1255–1263.

Ernst, R., Klemm, R., Schmitt, L., and Kuchler, K. (2005). Yeast ATP-binding cassette transporters: cellular cleaning pumps. Methods Enzymol. *400*, 460–484.

Ernst, R., Koch, J., Horn, C., Tampe, R., and Schmitt, L. (2006). Engineering ATPase activity in the isolated ABC cassette of human TAP1. J. Biol. Chem. *281*, 27471–27480.

Ernst, R., Kueppers, P., Klein, C.M., Schwarzmueller, T., Kuchler, K., and Schmitt, L. (2008). A mutation of the H-loop selectively affects rhodamine transport by the yeast multidrug ABC transporter Pdr5. Proc. Natl. Acad. Sci. USA *105*, 5069–5074.

Ernst, R., Kueppers, P., Stindt, J., Kuchler, K., and Schmitt, L. (2010). Multidrug efflux pumps: substrate selection in ATP-binding cassette multidrug efflux pumps – first come, first served? FEBS J. *277*, 540–549.

Ferreira-Pereira, A., Marco, S., Decottignies, A., Nader, J., Goffeau, A., and Rigaud, J.L. (2003). Three-dimensional reconstruction

of the *Saccharomyces cerevisiae* multidrug resistance protein Pdr5p. J. Biol. Chem. *278*, 11995–11999.

Fitzpatrick, D.A., Logue, M.E., Stajich, J.E., and Butler, G. (2006). A fungal phylogeny based on 42 complete genomes derived from supertree and combined gene analysis. BMC Evol. Biol. *6*, 99.

Gadsby, D.C., Dousmanis, A.G., and Nairn, A.C. (1998). ATP hydrolysis cycles and the gating of CFTR Cl^- channels. Acta Physiol. Scand. (Suppl.) *643*, 247–256.

Gadsby, D.C., Vergani, P., and Csanady, L. (2006). The ABC protein turned chloride channel whose failure causes cystic fibrosis. Nature *440*, 477–483.

Gerber, S., Comellas-Bigler, M., Goetz, B.A., and Locher, K.P. (2008). Structural basis of trans-inhibition in a molybdate/tungstate ABC transporter. Science *321*, 246–250.

Ghaemmaghami, S., Huh, W.K., Bower, K., Howson, R.W., Belle, A., Dephoure, N., O'Shea, E.K., and Weissman, J.S. (2003). Global analysis of protein expression in yeast. Nature *425*, 737–741.

Golin, J., Ambudkar, S.V., Gottesman, M.M., Habib, A.D., Sczepanski, J., Ziccardi, W., and May, L. (2003). Studies with novel Pdr5p substrates demonstrate a strong size dependence for xenobiotic efflux. J. Biol. Chem. *278*, 5963–5969.

Golin, J., Ambudkar, S.V., and May, L. (2007a). The yeast Pdr5p multidrug transporter: how does it recognize so many substrates? Biochem. Biophys. Res. Commun. *356*, 1–5.

Golin, J., Kon, Z.N., Wu, C.P., Martello, J., Hanson, L., Supernavage, S., Ambudkar, S.V., and Sauna, Z.E. (2007b). Complete inhibition of the Pdr5p multidrug efflux pump ATPase activity by its transport substrate clotrimazole suggests that GTP as well as ATP may be used as an energy source. Biochemistry *46*, 13109–13119.

Guan, W., Jiang, H., Guo, X., Mancera, E., Xu, L., Li, Y., Steinmetz, L., and Gu, Z. (2010). Antagonistic changes in sensitivity to antifungal drugs by mutations of an important ABC transporter gene in a fungal pathogen. PLoS One *5*, e11309.

Gutmann, D.A., Ward, A., Urbatsch, I.L., Chang, G., and van Veen, H.W. (2010). Understanding polyspecificity of multidrug ABC transporters: closing in on the gaps in ABCB1. Trends Biochem. Sci. *35*, 36–42.

Hanekop, N., Zaitseva, J., Jenewein, S., Holland, I.B., and Schmitt, L. (2006). Molecular insights into the mechanism of ATP-hydrolysis by the NBD of the ABC-transporter HlyB. FEBS Lett. *580*, 1036–1041.

Hanson, L., May, L., Tuma, P., Keeven, J., Mehl, P., Ferenz, M., Ambudkar, S.V., and Golin, J. (2005). The role of hydrogen bond acceptor groups in the interaction of substrates with Pdr5p, a major yeast drug transporter. Biochemistry *44*, 9703–9713.

Hirata, D., Yano, K., Miyahara, K., and Miyakawa, T. (1994). *Saccharomyces cerevisiae* YDR1, which encodes a member of the ATP-binding cassette (ABC) superfamily, is required for multidrug resistance. Curr. Genet. *26*, 285–294.

Holmes, A.R., Tsao, S., Lamping, E., Niimi, K., Monk, B.C., Tanabe, K., Niimi, M., and Cannon, R.D. (2006). Amino acid residues affecting drug pump function in *Candida albicans* – *C. albicans* drug pump function. Nippon Ishinkin Gakkai Zasshi *47*, 275–281.

Jardetzky, O. (1966). Simple allosteric model for membrane pumps. Nature *211*, 969–970.

John, K., Kubelt, J., Muller, P., Wustner, D., and Herrmann, A. (2002). Rapid transbilayer movement of the fluorescent sterol dehydroergosterol in lipid membranes. Biophys. J. *83*, 1525–1534.

Jones, P.M. and George, A.M. (1999). Subunit interactions in ABC transporters: towards a functional architecture. FEMS Microbiol. Lett. *179*, 187–202.

Jones, P.M., O'Mara, M.L., and George, A.M. (2009). ABC transporters: a riddle wrapped in a mystery inside an enigma. Trends Biochem. Sci. *34*, 520–531.

Kadaba, N.S., Kaiser, J.T., Johnson, E., Lee, A., and Rees, D.C. (2008). The high-affinity *E. coli* methionine ABC transporter: structure and allosteric regulation. Science *321*, 250–253.

Karpowich, N., Martsinkevich, O., Millen, L., Yuan, Y.R., Dai, P.L., MacVey, K., Thomas, P.J., and Hunt, J.F. (2001). Crystal structures of the MJ1267 ATP binding cassette reveal an induced-fit effect at the ATPase active site of an ABC transporter. Structure *9*, 571–586.

Kimchi-Sarfaty, C., Oh, J.M., Kim, I.W., Sauna, Z.E., Calcagno, A.M., Ambudkar, S.V., and Gottesman, M.M. (2007). A 'silent' polymorphism in the MDR1 gene changes substrate specificity. Science *315*, 525–528.

Kolaczkowski, M., van der Rest, M., Cybularz-Kolaczkowska, A., Soumillion, J.P., Konings, W.N., and Goffeau, A. (1996). Anticancer drugs, ionophoric peptides, and steroids as substrates of the yeast multidrug transporter Pdr5p. J. Biol. Chem. *271*, 31543–31548.

Krasowska, A., Lukaszewicz, M., Bartosiewicz, D., and Sigler, K. (2010). Cell ATP level of *Saccharomyces cerevisiae* sensitively responds to culture growth and drug-inflicted variations in membrane integrity and PDR pump activity. Biochem. Biophys. Res. Commun. *395*, 51–55.

Kumar, A., Shukla, S., Mandal, A., Ambudkar, S.V., and Prasad, R. (2010). Divergent signature motifs of nucleotide binding domains of ABC multidrug transporter, CaCdr1p of pathogenic *Candida albicans*, are functionally asymmetric and noninterchangeable. Biochim. Biophys. Acta *1798*, 1757–1766.

Lamping, E., Baret, P.V., Holmes, A.R., Monk, B.C., Goffeau, A., and Cannon, R.D. (2010). Fungal PDR transporters: phylogeny, topology, motifs and function. Fungal Genet. Biol. *47*, 127–142.

Li-Blatter, X., Nervi, P., and Seelig, A. (2009). Detergents as intrinsic P-glycoprotein substrates and inhibitors. Biochim. Biophys. Acta *1788*, 2335–2344.

Linton, K.J. (2007). Structure and function of ABC transporters. Physiology (Bethesda) *22*, 122–130.

Locher, K.P. (2009). Review. Structure and mechanism of ATP-binding cassette transporters. Philos. Trans. R. Soc. Lond. B Biol. Sci. *364*, 239–245.

Monk, B.C. and Goffeau, A. (2008). Outwitting multidrug resistance to antifungals. Science *321*, 367–369.

Nakamura, K., Niimi, M., Niimi, K., Holmes, A.R., Yates, J.E., Decottignies, A., Monk, B.C., Goffeau, A., and Cannon, R.D. (2001). Functional expression of *Candida albicans* drug efflux pump Cdr1p in a *Saccharomyces cerevisiae* strain deficient in membrane transporters. Antimicrob. Agents Chemother. *45*, 3366–3374.

Nikaido, K. and Ames, G.F. (1999). One intact ATP-binding subunit is sufficient to support ATP hydrolysis and translocation in an ABC transporter, the histidine permease. J. Biol. Chem. *274*, 26727–26735.

Oancea, G., O'Mara, M.L., Bennett, W.F., Tieleman, D.P., Abele, R., and Tampe, R. (2009). Structural arrangement of the transmission interface in the antigen ABC transport complex TAP. Proc. Natl. Acad. Sci. USA *106*, 5551–5556.

Oldham, M.L., Khare, D., Quiocho, F.A., Davidson, A.L., and Chen, J. (2007). Crystal structure of a catalytic intermediate of the maltose transporter. Nature *450*, 515–521.

Oswald, C., Holland, I.B., and Schmitt, L. (2006). The motor domains of ABC-transporters. What can structures tell us? Naunyn-Schmiedebergs Arch. Pharmacol. *372*, 385–399.

Pall, M.L. and Kelly, K.A. (1971). Specificity of transinhibition of amino acid transport in *Neurospora*. Biochem. Biophys. Res. Commun. *42*, 940–947.

Procko, E., Ferrin-O'Connell, I., Ng, S.L., and Gaudet, R. (2006). Distinct structural and functional properties of the ATPase sites in an asymmetric ABC transporter. Mol. Cell *24*, 51–62.

Procko, E., O'Mara, M.L., Bennett, W.F., Tieleman, D.P., and Gaudet, R. (2009). The mechanism of ABC transporters: general lessons from structural and functional studies of an antigenic peptide transporter. FASEB J. *23*, 1287–1302.

Putman, M., van Veen, H.W., and Konings, W.N. (2000). Molecular properties of bacterial multidrug transporters. Microbiol. Mol. Biol. Rev. *64*, 672–693.

Reich-Slotky, R., Panagiotidis, C., Reyes, M., and Shuman, H.A. (2000). The detergent-soluble maltose transporter is activated by maltose binding protein and verapamil. J. Bacteriol. *182*, 993–1000.

Safa, A.R. (2004). Identification and characterization of the binding sites of P-glycoprotein for multidrug resistance-related drugs and modulators. Curr. Med. Chem. Anticancer Agents *4*, 1–17.

Sauna, Z.E. and Ambudkar, S.V. (2000). Evidence for a requirement for ATP hydrolysis at two distinct steps during a single turnover of the catalytic cycle of human P-glycoprotein. Proc. Natl. Acad. Sci. USA *97*, 2515–2520.

Sauna, Z.E., Bohn, S.S., Rutledge, R., Dougherty, M.P., Cronin, S., May, L., Xia, D., Ambudkar, S.V., and Golin, J. (2008). Mutations define cross-talk between the N-terminal nucleotide-binding domain and transmembrane helix-2 of the yeast multidrug transporter Pdr5: possible conservation of a signaling interface for coupling ATP hydrolysis to drug transport. J. Biol. Chem. *283*, 35010–35022.

Schmitt, L. and Tampé, R. (2002). Structure and mechanism of ABC-transporters. Cur. Opin. Struc. Biol. *12*, 754–760.

Schuller, C., Mamnun, Y.M., Wolfger, H., Rockwell, N., Thorner, J., and Kuchler, K. (2007). Membrane-active compounds activate the transcription factors Pdr1 and Pdr3 connecting pleiotropic drug resistance and membrane lipid homeostasis in *Saccharomyces cerevisiae*. Mol. Biol. Cell *18*, 4932–4944.

Seeger, M.A. and van Veen, H.W. (2009). Molecular basis of multidrug transport by ABC transporters. Biochim. Biophys. Acta *1794*, 725–737.

Seelig, A. and Gatlik-Landwojtowicz, E. (2005). Inhibitors of multidrug efflux transporters: their membrane and protein interactions. Mini Rev. Med. Chem. *5*, 135–151.

Senior, A.E. and Gadsby, D.C. (1997). ATP hydrolysis cycles and mechanism in P-glycoprotein and CFTR. Semin. Cancer Biol. *8*, 143–150.

Shapiro, A.B. and Ling, V. (1997). Positively cooperative sites for drug transport by P-glycoprotein with distinct drug specificities. Eur. J. Biochem. *250*, 130–137.

Shukla, S., Rai, V., Banerjee, D., and Prasad, R. (2006). Characterization of Cdr1p, a major multidrug efflux protein of *Candida albicans*: purified protein is amenable to intrinsic fluorescence analysis. Biochemistry *45*, 2425–2435.

Siarheyeva, A., Liu, R., and Sharom, F.J. (2010). Characterization of an asymmetric occluded state of P-glycoprotein with two bound nucleotides: implications for catalysis. J. Biol. Chem. *285*, 7575–7586.

Smith, P.C., Karpowich, N., Millen, L., Moody, J.E., Rosen, J., Thomas, P.J., and Hunt, J.F. (2002). ATP binding to the motor domain from an ABC transporter drives formation of a nucleotide sandwich dimer. Mol. Cell *10*, 139–149.

Steck, T.L., Ye, J., and Lange, Y. (2002). Probing red cell membrane cholesterol movement with cyclodextrin. Biophys. J. *83*, 2118–2125.

Szakacs, G., Paterson, J.K., Ludwig, J.A., Booth-Genthe, C., and Gottesman, M.M. (2006). Targeting multidrug resistance in cancer. Nat. Rev. Drug Discov. *5*, 219–234.

Taubes, G. (2008). The bacteria fight back. Science *321*, 356–361.

Tombline, G., Muharemagic, A., White, L.B., and Senior, A.E. (2005). Involvement of the 'occluded nucleotide conformation' of P-glycoprotein in the catalytic pathway. Biochemistry *44*, 12879–12886.

Tsai, M.F., Li, M., and Hwang, T.C. (2010). Stable ATP binding mediated by a partial NBD dimer of the CFTR chloride channel. J. Gen. Physiol. *135*, 399–414.

Turk, D., Hall, M.D., Chu, B.F., Ludwig, J.A., Fales, H.M., Gottesman, M.M., and Szakacs, G. (2009). Identification of compounds selectively killing multidrug-resistant cancer cells. Cancer Res. *69*, 8293–8301.

Tutulan-Cunita, A.C., Mikoshi, M., Mizunuma, M., Hirata, D., and Miyakawa, T. (2005). Mutational analysis of the yeast multidrug resistance ABC transporter Pdr5p with altered drug specificity. Genes Cells *10*, 409–420.

Wada, S., Niimi, M., Niimi, K., Holmes, A.R., Monk, B.C., Cannon, R.D., and Uehara, Y. (2002). *Candida glabrata* ATP-binding cassette transporters Cdr1p and Pdh1p expressed in a *Saccharomyces cerevisiae* strain deficient in membrane transporters show phosphorylation-dependent pumping properties. J. Biol. Chem. *277*, 46809–46821.

Yuan, Y.R., Blecker, S., Martsinkevich, O., Millen, L., Thomas, P.J., and Hunt, J.F. (2001). The crystal structure of the MJ0796 ATP-binding cassette. Implications for the structural consequences of ATP hydrolysis in the active site of an ABC transporter. J. Biol. Chem. *276*, 32313–32321.

Zaitseva, J., Jenewein, S., Jumpertz, T., Holland, I.B., and Schmitt, L. (2005). H662 is the linchpin of ATP hydrolysis in the nucleotide-binding domain of the ABC transporter HlyB. EMBO J. *24*, 1901–1910.

Received September 3, 2010; accepted October 12, 2010

Proportionate work on manuscript: 50%

Journal: Biological Chemistry

Impact factor: 2.683

Publication V

Extending the yeast based Pdr1-3 expression strategy for membrane proteins

Rakeshkumar P. Gupta[1], Petra Kueppers[1], Nils Hanekop[1] & Lutz Schmitt[1,*]

1: Institute of Biochemistry, Heinrich Heine University Düsseldorf, Universitätsstr. 1, 40225 Düsseldorf, Germany

*: To whom correspondence should be addressed:
Lutz Schmitt
Institute of Biochemistry
Heinrich Heine University Duesseldorf
Universitaetsstr. 1
40225 Duesseldorf, Germany
Phone: +49(0)211-81-10773
Fax: +49(0)211-81-15310
Email: lutz.schmitt@hhu.de

Abstract

Overexpression of membrane proteins has been a bottleneck for their functional and structural study for a long time. Heterologous expression of membrane proteins presents unique challenges for cloning and expression. *S. cerevisiae* is a potential host system with significant closeness to higher eukaryotes and provides opportunity for attempts to express membrane proteins. In the past, bakers yeast containing mutations within the transcriptional regulator Pdr1 has been used to overexpress various membrane proteins including for example the ABC transporters Pdr5 and Yor1, respectively. In this study we exploited this system and tried to express 3 membrane proteins in yeast along with Pdr5 and Yor1 viz. Rsb1, Mdl1 and Drs2. Out of these five, we could express all membrane proteins although at different levels. Satisfactory yields were obtained for three examples i.e Pdr5, Yor1 and Drs2. Rsb1 expression was comparatively low and Mdl1 was rather unsatisfactory. Thus, we demonstrate here an extension of the application of this yeast based expression system that is suitable for cloning and expression of a wide variety of membrane proteins.

Keywords: ATP Binding Cassette (ABC) transporters, multidrug resistance, P-type ATPases, flippases, membrane protein overexpression.

Abbreviations: MDR- Multidrug resistance, PDR- Pleiotropic drug resistance, LTE- Lipid translocating enzyme.

Introduction

Membrane proteins have been under study for their important roles in the maintenance of vital cellular functions and, especially in fungi, providing resistance against toxic compounds (Klein et al., 2011; Monk and Goffeau, 2008; Niimi et al., 2005). It is this observation of multidrug resistance (MDR) phenomenon observed in cancer and during fungal infections, which fuelled increasing interest in attempts to uncover the structure and function of membrane proteins conferring MDR or pleiotropic drug resistance (PDR) as it is called in fungi (DeRisi et al., 2000).

Membrane protein expression in heterologous systems has proven particularly difficult for many membrane proteins especially human ones, due to various reasons. The major difficulty presented is low expression, mis-folding, mis-trafficking or even in the case of expression low or no functionality (Frelet-Barrand et al., 2010; Li et al., 2009; Midgett and Madden, 2007; Monne et al., 2005). Post-translational modifications present another challenge, which significantly affects the proper functioning of heterologously expressed proteins. A wide variety of host systems have been in use for trying to overexpress membrane proteins for study ranging from *E. coli* to insect cell lines. The bakers yeast *S. cerevisiae* is one such host system that has over time proven its usefulness in providing a platform for expression of membrane proteins (Osterberg et al., 2006).

The phenomenon of pleiotropic drug (PDR) resistance is the yeast counterpart of the multidrug resistance (MDR) phenomenon at work in higher eukaryotes (Balzi and Goffeau, 1995). In native yeast cells the *pdr* genes are under strict control of the transcription factors Pdr1 and Pdr3 and are up-regulated whenever the yeast cells are under stress from cytotoxic compounds. The Pdr proteins, most notably Pdr5, Snq2 and Yor1 among others are part of this entire network of membrane proteins localized in the plasma membrane, and extrude cytotoxic compounds to the extracellular surface (Rogers et al., 2001). In the late 1980s it was discovered that mutations in the transcriptional regulator Pdr1 (Pdr1-3) led to huge increase in

expression levels of Pdr5 (Balzi et al., 1987). This was instrumental in producing sufficient amount of Pdr5 for biochemical and structural studies ever since. As this system worked beautifully for overexpression of Pdr5, it has been used in the past for different membrane proteins from fungi and in one case even from humans (Decottignies et al., 1998; Lamping et al., 2007; Nakamura et al., 2001). We were intrigued by the obvious potential of this system and tried to overexpress other membrane proteins instead of Pdr5 using the approach of employing a strong and constitutive Pdr5 promoter in a genetic background consisting a mutated Pdr1 (Balzi et al., 1987; Decottignies et al., 1998; Lamping et al., 2007; Nakamura et al., 2001). For this purpose, we chose three membrane proteins along with Pdr5 and Yor1 to be tested. These included a member of the lipid-translocating exporter (LTE), Rsb1 from *S. cerevisiae*, that is involved in flipping sphingolipid long chain bases from the cytoplasmic to the extracellular side of the plasma membrane (Kihara and Igarashi, 2002) and the mitochondrial half-size ABC transporter Mdl1, which is responsible for providing resistance towards oxidative stress (Hofacker et al., 2007; Zutz et al., 2009). In our study, we employed the genetically altered version Mdl1 Δ59 lacking the first 59 N-terminal amino acids. This deletion localizes the protein to endoplasmic reticulum microsomes of *S. cerevisiae* (further details are provided in Results). As a third example, the aminophospholipid translocase Drs2, a member of the P4-type ATPase family, that is localized in Golgi membranes of *S. cerevisiae* and is responsible for maintaining lipid asymmetry was used (Chen et al., 1999; Lenoir et al., 2009b; Zhou and Graham, 2009).

Our expression strategy involved a 2-step approach – first the gene of interest is cloned and propagated in *E. coli* on a customized plasmid, which leads to quick and easy handling as well as sufficient quantities of genetic material for the next step. The second step comprises of isolation of the plasmid followed by restriction cleavage to release the gene of interest along with other DNA elements comprising an auxotrophy marker, Pdr5 promoter and an N-terminal 14 histidine tag. This is followed by transformation in competent yeast cells and by homologous recombination the gene of interest is chromosomally incorporated (Figure 1). Using this approach out of the five proteins tested, we

could overexpress 3 membrane proteins, while Rsb1 levels were comparatively low. Mdl1 Δ59 expression was rather unsatisfactory, which could be due to its ER localization and some other factors discussed later.

The approach we have utilized for expressing membrane proteins in *S. cerevisiae* can in principle be used to express any membrane protein as shown in previous studies for ABC transporters, secondary transporters of the major facilitator superfamily, a membrane-bound cytochrome P450 enzyme and human P-glycoprotein (MDR1 or ABC B1) (Balzi et al., 1994; Decottignies et al., 1998; Ernst et al., 2008; Lamping et al., 2007; Nakamura et al., 2001).

Our results suggest that this yeast-based membrane protein expression system might be a promising approach if protein specific information on localization and stability are present and sufficient yields of membrane proteins can be obtained in many cases. This is of particular interest for membrane proteins native to yeast or higher eukaryotes due to similarities in protein trafficking, post-translational modifications, similar membrane environment as well as from a practical point of view due to the ease of growing yeast in the laboratories, genetic manipulation and subsequent purification.

Materials and Methods

Growth media and chemicals

Yeast cells were cultured in YPD medium (10g/l Yeast extract, 20g/l Peptone/Tryptone and 20g/l Glucose). All chemicals were procured from Carl Roth. The detergents used for solubilisation- DDM and Fos-choline 14 were purchased from Anatrace. Anti-Histidine antibody was purchased from Qiagen, α-Pdr5 antibody was kindly provided by Dr. Karl Kuchler, Vienna Biocenter, α-Drs2 antibody was kindly provided by Dr. J. Holthuis, Utrecht University and α-Mdl1 was a kind gift from Dr. R. Tampe, University of Frankfurt. Asolectin was purchased from Fluka. Protease inhibitor tablets were purchased from Roche. Bradford's reagent was purchased from Thermo Scientific.

Yeast strains

The following *S. cerevisiae* strains were used in this study: YALF-A1 (*MATa; ura3-52 trp 1-1 leu 2-3, his 3-11, 15 ade 2-1 PDR 1-3*), and YRE1001 (*MATa; ura3-52 trp 1-1 leu 2-3, his 3-11, 15 ade 2-1 PDR 1-3 pdr5pdr5promΔ::TRP1*). Details about plasmid and strain construction can be found in (Ernst et al., 2008) and Supplementary table S1. Cdc50 plasmid construct was a kind gift from Dr. J. Holthuis, Utrecht University.

Cloning strategy

The gene of interest is first amplified and cloned in pRE5 plasmid which already possesses the DNA elements for histidine auxotrophy, strong Pdr5 promoter, an N-terminus 14 histidine tag and 5' as well as 3' overhangs for subsequent cloning in *S. cerevisiae* cells (Figure 1). pRE5 plasmid is propagated in *E. coli* and isolated for further processing. The plasmid is cleaved near the overhangs using the restriction enzymes SpeI and ApaI. The isolated fragment is then transformed into competent *S. cerevisiae* cells lacking the Pdr5 promoter and possessing a Trp^+ selectable marker instead. The transformed cells are plated on –His plates and incubated for 48-96 hours

at 30°C. PCR and DNA sequencing confirmed the proper integration of the cloning.

Isolation of plasma membranes

Total membrane isolation

Cells were grown in YPD medium at 30°C. At OD_{600} of 1.5, the nitrogen source was replenished by addition of a 10^{th} volume of 5X YP (50 g/liter yeast extract; 100 g/liter tryptone/peptone). Cells were harvested at OD_{600} of 3.5. The isolation of plasma membranes was performed as described in (Ernst et al., 2008; Kolaczkowski et al., 1996).

Isolation of Endoplasmic reticulum microsomes

The isolation of ER microsomes was accomplished using a modification of the protocol by Carman and Fischl (Carman and Fischl, 1992) in combination with the Serrano protocol (Serrano, 1988). Yeast cells from 6-8l (30-50g) expression cultures were thawed and 12ml of lysis buffer (TES buffer: 50mM Tris-HCl pH 7.8, 1mM EDTA, 0.3M sucrose, 10mM β-mercaptoethanol) was added per liter of cell culture. Cell lysis was carried out on ice with 200-300ml glass beads along with protease inhibitor tablets. After cell lysis the cell suspension obtained was centrifuged at 1500g for 10 min (4°C) to remove cell debris. Subsequently, the suspension was centrifuged at 27,000g for 10 min (4°C) and the supernatant discarded. The pellets were washed with 100ml of TES buffer (10 min, 27,000g, 4°C) and discarded, and the combined supernatants were used for sedimentation of the microsomes by centrifugation (75 min, 180,000g, 4°C). For final step before purification the membranes were resuspended in 15ml Buffer A (50mM Tris-HCl pH 7.8, NaCl 50mM and Glycerol 10%) with 15mM β-mercaptoethanol. Protein concentration was measured by Bradford's method of protein estimation.

Isolation of Golgi membranes

For isolation of Golgi membranes containing Drs2 the Serrano protocol was slightly modified. Yeast cells from 6-8l expression cultures were used to isolate membranes. The procedure until the plasma membrane isolation is

essentially the same as described in (Ernst et al., 2008). After the centrifugation step at 20,000g, 20 min (4°C), the supernatant instead of the pellet was processed further. This supernatant was ultracentrifuged at 180,000g for 75min (4°C). The pellet was resuspended in 2ml of Buffer A per liter of culture. Further processing of the membranes for purification was the same as total membranes and microsomes.

Affinity purification and Size-exclusion chromatography

For purification of the N-terminal 14 histidine tagged proteins, immobilized metal ion affinity chromatography (IMAC) purification technique was used. The membrane suspensions were first homogenized and adjusted to a concentration of 10mg/ml. The solubilization was carried out with constant stirring of the suspension for 60 min at 4^0C after addition of the detergent in a mass ratio of 1:1 (protein : detergent). Following this the non-solubilized fraction was separated by ultracentrifugation at 180,000g for 60 min at 4°C. A 1ml HiTrap Chelating column loaded with Zn^{2+} was used for purification. Column equilibration was done using low histidine buffer (50mM Tris-HCl pH 7.8, 500mM NaCl, 2.5mM L-histidine, 0.05% or 0.1% detergent). The solubilized protein fraction was loaded onto the column. Non-specifically bound proteins were eluted with a step gradient using mixed ratios of low and high histidine buffer (50mM Tris-HCl pH 7.8, 500mM NaCl, 100mM L-histidine, 0.05% or 0.1% detergent). The elution was carried out with a significantly increased proportion of the high histidine buffer (51.25mM L-histidine). The individual fractions were treated with 4mM TCEP and 20mM DTT and analyzed by SDS-PAGE. For subsequent gel filtration analysis, the protein fractions were pooled and concentrated using Amicon ultrafiltration (Amicon Ultra 4) devices (100kDa and 30kDa MWCO). The size exclusion chromatography was performed using a HR10/30 Superose 6 column (GE Healthcare). The column was equilibrated prior to loading the sample with Buffer A with varying amounts of detergent. IMAC and size exclusion chromatography was performed on the Akta protein purification systems (GE Healthcare).

Results

Expression of the 'control' full size ABC transporters Pdr5 and Yor1

Pdr5 has been characterized for its role in multidrug resistance in various studies (Conseil et al., 2000; Kolaczkowski et al., 1998; Rogers et al., 2001). Its functional similarity to human multidrug resistance protein Pgp makes it a vital candidate for elucidating the mechanisms of action of MDR ABC transporters. Its function (Balzi et al., 1994; Bissinger and Kuchler, 1994; Hirata et al., 1994) and expression is well established and was used in the context of our cloning strategy (Figure 1) to purify this ABC transporter as an internal control for the capability of the system. Furthermore, it is the only yeast MDR ABC transporter, for which low-resolution structural information is available (Ferreira-Pereira et al., 2003) as well as a homology model (Rutledge et al., 2011) that is based on the crystal structures of mouse P-gp (Aller et al., 2009) and Sav1866 (Dawson and Locher, 2006). As outlined in Material and Methods, Pdr5 could be solubilized and purified to homogeneity using a two-step purification protocol with a yield of approximately 0.75 mg / l yeast culture. The results are similar to previously reported protocols (Ferreira-Pereira et al., 2003).

Yor1, which has been characterized as a multidrug transporter as well, is involved in the extrusion of a wide variety of toxic compounds from the yeast cell (Decottignies et al., 1998; Katzmann et al., 1999; Katzmann et al., 1995). Both Pdr5 and Yor1, are under tight control of the transcription factors Pdr1 and Pdr3 (Balzi and Goffeau, 1995; Ernst et al., 2005). Following published protocols (Decottignies et al., 1998), Yor1 was over-expressed in the Pdr1-3 background (Balzi et al., 1987) employing again the cloning strategy outlined in Figure 1. Subsequently, it was solubilized and purified in a similar way to N14His Pdr5 with DDM (0.01% DDM, 0.5mg/ml asolectin; further details are provided in Materials and Methods) with yield of approximately 0.25 mg / l yeast culture.

Expression and purification of the LTE transporter Rsb1 from *S. cerevisiae*

Rsb1 is an integral membrane protein involved in transport of the sphingolipid long chain base (LCB) from the cytoplasmic side to the extracellular side of the yeast plasma membrane (Kihara and Igarashi, 2004; Manente and Ghislain, 2009). This is instrumental in the control of sphingolipid metabolism (Kihara and Igarashi, 2002). Because of this interesting function and an anticipated possibility to study this flippase also *in* vitro, we selected Rsb1 for expression studies in the context of the yeast based Pdr1-3 expression strategy. Similar to Pdr5 and Yor1, the gene of Rsb1 was integrated in the chromosome of *S. cerevisiae* by homologous recombination. Subsequently, Rsb1 positive clones were used for expression and purification (details are provided in Materials and Methods). The LTE flippase was solubilized and purified identically to Pdr5 and Yor1. Thus, neither elaborated screening for the most appropriate expression conditions nor any screening for the most suited detergent for efficient solubilzation was performed. Nevertheless and as summarized in Figure 2, it was possible to purify N14His Rsb1 to homogeneity with yields of 0.06mg/l cell culture (Figure 2 upper panel). This is obvious by a factor of 4 lower than Yor1 and a factor of 10 lower than Pdr5, but we are confident that further optimization of expression conditions and choice of the proper detergent will increase the yield further.

Expression and purification of the fusion proteins Mdl1 Δ59 and Drs2

Expression attempts employing the 'Pdr1-3 system' for the half size transporter Mdl1 led to very low yields of the protein under standardized conditions employed for Pdr5 and Yor1 (data not shown). The transporter is localized in the mitochondria and is probably responsible for the quality control in peptide transport (Hofacker et al., 2007) among other functions and also in regulation of response to oxidative stress (Zutz et al., 2009). On the other hand, the genetically modified Mdl1 Δ59, which lacks the first 59 N-terminal amino acids, is localized to the ER due to a remote signal sequence at the N-terminus (Gompf et al., 2007). Therefore, on the one hand the method of Fischl and Carman (Carman and Fischl, 1992) was employed for

purification of ER-microsomes. On the other hand, the isolation of total membranes was carried out separately. In contrast to Pdr1, Yor1 and Rsb1, another detergent Fos-choline 14 was also used for solubilization in addition to DDM. In both detergents, a large portion of the protein remained in the pellet after solubilization or was removed in form of aggregates, which therefore led to drastic reduction in protein yields after purification that could be visualized only by Western blot. Interestingly and as shown in Figure 2 lower panel, Mdl1 Δ59 was mainly detected as the full size dimer (130kDa) in the purified fractions by Western blotting, while the expected half size monomer (62kDa) was present as a minor species. This finding clearly requires further investigations, but our studies demonstrate that an over-expression and purification of this Mdl1 variant is in principle possible even without optimizing expression conditions or the choice of the appropriate detergent.

The last example that we chose for over-expression studies in the Pdr1-3 background was Drs2. This member of the P-type ATPase subfamily IV, has been demonstrated to be indeed an aminophospholipid translocase (Lenoir et al., 2009b; Zhou and Graham, 2009) which is involved in maintaining lipid asymmetry in post-golgi secretory vesicles (Chen et al., 1999; Furuta et al., 2007). In our studies, Drs2 required additional efforts for its expression. The protocol for total membrane isolation and golgi membrane isolation did not yield satisfactory amounts of Drs2 after purification (data not shown). One possible reason might be our naive assumption that the cellular interaction partner of Drs2, Cdc50 (Lenoir et al., 2009b; Paulusma et al., 2008), was not required for achieving expression of isolated Drs2. Consequently, we tried to express Drs2 harbouring cells (chromosomally expressed) along with a plasmid containing Cdc50, which led to expression of Drs2 purified subsequently from Golgi membranes (Figure 2 upper panel; details are provided in Materials and Methods). The yield of purified Drs2 after this chromosomal / plasmid-based co-expression of Drs2 and Cdc50 was approximately 0.15mg/l yeast culture. This yield seems to be comparable with published data (Lenoir et al., 2009b; Zhou and Graham, 2009), but we like to

stress that in contrast to the reported data no optimization of expression, solubilization or purification were performed.

Discussion

Saccharomyces cerevisiae has been a model of choice for a number of research areas such as cell biology, molecular biology and others due to a principle similarity of many cellular processes to those operating in higher eukaryotes. The sequencing of the yeast genome (Goffeau et al., 1996) opened new prospects to exploit the wealth of knowledge available for use in genetic manipulation and study of clinically relevant proteins. The transcription factors Pdr1 and Pdr3 control expression of many genes part of which are directly involved in the multidrug resistance phenomenon seen in yeast (Balzi et al., 1987; DeRisi et al., 2000; Simonics et al., 2000). The discovery that a mutation in the allele Pdr1-3 induces overexpression of the MDR protein Pdr5 (Balzi et al., 1994) was key to opening new opportunities to overexpress ABC transporters using this system. Although this system of expression had been shown to work very efficiently for Pdr5 (Balzi et al., 1994) and other membrane proteins from yeast (Decottignies et al., 1998; Lamping et al., 2007; Nakamura et al., 2001) and one from human (Lamping et al., 2007), we wanted to further explore the principle possibility and potential of expressing membrane proteins using this method. Therefore, on the basis of this functional unit from the constitutive Pdr5 promoter in a deletion strain, a genetically modified cloning and purification strategy for establishing a generally applicable method was developed for this work (Ernst et al., 2008). In addition a separable 14Histidine affinity tag was introduced to allow rapid purification of the expressed protein using affinity chromatography.

In principle, expression of any protein is feasible downstream of the strong and constitutive Pdr5 promoter. In this study we tested five membrane proteins from different families for their expression and could obtain satisfactory yields for at least three of them (Figure 2 upper panel) viz. Pdr5, Yor1 and Drs2. Obviously, the expression of Pdr5 and Yor1 has been described and we used it as an internal control of the system. Our yields of purified Pdr5 and Yor1 are comparable to those reported in the literature (Decottignies et al., 1998; Decottignies et al., 1994; Kolaczkowski et al., 1998).

Out of these three well-expressed membrane proteins, Pdr5 and Yor1 are localized in the plasma membrane of yeast cells and also have some substrate overlap (Kolaczkowska et al., 2008). As these proteins are native to yeast, the correct post-translational modifications and folding are expected along with their localization in the plasma membrane. The ATP-dependent long chain base (LCB) translocase Rsb1 (Kihara and Igarashi, 2002, 2004), which is a member of the LTE family, was also expressed albeit at relatively low levels when compared with Pdr5 or Yor1. The majority of Rsb1 apparently localizes to the endoplasmic reticulum (ER) (Kihara and Igarashi, 2004), where it translocates LCB retrieved from the plasma membrane for subsequent phosphorylation. Interestingly, it appears to be under the control of Pdr1, but not of Pdr3 and expression levels of Rsb1 are upregulated in Pdr5 and / or Yor1 knock-out strains (Kihara and Igarashi, 2004). Since Rsb1 is involved in maintaining lipid asymmetry, the reduced expression levels of Rsb1 might be a cellular response to cope with Rsb1-induced changes in lipid composition of the individual leaflets of the bilayer. However, Kihara and Igarashi (Kihara and Igarashi, 2004) did not report any detrimental influence of Rsb1 expression on vitality of yeast cells nor did we notice any toxic effects upon expression of Rsb1 on the growth behaviour of yeast cells (data not shown). Thus, the reduced expression levels might be due to the localization of Rsb1 (ER versus plasma membrane) or other unknown intrinsic factors of this particular membrane protein.

Mdl1 expression was the lowest, which could possibly be due to the modified gene lacking N-terminal signal sequence that directs it to mitochondria under native conditions. But after cleavage it is directed and is localized in ER-microsomes (Gompf et al., 2007). The effect of this genetic modification on the expression, folding and localization could not be determined, although functional data of Mdl suggest that a re-targeting of this ABC transporter does not interfere with function (Hofacker et al., 2007). Small amounts of monomeric and dimeric Mdl1 were purified and observed as seen in Figure 2 lower panel. A previous study reported reduced Mdl1 Δ59 levels upon cleavage of the N-terminal signal sequence (Gompf et al., 2007) and is

supported by the low expression levels observed by us. Additionally, this reduction in expression was independent of the position of the affinity tag on the N- or C-terminus, therefore the negative impact on the proper processing or localization of the protein by the N-terminally fused 14-Histidine tag in the ER is very unlikely.

The P-type ATPase Drs2, which maintains lipid asymmetry in *S. cerevisiae* (Zhou and Graham, 2009), interacts *in vivo* with the cell division protein Cdc50 (Lenoir et al., 2009b). Initial expression studies of Drs2 in the absence of Cdc50 were not successful (data not shown). However, the expression level was significantly improved with the co-expression of Cdc50 in Drs2 containing cells. Here, Cdc50 was added *in trans* in a plasmid, while Drs2 was integrated in the chromosome under the control of the Pdr5 promoter. Although we could not detect co-elution of Drs2 with Cdc50 after purification it is possible that Cdc50 and Drs2 interact and Drs2 is stabilized within the cell due to this interaction. This is in agreement with previous studies where Cdc50 was shown to be necessary for expression and correct localization of Drs2 within the membrane (Lenoir et al., 2009a). This also highlights the importance of additional catalytic subunits in proper functioning of relevant proteins.

Our cloning strategy here employs the selectable marker for Histidine auxotrophy. This is an essential factor that makes specific modification of target genes and subsequent verification possible. Similar strategies have been used previously utilizing the Pdr5 promoter for expression of fungal ABC transporters Cdr1 (Lamping et al., 2007; Nakamura et al., 2001). The valuable property of the model organism of homologous recombination is the basis for our cloning strategy of introducing proteins in the genome for over expression. This also provides opportunity for further genetic modifications to study the biochemical properties of the proteins being expressed as well as manipulations in relation to expression of the interaction partners are possible in yeast. In summary, four of the five tested membrane proteins could be successfully expressed and purified at significant levels. This emphasises the potential of the Pdr1-3 based expression strategy. Interestingly, expression

was most efficient for those membrane proteins that are localized to the plasma membrane, while the two examples that are targeted to the ER (Mdl1 and Rsb1) showed severely reduced levels of expression. Since we have no indication that these proteins are toxic, one way of interpreting the data is that the membrane space of the ER is more limited than that of the plasma membrane. Thus, the reduced levels of expression are a consequence of a overcrowding within the membrane that prohibits further expression of these membrane proteins. Nevertheless, heterologous expression and purification of membrane proteins is possible with this strategy although some protein specific knowledge would be very helpful in optimising the isolation and purification conditions for specific proteins.

Acknowledgements

We thank Robert Ernst, University of Frankfurt, and Karl Kuchler, Medical University of Vienna, for many stimulating discussion and support of the project. We are indebted to Robert Tampé, University of Frankfurt, Jost Holthuis, University of Osnabrück, for the kind gifts of antibodies and plasmids. This project was funded by grant from the (grant Schm1279/5-3) and the EU (EDICT (European Drug Initiative on Channels and Transporters) FP7 Theme [Health-2007-2.1.1.-5]) to L.S..

References

Aller, S.G., Yu, J., Ward, A., Weng, Y., Chittaboina, S., Zhuo, R., Harrell, P.M., Trinh, Y.T., Zhang, Q., Urbatsch, I.L., Chang, G., (2009) Structure of P-glycoprotein reveals a molecular basis for poly-specific drug binding. Science 323, 1718-1722.

Balzi, E., Chen, W., Ulaszewski, S., Capieaux, E., Goffeau, A., (1987) The multidrug resistance gene PDR1 from Saccharomyces cerevisiae. J Biol Chem 262, 16871-16879.

Balzi, E., Goffeau, A., (1995) Yeast multidrug-resistance - the pdr network Journal of Bioenergetics and Biomembranes 27, 71-76.

Balzi, E., Wang, M., Leterme, S., Van Dyck, L., Goffeau, A., (1994) PDR5, a novel yeast multidrug resistance conferring transporter controlled by the transcription regulator PDR1. J Biol Chem 269, 2206-2214.

Bissinger, P.H., Kuchler, K., (1994) Molecular cloning and expression of the Saccharomyces cerevisiae STS1 gene product. A yeast ABC transporter conferring mycotoxin resistance. J Biol Chem 269, 4180-4186.

Carman, G.M., Fischl, A.S., (1992) Phosphatidylinositol synthase from yeast. Methods Enzymol 209, 305-312.

Chen, C.Y., Ingram, M.F., Rosal, P.H., Graham, T.R., (1999) Role for Drs2p, a P-type ATPase and potential aminophospholipid translocase, in yeast late Golgi function. J Cell Biol 147, 1223-1236.

Conseil, G., Decottignies, A., Jault, J.M., Comte, G., Barron, D., Goffeau, A., Di Pietro, A., (2000) Prenyl-flavonoids as potent inhibitors of the Pdr5p multidrug ABC transporter from Saccharomyces cerevisiae. Biochemistry 39, 6910-6917.

Dawson, R.J., Locher, K.P., (2006) Structure of a bacterial multidrug ABC transporter. Nature 443, 180-185.

Decottignies, A., Grant, A.M., Nichols, J.W., de Wet, H., McIntosh, D.B., Goffeau, A., (1998) ATPase and multidrug transport activities of the overexpressed yeast ABC protein Yor1p. J Biol Chem 273, 12612-12622.

Decottignies, A., Kolaczkowski, M., Balzi, E., Goffeau, A., (1994) Solubilization and characterization of the overexpressed PDR5 multidrug resistance nucleotide triphosphatase of yeast. J. Biol. Chem. 269, 12797-12803.

DeRisi, J., van den Hazel, B., Marc, P., Balzi, E., Brown, P., Jacq, C., Goffeau, A., (2000) Genome microarray analysis of transcriptional activation in multidrug resistance yeast mutants. FEBS Lett 470, 156-160.

Ernst, R., Klemm, R., Schmitt, L., Kuchler, K., (2005) Yeast ABC-transporters - Cellular cleaning pumps. Methods Enzymol. 400, 460-484.

Ernst, R., Kueppers, P., Klein, C.M., Schwarzmueller, T., Kuchler, K., Schmitt, L., (2008) A mutation of the H-loop selectively affects rhodamine transport by the yeast multidrug ABC transporter Pdr5. Proc Natl Acad Sci U S A 105, 5069-5074.

Ferreira-Pereira, A., Marco, S., Decottignies, A., Nader, J., Goffeau, A., Rigaud, J.L., (2003) Three-dimensional reconstruction of the Saccharomyces cerevisiae multidrug resistance protein Pdr5p. J Biol Chem 278, 11995-11999.

Frelet-Barrand, A., Boutigny, S., Kunji, E.R., Rolland, N., (2010) Membrane protein expression in Lactococcus lactis. Methods in molecular biology 601, 67-85.
Furuta, N., Fujimura-Kamada, K., Saito, K., Yamamoto, T., Tanaka, K., (2007) Endocytic recycling in yeast is regulated by putative phospholipid translocases and the Ypt31p/32p-Rcy1p pathway. Mol Biol Cell 18, 295-312.
Goffeau, A., Barrell, B.G., Bussey, H., Davis, R.W., Dujon, B., Feldmann, H., Galibert, F., Hoheisel, J.D., Jacq, C., Johnston, M., Louis, E.J., Mewes, H.W., Murakami, Y., Philippsen, P., Tettelin, H., Oliver, S.G., (1996) Life with 6000 genes. Science 274, 546, 563-547.
Gompf, S., Zutz, A., Hofacker, M., Haase, W., van der Does, C., Tampe, R., (2007) Switching of the homooligomeric ATP-binding cassette transport complex MDL1 from post-translational mitochondrial import to endoplasmic reticulum insertion. FEBS J 274, 5298-5310.
Hirata, D., Yano, K., Miyahara, K., Miyakawa, T., (1994) Saccharomyces cerevisiae YDR1, which encodes a member of the ATP-binding cassette (ABC) superfamily, is required for multidrug resistance. Curr Genet 26, 285-294.
Hofacker, M., Gompf, S., Zutz, A., Presenti, C., Haase, W., van der Does, C., Model, K., Tampe, R., (2007) Structural and functional fingerprint of the mitochondrial ATP-binding cassette transporter Mdl1 from Saccharomyces cerevisiae. J Biol Chem 282, 3951-3961.
Katzmann, D.J., Epping, E.A., Moye-Rowley, W.S., (1999) Mutational disruption of plasma membrane trafficking of Saccharomyces cerevisiae Yor1p, a homologue of mammalian multidrug resistance protein. Mol Cell Biol 19, 2998-3009.
Katzmann, D.J., Hallstrom, T.C., Voet, M., Wysock, W., Golin, J., Volckaert, G., Moye-Rowley, W.S., (1995) Expression of an ATP-binding cassette transporter-encoding gene (YOR1) is required for oligomycin resistance in Saccharomyces cerevisiae. Mol Cell Biol 15, 6875-6883.
Kihara, A., Igarashi, Y., (2002) Identification and characterization of a Saccharomyces cerevisiae gene, RSB1, involved in sphingoid long-chain base release. J Biol Chem 277, 30048-30054.
Kihara, A., Igarashi, Y., (2004) Cross talk between sphingolipids and glycerophospholipids in the establishment of plasma membrane asymmetry. Mol Biol Cell 15, 4949-4959.
Klein, C., Kuchler, K., Valachovic, M., (2011) ABC proteins in yeast and fungal pathogens. Essays Biochem 50, 101-119.
Kolaczkowska, A., Kolaczkowski, M., Goffeau, A., Moye-Rowley, W.S., (2008) Compensatory activation of the multidrug transporters Pdr5p, Snq2p, and Yor1p by Pdr1p in Saccharomyces cerevisiae. FEBS Lett 582, 977-983.
Kolaczkowski, M., Kolaczowska, A., Luczynski, J., Witek, S., Goffeau, A., (1998) In vivo characterization of the drug resistance profile of the major ABC transporters and other components of the yeast pleiotropic drug resistance network. Microb Drug Resist 4, 143-158.
Kolaczkowski, M., van der Rest, M., Cybularz-Kolaczkowska, A., Soumillion, J.P., Konings, W.N., Goffeau, A., (1996) Anticancer drugs, ionophoric peptides, and steroids as substrates of the yeast multidrug transporter Pdr5p. J Biol Chem 271, 31543-31548.

Lamping, E., Monk, B.C., Niimi, K., Holmes, A.R., Tsao, S., Tanabe, K., Niimi, M., Uehara, Y., Cannon, R.D., (2007) Characterization of three classes of membrane proteins involved in fungal azole resistance by functional hyperexpression in Saccharomyces cerevisiae. Eukaryot Cell 6, 1150-1165.
Lenoir, G., Williamson, P., Puts, C.F., Holthuis, J.C., (2009a) Cdc50p plays a vital role in the ATPase reaction cycle of the putative aminophospholipid transporter Drs2p. J Biol Chem 284, 17956-17967.
Lenoir, G., Williamson, P., Puts, C.F., Holthuis, J.C., (2009b) Cdc50p plays a vital role in the ATPase reaction cycle of the putative aminophospholipid transporter Drs2p. The Journal of biological chemistry 284, 17956-17967.
Li, M., Hays, F.A., Roe-Zurz, Z., Vuong, L., Kelly, L., Ho, C.M., Robbins, R.M., Pieper, U., O'Connell, J.D., 3rd, Miercke, L.J., Giacomini, K.M., Sali, A., Stroud, R.M., (2009) Selecting optimum eukaryotic integral membrane proteins for structure determination by rapid expression and solubilization screening. Journal of molecular biology 385, 820-830.
Manente, M., Ghislain, M., (2009) The lipid-translocating exporter family and membrane phospholipid homeostasis in yeast. FEMS Yeast Res 9, 673-687.
Midgett, C.R., Madden, D.R., (2007) Breaking the bottleneck: eukaryotic membrane protein expression for high-resolution structural studies. J Struct Biol 160, 265-274.
Monk, B.C., Goffeau, A., (2008) Outwitting multidrug resistance to antifungals. Science 321, 367-369.
Monne, M., Chan, K.W., Slotboom, D.J., Kunji, E.R., (2005) Functional expression of eukaryotic membrane proteins in Lactococcus lactis. Protein Sci.
Nakamura, K., Niimi, M., Niimi, K., Holmes, A.R., Yates, J.E., Decottignies, A., Monk, B.C., Goffeau, A., Cannon, R.D., (2001) Functional expression of Candida albicans drug efflux pump Cdr1p in a Saccharomyces cerevisiae strain deficient in membrane transporters. Antimicrob Agents Chemother 45, 3366-3374.
Niimi, M., Wada, S., Tanabe, K., Kaneko, A., Takano, Y., Umeyama, T., Hanaoka, N., Uehara, Y., Lamping, E., Niimi, K., Tsao, S., Holmes, A.R., Monk, B.C., Cannon, R.D., (2005) Functional analysis of fungal drug efflux transporters by heterologous expression in Saccharomyces cerevisiae. Jpn J Infect Dis 58, 1-7.
Osterberg, M., Kim, H., Warringer, J., Melen, K., Blomberg, A., von Heijne, G., (2006) Phenotypic effects of membrane protein overexpression in Saccharomyces cerevisiae. Proc Natl Acad Sci U S A 103, 11148-11153.
Paulusma, C.C., Folmer, D.E., Ho-Mok, K.S., de Waart, D.R., Hilarius, P.M., Verhoeven, A.J., Oude Elferink, R.P., (2008) ATP8B1 requires an accessory protein for endoplasmic reticulum exit and plasma membrane lipid flippase activity. Hepatology 47, 268-278.
Rogers, B., Decottignies, A., Kolaczkowski, M., Carvajal, E., Balzi, E., Goffeau, A., (2001) The pleitropic drug ABC transporters from Saccharomyces cerevisiae. J Mol Microbiol Biotechnol 3, 207-214.
Rutledge, R.M., Esser, L., Ma, J., Xia, D., (2011) Toward understanding the mechanism of action of the yeast multidrug resistance transporter Pdr5p: a molecular modeling study. Journal of structural biology 173, 333-344.

Serrano, R., (1988) H+-ATPase from plasma membranes of Saccharomyces cerevisiae and Avena sativa roots: purification and reconstitution. Methods Enzymol 157, 533-544.
Simonics, T., Kozovska, Z., Michalkova-Papajova, D., Delahodde, A., Jacq, C., Subik, J., (2000) Isolation and molecular characterization of the carboxy-terminal pdr3 mutants in Saccharomyces cerevisiae. Curr Genet 38, 248-255.
Zhou, X., Graham, T.R., (2009) Reconstitution of phospholipid translocase activity with purified Drs2p, a type-IV P-type ATPase from budding yeast. Proceedings of the National Academy of Sciences of the United States of America 106, 16586-16591.
Zutz, A., Gompf, S., Schagger, H., Tampe, R., (2009) Mitochondrial ABC proteins in health and disease. Biochim Biophys Acta 1787, 681-690.

Figure Legends

Figure 1. Schematic representation of the cloning strategy employed in this study. The gene of interest is cloned and is preceded by an auxotrophy marker for histidine, Pdr5 promoter and N-terminus 14His tag for further purification. This entire DNA segment is part of the pRE5 plasmid and is propagated in *E. coli*. Plasmid isolation and subsequent restriction digestion releases this fragment and it is then transformed into competent *S. cerevisiae* cells where it undergoes homologous recombination and the gene of interest is chromosomally integrated.

Figure 2. Upper panel - Coomassie stained gel showing Pdr5, Yor1, Rsb1 and Drs2. Lower panel - Western blots of Pdr5 with α-Pdr5 antibodies, Yor1 and Rsb1 with anti-His antibodies, Drs2 with α-Drs2 antibodies and Mdl1 with an α-Mdl1 antibodies. An asterisk next to the SDS PAGE gels indicates the purified protein.

Table Legends

Table 1 Primers used in this study.

Figures

Figure 1.

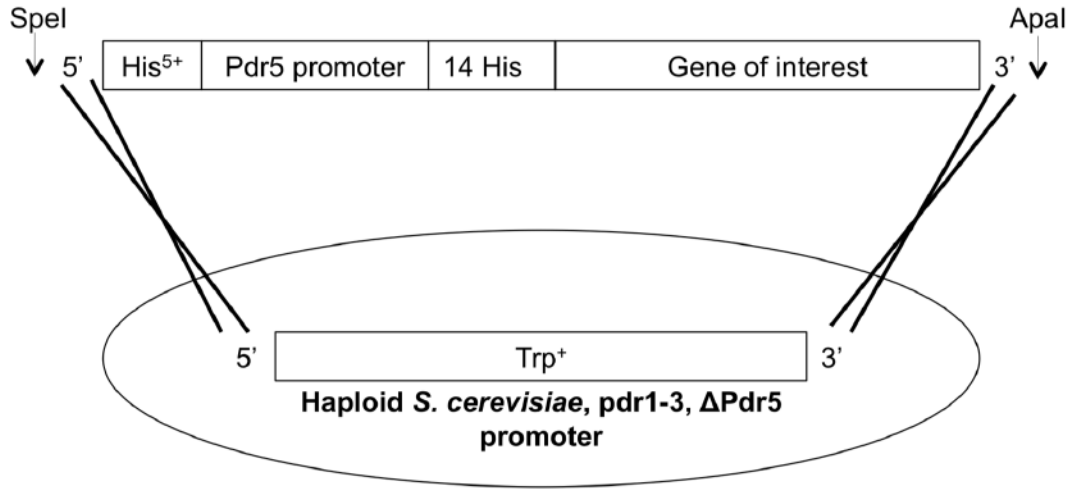

Figure 2.

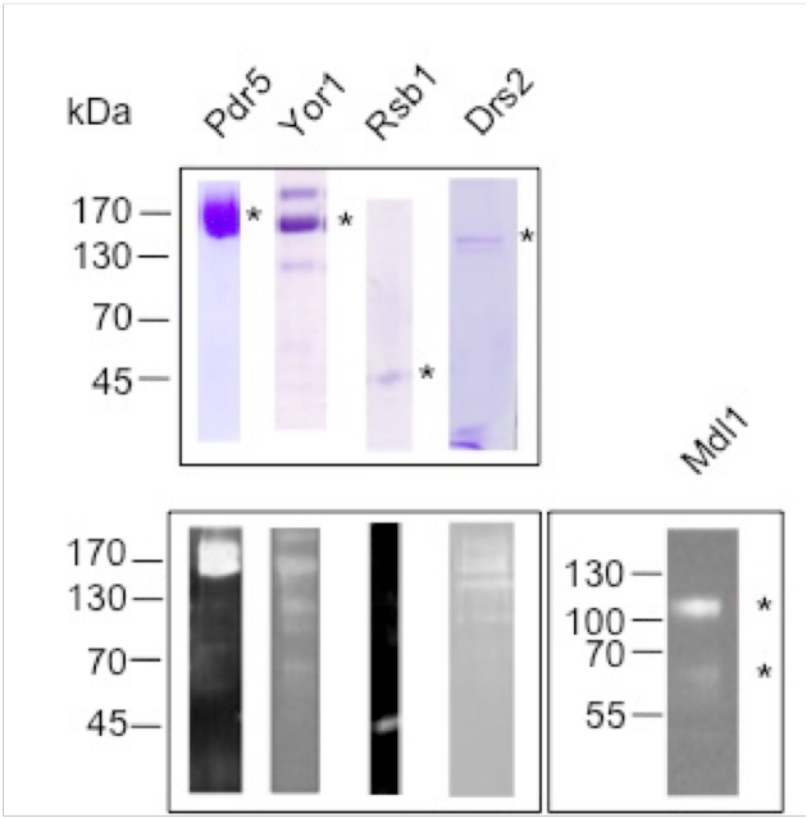
kDa
Pdr5
Yor1
Rsb1
Drs2
170
130
70
45
*
*
*
*
170
130
70
45
Mdl1
130
100
70
55
*
*

Table 1.

Primers used for cloning	Sequence
Pdr5-S	CCTATTACAATAAACAATTAAGCCATACTCGCAACAA TTTGCCTCATCGATGAATTCGAGCTCG
Pdr5-AS	CGTCGTTGACGTTATTGTTAAGCTTGGCCTCGGGCA TTCTACCTTCAATACCACC
Yor1-S	CGCTTCTATTTTCCTCCCCACCGCGAGGCGGAAATG TCATCGATGAATTCGAGCTCG
Yor1-AS	CCAGCTCCGTCTCCGAAACTGCATCCCCCACGGTAA TCGTTCTACCTTCAATACCACCACCATGGTGATG
Rsb1-S	CGACGTTGCCTAGTAGTTGTGGCAGCTCCGATAGTT GACATTCTCATCGATGAATTCGAGCTCG
Rsb1-AS	GGCAAAAGACTGCCTAACGTATTATTTGTTGCGTTGG ATCTACCTTCAATACCACCACCATGGTGATG
Mdl1 Δ59-S	GTGGCTGGTACTGGCGTTTCGTTTAGGCGCATCGAGCCGAGA CTTCATCGATGAATTCGAGCTCG
Mdl1 Δ59-AS	GGGCTTGGTGGACTTCTTTCCTTGCGCAATGTCTGA TTGTCTACCTTCAATACCACCACCATGGTGATG
Drs2-S	CGGATGAAATGTCACTGAAATCTTCCTGATCACGTGATTGGC TTTCATCGATGAATTCGAGCTCG
Drs2-AS	CGTGTCGTCCTCCCCAGGTTTCCTCTTTGGGGGGGT TTCTCTGTCGTCATTTCTACCTTCAATACCACCACCA

S: Sense; AS: Antisense

Proportionate work on the manuscript: 50%

Journal: Journal of Biotechnology (to be submitted shortly)

Impact factor: 3.183

Publication VI

Alternate mechanisms of overcoming drug resistance in *Saccharomyces cerevisiae* revealed by complete proteome analysis

Rakeshkumar P. Gupta[1], Anja Stefanski[2], Kai Stühler[2], Nils Hanekop[1] and Lutz Schmitt[1,*]

1: Institute of Biochemistry, Heinrich Heine University Düsseldorf, Universitätsstr. 1, 40225 Düsseldorf Germany

2: Molecular Proteomics Laboratory, BMFZ, Heinrich Heine University Düsseldorf, Universitätsstr. 1, 40225 Düsseldorf Germany

*: To whom correspondence should be addressed:
Lutz Schmitt
Institute of Biochemistry
Heinrich Heine University Düsseldorf
Universitätsstr. 1
40225 Düsseldorf, Germany
Phone: +49(0)211-81-10773
Fax: +49(0)211-81-15310
Email: lutz.schmitt@hhu.de

Abstract

Saccharomyces cerevisiae is an organism well known for its ability to adapt to various kinds of stress. Stress posed by toxic compounds is dealt by extruding it to the extracellular surface using multidrug efflux pumps as one of the means of survival. Pdr5 is one such membrane protein that protects the yeast cells from xenotoxic compounds. In a previous study we observed increased resistance of certain mutants of Pdr5 that exhibited increased tolerance towards the dye rhodamine 6g, although these mutants were incapable of transporting the drug due to non-functional Pdr5. In this study we subjected the mutant and wildtype cells to complete quantitative proteome analysis to better understand the basis for the increased resistance. Our initial observations hint at alternate mechanisms of drug tolerance by increased glycolytic flux in the mutant as compared to wildtype in the presence of rhodamine 6g. This pathway is also dependent on the presence or absence of a functional Pdr5 protein in the membrane possibly due to Pdr5 interactions with hexose transporters. This interaction seems to be different in the wildtype and mutant proteins due to differences in post-translational modifications. In essence this is one of the first studies revealing possible interaction of Pdr5 in activating an alternate drug resistance pathway in yeast.

Keywords

Pleiotropic drug resistance, mass spectrometry, ATP binding cassette transporter

Introduction

Multidrug resistance is a phenomenon commonly encountered during chemotherapy of cancer patients and poses a major hurdle in treatment. It is also relevant in treatment of fungal infections among immunocompromised individuals (*1*). Pleiotropic drug resistance (PDR) is the same phenomena observed in fungi and comprises of the PDR network including multidrug efflux proteins, major facilitator superfamily proteins (MFS) and their transcriptional regulators (*2, 3*). Pdr5 is one such ATP binding cassette transporter from *Saccharomyces cerevisiae.* It is a full size transporter of 170 kDa and is localized in the plasma membrane of yeast. Although its physiological substrate is still unknown, it is responsible for extrusion of a variety of compounds from the cell to the extracellular surface up on encountering (*4*).

The full size transporter possesses two cytoplasmically located nucleotide binding domains (NBDs) that bind and hydrolyze nucleotides (mainly ATP) and use it as an energy source to transport substrates across the membrane bilayer. In addition there are two transmembrane domains (TMDs) that span the bilayer and possess the substrate binding pocket(s). Pdr5 belongs to the category of uncoupled ABC transporters, which hydrolyze ATP constantly regardless of any substrate being present and display no substrate stimulated increase in ATPase activity (*5, 6*). In addition Pdr5 along with other fungal ABC transporters displays a degenerate nucleotide binding site (NBS) that characterizes the ability to hydrolyze ATP at only one canonical site out of the two due to absence of key residues at the degenerate site (*6, 7*). In a previous study we exchanged all the degenerate amino acid residues with their consensus counterparts and studied its effects on protein function and *in vivo* drug resistance (manuscript submitted for publication). Our observations revealed that a number of mutants displayed increased resistance towards rhodamine 6g as compared to the wild type cells, although these mutants were unable to transport rhodamine 6g and possessed low if any Pdr5 specific ATPase activity (manuscript submitted for publication). Chiefly among these mutants was the ABHC mutant that has a completely restored degenerate NBS comprising of the mutations in Walker A - P195S, C199K; Walker B – N334E, H

loop – Y367H and C loop – N1011S, V1012G, E1013G. This mutant was named 'ABHC' mutant and shall be referred as such henceforth. Microscopic examination of these cells showed accumulation of rhodamine 6g within the cells in addition to them being viable. Mechanisms to overcome drug resistance in yeast have been studied in the past. Vacuolar accumulation or biotransformation of the toxic compound are some of the methods that the yeast cell employs to counteract drug toxicity (*8-11*). We on the other hand observed an accumulation of the drug throughout the cytoplasm and the emission spectra of the dye remained the same. Hence we subjected the cells to complete quantitative proteome analysis using mass spectrometry to understand the molecular basis of this increased drug tolerance. Our initial observations point in a direction of the involvement of Pdr5 interaction with other membrane proteins including hexose transporters residing in the membrane that leads to increased import and accumulation of glucose in the ABHC mutant as compared to wild type. This interaction seems to be dependent up on post-translational modifications of Pdr5, which are presumably different in the wild type and ABHC mutant.

This is the first study suggesting a direct role of the interaction of an ABC transporter with other membrane proteins in initiating alternate mechanisms of drug resistance in yeast.

Materials and Methods

Yeast Strains and Plasmid Mutagenesis

Yeast strains were cultured in YPD medium containing 10g/l yeast extract, 20g/l peptone and 2% glucose. The following *S. cerevisiae* strains were used in this study: YALF-A1 (*MATa; ura3-52 trp 1-1 leu 2-3, his 3-11, 15 ade 2-1 PDR 1-3*), YHW-A5 (*MATa; ura3-52 trp 1-1 leu 2-3, his 3-11, 15 ade 2-1 PDR 1-3 pdr5Δ::TRP1*), and YRE1001 (*MATa; ura3-52 trp 1-1 leu 2-3, his 3-11, 15 ade 2-1 PDR 1-3 pdr5pdr5promΔ::TRP1*). Details about plasmid and strain construction can be found in (*6*) and supplementary table S1. Site-directed mutagenesis of *pdr5* was performed on plasmid pRE5 with the QuickChange II XL site-directed mutagenesis kit (Stratagene).

Liquid drug assay

Rhodamine 6g (R6G) was obtained from Sigma-Aldrich. All drug stock solutions were prepared in dimethyl sulfoxide (DMSO, Acros Organics) and further dilutions were carried out in sterile water. Assay was carried out in sterile 96 well microtiter plates (Falcon) with 20 µl drug, 180 µl YPD medium and 50 µl of OD_{600} 0.2 yeast culture. Plates were incubated at 30°C for 48 hours and OD_{600} was measured with an elisa plate reader (Fluostar-Optima).

Quantitative Proteome analysis using Mass spectrometry

Mass spectrometric analyses of whole cell lysates were carried out using a label-free MS approach for quantification. Extracted peptides were analyzed with a nano-HPLC/ESI-MS system (RSLCnano™ U3000 HPLC, Thermo Fisher Scientific, Bremen, Germany) online coupled with a LTQ Orbitrap Elite™ (Thermo Fisher Scientific, Bremen, Germany) mass spectrometer equipped with a nano-electrospray ion source (nano-ESI). 300 ng of each sample were loaded onto a C_{18} trapping column (Acclaim PepMap C_{18}, 2 cm × 100 μm × 5 μm, 100 Å, Thermo Fisher Scientific) and desalted with 0.1% trifluoroacetic acid (TFA) for 10 minutes. Peptides were eluted from the trap column and subsequently separated using an analytical column (Acclaim PepMap RSLC C_{18}; 25 cm × 75 μm × 2 μm, 100 Å, Thermo Fisher Scientific) for 120 minutes with a

flow rate of 300 nL/min before spraying into the MS. The mobile phase for chromatography consisted of 0.1% formic acid in water (solvent A) and 84% acetonitrile, 0.1% formic acid in water (solvent B). The gradient started with 4% B, ramped to 10% B in 5 min, 20% B in 62 min, 30% B in 35 min, 40% B in 15 min and 95% B in 2 min. System parameters were as follows: spray voltage, 1.4 kV; ion transfer tube temperature, 275 °C; collision gas, helium; collision gas pressure, 1.3 mTorr; normalized collision energy for MS/MS, 35%. The Orbitrap Elite was operated in a TOP20 data-dependent mode to automatically switch between MS and MS/MS acquisition. MS-spectra were acquired in the Orbitrap with a mass range of 350-1700 m/z and a resolution of 60,000. Polysiloxane (445.120030 Th) was used as lock mass. For MS/MS, ions were isolated with an isolation width of 2 m/z and fragmented using collision-induced dissociation (CID). MS/MS-spectra were acquired in the linear ion trap in centroid mode. Target ions selected for MS/MS were dynamically excluded for 45 sec. The ion selection threshold for MS/MS was 500 counts. For protein identification Proteome Discoverer™ (version 1.3, Thermo Fisher Scientific) and MASCOT™ search engine (version 2.4.1, Matrix Science, London, UK) were used. MS/MS-spectra were searched against the UniProtKB/Swiss-Prot database (7799 yeast sequences; date 25/09/2013). Search parameters were as follows: enzyme: trypsin; 2 maximum missed cleavage sites; taxonomy: *Saccharomyces cerevisiae*; 10 ppm precursor mass tolerance; 0.4 Da fragment mass tolerance; oxidation of methionine as dynamic modification; carbamidomethylation of cysteine as fixed modification. The false discovery rate (FDR) was set to 1% ($p \leq 0.01$). If identified peptides are shared between two proteins, these are combined and reported as one protein group. Label-free quantification was carried out using ProgenesisTM LC-MS (Nonlinear Dynamics, Newcastle upon Tyne, UK). A minimum of 2 unique peptides were required for quantification. Proteins with a significant (anova <0.01) abundance change of 2.0 were considered as differentially regulated. Proteins with less than 2 quantifiable peptides were excluded.

Results

Proteome analysis reveals significant differences between WT and ABHC mutant

Initial observations during the liquid drug assay with rhodamine 6g displayed increase of resistance in the ABHC mutant as compared to Pdr5WT (Figure 1). Concentration of more than 7.5μg/ml dye was detrimental to the wildtype cells while the ABHC mutant could withstand 15μg/ml rhodamine 6g. Although biochemical data suggested that the ABHC mutant was unable to transport rhodamine 6g and that the Pdr5 specific ATPase activity was also very low (Table 1)(data taken from the submitted manuscript). This raised questions about the reasons for the increased drug tolerance in this particular mutant. To check whether any other transporters are counterbalacing the transport deficient Pdr5 mutant and in fact transporting rhodamine 6g, we analysed the cells from the liquid drug assay using confocal microscopy. Here, it was evident that there is accumulation of rhodamine 6g within the ABHC mutant cells and strikingly that these cells are alive as well as could tolerate twice as much rhodamine 6g when compared to the wildtype cells (data from submitted manuscript). In order to understand the underlying molecular mechanisms we subjected the wildtype and ABHC mutant cells with and without rhodamine 6g to a complete quantitative proteome analysis. The data obtained is summarized in Tables 2 and 3. As can clearly be observed there is significantly increased levels of glycolytic enzymes in the ABHC mutant cells after exposure to rhodamine 6g as compared to wildtype. This observation holds true for both concentrations of rhodamine 6g tested i.e 6 μg/ml for both WT and ABHC (Table 2) and 7.5 μg/ml for WT and 15 μg/ml for ABHC (Table 3). Also surprisingly it was noted that the fold increase in the levels of glycolytic enzymes was greater when the concentration of rhodamine 6g was higher. This observation also revealed significant down regulation of mitochondrial enzymes involved in ATP synthesis. Alcohol dehydrogenase levels were also significantly up regulated in the ABHC mutant with 15 μg/ml rhodamine 6g. Interestingly the TCA cycle enzymes for the ABHC mutants relatively recovered in the presence of higher concentration of the drug, this could possibly be due to increase in expression levels following an initial down regulation due to

increased cellular energy levels. The most significant changes in the protein levels obtained for wildtype and ABHC mutants in the presence of 6 μg/ml rhodamine 6g are graphically represented in Figure 2 A-D. The proteins being down regulated in the presence of the dye although similar in proportion but are significantly different in terms of numbers between wildtype and ABHC (Figure 2A and 2B). Notably the TCA cycle enzymes and electron transport chain enzymes are down regulated only in the ABHC mutant (Figure 2B). In addition the protein level up regulation in both the wildtype and ABHC mutant in the presence of rhodamine 6g is displayed in Figure 2C and 2D. Notably here too the number of proteins up regulated in the ABHC mutant is significantly higher. Also the presence of glycolytic enzymes is seen clearly for the mutant (Figure 2D) where it is up regulated.

Effect of glucose on growth rates

The analysis of the proteome analysis revealed differences in glycolytic rates of the ABHC and wildtype cells. In order to investigate this we carried out liquid drug assays with varying glucose concentrations (1%-4%) with the mutants and included two additional controls i.e. ΔPdr5, which is a knock-out strain lacking Pdr5 and the Pdr5 K911A mutant, which is a mutant of Pdr5 that is phenotypically similar to ABHC in terms of low ATPase activity and no rhodamine 6g transport. The results of this experiment are summarized in Figure 3. As can be noted, the wildtype cells are the slowest to adapt to low concentrations of glucose (1%) (Figure 3A), while the ABHC, ΔPdr5 and K911A cells are much faster adapting and consequently are capable in glucose uptake at low as well as high concentrations of glucose (Figure 3 B-D). This is an important observation considering that the mitochondrial energy generating machinery is down regulated (Table 2 and 3), and glycolysis is the only source of energy for these cells (although less efficient). The wildtype cells which possess a functionally active Pdr5 that is capable of transporting rhodamine 6g also has a high level basal ATPase activity. This in turn seems to take a toll on the wildtype cells in a situation where rhodamine 6g affects mitochondria and the energy reserves in the cell are depleted. On the other hand the ABHC, ΔPdr5 and K911A mutant cells that have considerably low energy demands due to

inactive or complete absence of Pdr5 are able to cope with the challenge posed by rhodamine 6g in a much better way. It is also seen that the levels of a low affinity glucose transporter Hxt3 was being differentially regulated in the wildtype and ABHC mutant (Table 3). On exposure to rhodamine 6g this transporter was being down regulated to about 2 fold in wildtype while in the ABHC mutant there was 6 fold up regulation in its levels. Also one of the necessities for maintenance of high rates of glycolytic flux is the replenishment of NAD+ pools, this was indeed observed by the significant up regulation of alcohol dehydrogenase enzyme upon addition of rhodamine 6g to the ABHC mutant cells.

Discussion

Yeast cells possess multiple and redundant biochemical pathways that allow it to adapt and survive under stress from various internal and external sources (*12, 13*). The response of yeast cells under carbon, nitrogen and oxygen limiting conditions has been well studied (*14, 15*). Also the adaptation of these cells during fermentation with various carbon sources has been well documented (*12, 16*).

Our observation with the ABHC mutant being able to withstand elevated levels of rhodamine 6g as compared to wildtype without transporting it was extremely surprising and obviously counterintuitive. One needs to note that rhodamine 6g is not an extremely toxic compound unlike some others and cells possibly have time to adapt and respond to this source of stress. Pdr5 being a membrane protein has been shown to interact with a number of other membrane and cytosolic proteins (*17, 18*). Notably among this inventory are hexose transporters that reside in the membrane bilayer and are responsible for import of glucose inside the cell (*19, 20*). The interaction between Pdr5 and hexose transporters is a very likely scenario, although the effect of this interaction on the functioning of one or both partners is unknown. According to our observations with respect to the wildtype and ABHC mutant we detect important differences in the response of these two cell types to the presence of rhodamine 6g. The down regulation of mitochondrial ATP synthesis machinery clearly indicates low energy levels in the cells, while elevated glycolytic enzymes indicate presence of sufficient glucose and a response to generate more ATP. It seems the ABHC, ΔPdr5 and K911A cells are better in their response than the wildtype cells, although the ΔPdr5 and K911A cells are much more sensitive towards rhodamine 6g than ABHC or wildtype. This observation indicates that although ABHC, ΔPdr5 and K911A are phenotypically similar their response towards rhodamine 6g resistances is very different. This is likely a result of protein-protein interaction between Pdr5 and other (membrane) proteins. The response of the cell to up regulate glycolytic enzymes in the presence of rhodamine 6g occurs at a much earlier stage in the ABHC mutant as compared to wildtype. This is possible because the wildtype cells can actually

transport rhodamine 6g and the intracellular concentrations are fairly low until a certain threshold is reached (Figure 2A-D and Table 2, Table 3). The alternate mechanism of increased glucose metabolism as we believe is a result of Pdr5 interaction with hexose transporters residing in the membrane. This interaction in turn is different between wildtype and ABHC mutant owing to differences in post-translational modifications of these two proteins. This hypothesis also holds true for K911A, which is functionally deficient and ΔPdr5 that completely lacks Pdr5 and hence the alternate pathway is not activated and as a result the cells are hypersensitive towards rhodamine 6g. Our hypothesis is supported by observations where the transcriptional regulators, Pdr1 and Pdr3, controlling Pdr5 among other MDR transporters also regulate expression of hexose transporters (*20, 21*). Moreover glucose accumulation in anticipation of stress has also been shown with yeast cells (*22*). Retrograde phenomenon involving direct communication between mitochondria and nucleus via transcriptional factors has also been well studied (*23-25*). Although in our studies we could not detect and quantify these transcription factors possibly due to their low level of cellular expression, it cannot be ruled out that they indeed play a crucial role in our observation of increased drug resistance. The involvement of a multidrug efflux pump in such phenomena has not been seen prior to this study, moreover further details could reveal a much greater role for multidrug pumps in other physiological processes in the cell.

Acknowledgements

We thank Ulrich Schulte for important discussions and Marco Oldiges, Research Center Jülich for valuable experimental support. This work was funded by the Heinrich Heine University Düsseldorf..

References

1. Gottesman, M. M., and Ambudkar, S. V. (2001) Overview: ABC transporters and human disease, *J Bioenerg Biomembr 33*, 453-458.
2. Balzi, E., and Goffeau, A. (1991) Multiple or pleiotropic drug resistance in yeast, *Biochim Biophys Acta 1073*, 241-252.
3. Balzi, E., and Goffeau, A. (1994) Genetics and biochemistry of yeast multidrug resistance, *Biochim Biophys Acta 1187*, 152-162.
4. Rogers, B., Decottignies, A., Kolaczkowski, M., Carvajal, E., Balzi, E., and Goffeau, A. (2001) The pleitropic drug ABC transporters from Saccharomyces cerevisiae, *J Mol Microbiol Biotechnol 3*, 207-214.
5. Decottignies, A., Grant, A. M., Nichols, J. W., de Wet, H., McIntosh, D. B., and Goffeau, A. (1998) ATPase and multidrug transport activities of the overexpressed yeast ABC protein Yor1p, *J Biol Chem 273*, 12612-12622.
6. Ernst, R., Kueppers, P., Klein, C. M., Schwarzmueller, T., Kuchler, K., and Schmitt, L. (2008) A mutation of the H-loop selectively affects rhodamine transport by the yeast multidrug ABC transporter Pdr5, *Proc Natl Acad Sci U S A 105*, 5069-5074.
7. Gupta, R. P., Kueppers, P., Schmitt, L., and Ernst, R. (2011) The multidrug transporter Pdr5: a molecular diode?, *Biol Chem 392*, 53-60.
8. Rossignol, T., Kelly, B., Dobson, C., and d'Enfert, C. (2011) Endocytosis-mediated vacuolar accumulation of the human ApoE apolipoprotein-derived ApoEdpL-W antimicrobial peptide contributes to its antifungal activity in Candida albicans, *Antimicrob Agents Chemother 55*, 4670-4681.
9. Lee, M. E., Singh, K., Snider, J., Shenoy, A., Paumi, C. M., Stagljar, I., and Park, H. O. (2011) The Rho1 GTPase acts together with a vacuolar glutathione S-conjugate transporter to protect yeast cells from oxidative stress, *Genetics 188*, 859-870.
10. Han, X., Lai, L., Tian, F., Jiang, F. L., Xiao, Q., Li, Y., Yu, Q., Li, D., Wang, J., Zhang, Q., Zhu, B., Li, R., and Liu, Y. (2012) Toxicity of CdTe quantum dots on yeast Saccharomyces cerevisiae, *Small 8*, 2680-2689.
11. Liu, Z. L. (2011) Molecular mechanisms of yeast tolerance and in situ detoxification of lignocellulose hydrolysates, *Appl Microbiol Biotechnol 90*, 809-825.
12. Querol, A., Fernandez-Espinar, M. T., del Olmo, M., and Barrio, E. (2003) Adaptive evolution of wine yeast, *Int J Food Microbiol 86*, 3-10.
13. Gasch, A. P., and Werner-Washburne, M. (2002) The genomics of yeast responses to environmental stress and starvation, *Funct Integr Genomics 2*, 181-192.
14. Zhao, X. Q., and Bai, F. W. (2009) Mechanisms of yeast stress tolerance and its manipulation for efficient fuel ethanol production, *J Biotechnol 144*, 23-30.
15. Arbat, O. B., Semchyshyn, H. M., and Lushchak, V. I. (2008) [Acid stress in yeast Saccharomyces cerevisiae], *Ukr Biokhim Zh 80*, 19-31.
16. Bisson, L. F., Karpel, J. E., Ramakrishnan, V., and Joseph, L. (2007) Functional genomics of wine yeast Saccharomyces cerevisiae, *Adv Food Nutr Res 53*, 65-121.

17. Snider, J., Hanif, A., Lee, M. E., Jin, K., Yu, A. R., Graham, C., Chuk, M., Damjanovic, D., Wierzbicka, M., Tang, P., Balderes, D., Wong, V., Jessulat, M., Darowski, K. D., San Luis, B. J., Shevelev, I., Sturley, S. L., Boone, C., Greenblatt, J. F., Zhang, Z., Paumi, C. M., Babu, M., Park, H. O., Michaelis, S., and Stagljar, I. (2013) Mapping the functional yeast ABC transporter interactome, *Nat Chem Biol 9*, 565-572.
18. Stark, C., Breitkreutz, B. J., Chatr-Aryamontri, A., Boucher, L., Oughtred, R., Livstone, M. S., Nixon, J., Van Auken, K., Wang, X., Shi, X., Reguly, T., Rust, J. M., Winter, A., Dolinski, K., and Tyers, M. (2011) The BioGRID Interaction Database: 2011 update, *Nucleic Acids Res 39*, D698-704.
19. Wills, C. (1990) Regulation of sugar and ethanol metabolism in Saccharomyces cerevisiae, *Crit Rev Biochem Mol Biol 25*, 245-280.
20. Ozcan, S., and Johnston, M. (1999) Function and regulation of yeast hexose transporters, *Microbiol Mol Biol Rev 63*, 554-569.
21. Nourani, A., Wesolowski-Louvel, M., Delaveau, T., Jacq, C., and Delahodde, A. (1997) Multiple-drug-resistance phenomenon in the yeast Saccharomyces cerevisiae: involvement of two hexose transporters, *Mol Cell Biol 17*, 5453-5460.
22. Dikicioglu, D., Oc, S., Rash, B. M., Dunn, W. B., Pir, P., Kell, D. B., Kirdar, B., and Oliver, S. G. (2013) Yeast cells with impaired drug resistance accumulate glycerol and glucose, *Mol Biosyst 10*, 93-102.
23. Devaux, F., Carvajal, E., Moye-Rowley, S., and Jacq, C. (2002) Genome-wide studies on the nuclear PDR3-controlled response to mitochondrial dysfunction in yeast, *FEBS Lett 515*, 25-28.
24. Moye-Rowley, W. S. (2005) Retrograde regulation of multidrug resistance in Saccharomyces cerevisiae, *Gene 354*, 15-21.
25. Traven, A., Wong, J. M., Xu, D., Sopta, M., and Ingles, C. J. (2001) Interorganellar communication. Altered nuclear gene expression profiles in a yeast mitochondrial dna mutant, *J Biol Chem 276*, 4020-4027.
26. Tabas-Madrid, D., Nogales-Cadenas, R., and Pascual-Montano, A. (2012) GeneCodis3: a non-redundant and modular enrichment analysis tool for functional genomics, *Nucleic Acids Res 40*, W478-483.
27. Nogales-Cadenas, R., Carmona-Saez, P., Vazquez, M., Vicente, C., Yang, X., Tirado, F., Carazo, J. M., and Pascual-Montano, A. (2009) GeneCodis: interpreting gene lists through enrichment analysis and integration of diverse biological information, *Nucleic Acids Res 37*, W317-322.
28. Carmona-Saez, P., Chagoyen, M., Tirado, F., Carazo, J. M., and Pascual-Montano, A. (2007) GENECODIS: a web-based tool for finding significant concurrent annotations in gene lists, *Genome Biol 8*, R3.

Table Legends

Table 1.

Biochemical data on ATPase activity and rhodamine 6g transport for Pdr5 WT and ABHC mutant. Mean values of at least three independent experiments are shown and the error bars represent the SD.

Table 2.

Quantitative proteome analysis data depicting fold change in expression levels of respective enzymes in the presence of 6μg/ml rhodamine 6g as compared to without the drug for WT and ABHC mutant. An up regulation is highlighted in green, while down regulation is shown in red.

Table 3.

Quantitative proteome analysis data depicting fold change in expression levels of respective enzymes in the presence of 7.5μg/ml rhodamine 6g as compared to without the drug for WT and 15μg/ml rhodamine 6g for the ABHC mutant as compared to without the drug. Color coding is identical to Table 2

Figure Legends

Figure 1.

Graph representing resistance of different Pdr5 mutants towards rhodamine 6g.

Figure 2.

Graphical representation of the proteome data for Pdr5WT and ABHC mutant in the presence of 6 μg/ml rhodamine 6g. The cut-off threshold for fold change after exposure to rhodamine 6g v/s without rhodamine 6g was set at 1.25 for both data sets. The graphs represent number of proteins being down or up regulated. A. Pdr5WT down regulation, B. ABHC down regulation, C. Pdr5WT up regulation and D. ABHC up regulation. The data was analyzed using the GeneCodis3 analysis software (*26-28*).

Figure 3.

Growth curves of different mutants of Pdr5 in the presence of varying concentrations of rhodamine 6g and glucose. A. Pdr5WT, B. ABHC mutant, C. Delta Pdr5 and D. K911A.

Table 1.

	ATPase activity		R6G transport	
Mutant	**Km [mM]**	**Vmax [μmol/mg*min]**	**Km [nM]**	**Vmax (Relative decrease in fluorescence intensity in 700s)**
Pdr5WT	1.71 ± 0.71	1.33 ± 0.23	20.1 ± 2.9	83.52 ± 5.7
ABHC	1.80 ± 0.50	0.20 ± 0.03	No transport	0.68 ± 0.13

Table 2.

	Enzymes	**Fold change – with R6G/without R6G**	
		WT	**ABHC**
	Glycolysis		
1.	Hexokinase	1	1.8
2.	Phosphohexose isomerase	1.3	2
3.	Phosphofructokinase-1	No change	1.6
4.	Aldolase	No change	1.3
5.	Triosephosphate isomerase	No change	2.4
6.	Glyceraldehyde 3-phosphate dehydrogenase	No change	2
7.	Phosphoglycerate kinase	No change	1.4
8.	Phosphoglycerate mutase	No change	1.3
9.	Enolase	No change	1.6
10.	Pyruvate kinase	1	1.8
	Fermentation		
11.	Pyruvate decarboxylase	1.3	No change
12.	Alcohol dehydrogenase	1.1	2
	TCA cycle		
13.	Pyruvate dehydrogenase complex	No change	No change
14.	Citrate synthase	1.4	3.4
15.	Isocitrate dehydrogenase	1.2	1.3
16.	α-ketoglutarate dehydrogenase complex	No change	2.7
17.	Succinate dehydrogenase	No change	3.9
18.	Fumarase	No change	2.3
19.	Malate dehydrogenase	No change	2.3
	Oxidative phosphorylation		
20.	NADH dehydrogenase	No change	2.6
21.	Succinate dehydrogenase	No change	3.9
22.	Complex Q: cytochrome c oxido-reductase	1.3	3.3
23.	Cytochrome oxidase	1.4	2
24.	ATP synthase	No change	2

Table 3.

	Enzymes	Fold change – with R6G/without R6G	
		WT	ABHC
	Glycolysis		
1.	Hexokinase	2	5.5
2.	Phosphohexose isomerase	2	6
3.	Phosphofructokinase-1	0.7	2.7
4.	Aldolase	1.4	7
5.	Triosephosphate isomerase	1.6	6.4
6.	Glyceraldehyde 3-phosphate dehydrogenase	1.6	7
7.	Phosphoglycerate kinase	1.7	6.4
8.	Phosphoglycerate mutase	2.1	6.6
9.	Enolase	1.9	6
10.	Pyruvate kinase	1.7	5
	Fermentation		
11.	Pyruvate decarboxylase	1.5	8.3
12.	Alcohol dehydrogenase	1.4	5
	TCA cycle		
13.	Pyruvate dehydrogenase complex	1.3	2.3
14.	Citrate synthase	1.6	No change
15.	Isocitrate dehydrogenase	1.6	3
16.	α-ketoglutarate dehydrogenase complex	1.3	2
17.	Succinate dehydrogenase	1.2	1.8
18.	Fumarase	1.4	1.2
19.	Malate dehydrogenase	1.3	No change
	Oxidative phosphorylation		
13.	NADH dehydrogenase	1.9	1.3
14.	Succinate dehydrogenase	1.2	1.8
15.	Complex Q: cytochrome c oxido-reductase	1.6	1.6
16.	Cytochrome oxidase	1	4
17.	ATP synthase	1	4
	Other Protein		
18.	Hxt3, low affinity glucose transporter	2	6

Figure 1.

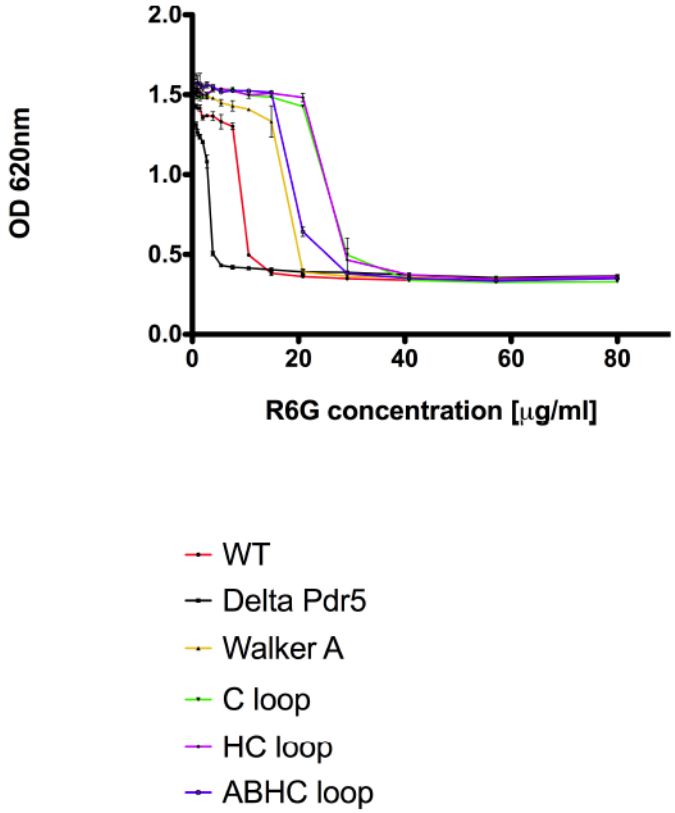
OD 620nm
2.0
1.5
1.0
0.5
0.0
0
20
40
60
80
R6G concentration [μg/ml]
WT
Delta Pdr5
Walker A
C loop
HC loop
ABHC loop

Figure 2.

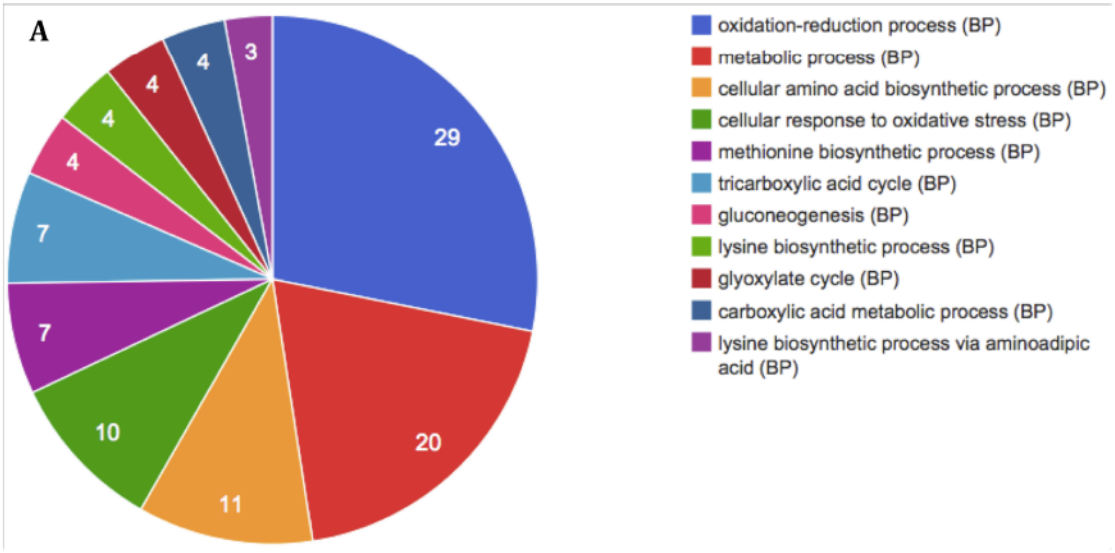
A
29
20
11
10
7
7
4
4
4
4
3
oxidation-reduction process (BP)
metabolic process (BP)
cellular amino acid biosynthetic process (BP)
cellular response to oxidative stress (BP)
methionine biosynthetic process (BP)
tricarboxylic acid cycle (BP)
gluconeogenesis (BP)
lysine biosynthetic process (BP)
glyoxylate cycle (BP)
carboxylic acid metabolic process (BP)
lysine biosynthetic process via aminoadipic acid (BP)

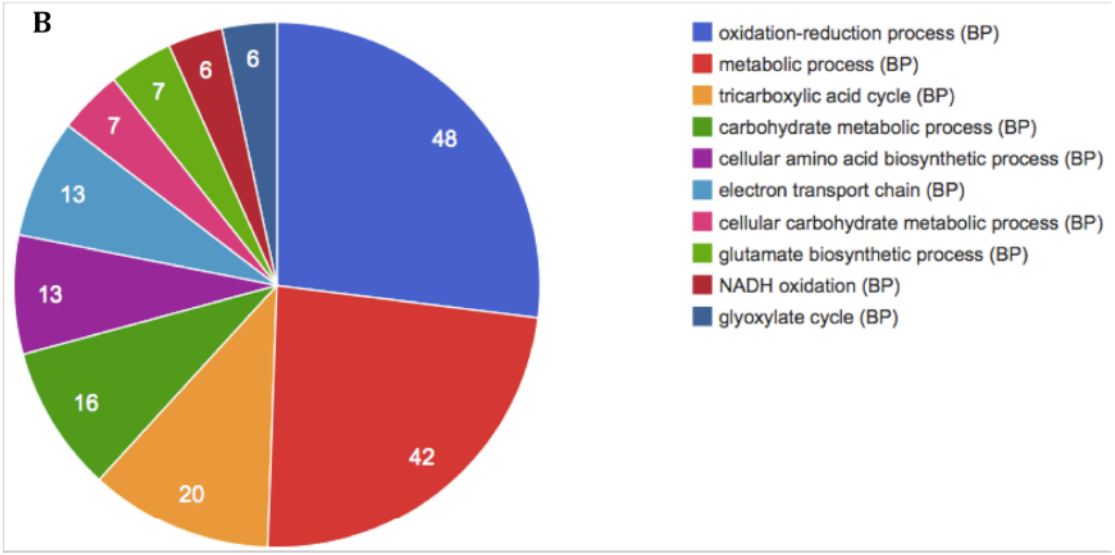
B
48
42
20
16
13
13
7
7
6
6
oxidation-reduction process (BP)
metabolic process (BP)
tricarboxylic acid cycle (BP)
carbohydrate metabolic process (BP)
cellular amino acid biosynthetic process (BP)
electron transport chain (BP)
cellular carbohydrate metabolic process (BP)
glutamate biosynthetic process (BP)
NADH oxidation (BP)
glyoxylate cycle (BP)

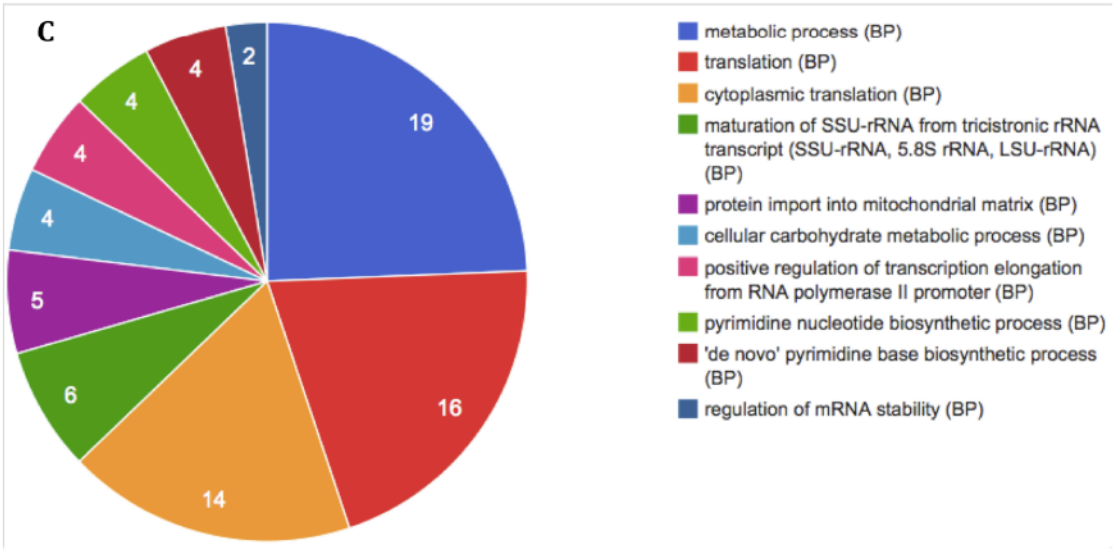
C
19
16
14
6
5
4
4
4
4
2
metabolic process (BP)
translation (BP)
cytoplasmic translation (BP)
maturation of SSU-rRNA from tricistronic rRNA transcript (SSU-rRNA, 5.8S rRNA, LSU-rRNA) (BP)
protein import into mitochondrial matrix (BP)
cellular carbohydrate metabolic process (BP)
positive regulation of transcription elongation from RNA polymerase II promoter (BP)
pyrimidine nucleotide biosynthetic process (BP)
'de novo' pyrimidine base biosynthetic process (BP)
regulation of mRNA stability (BP)

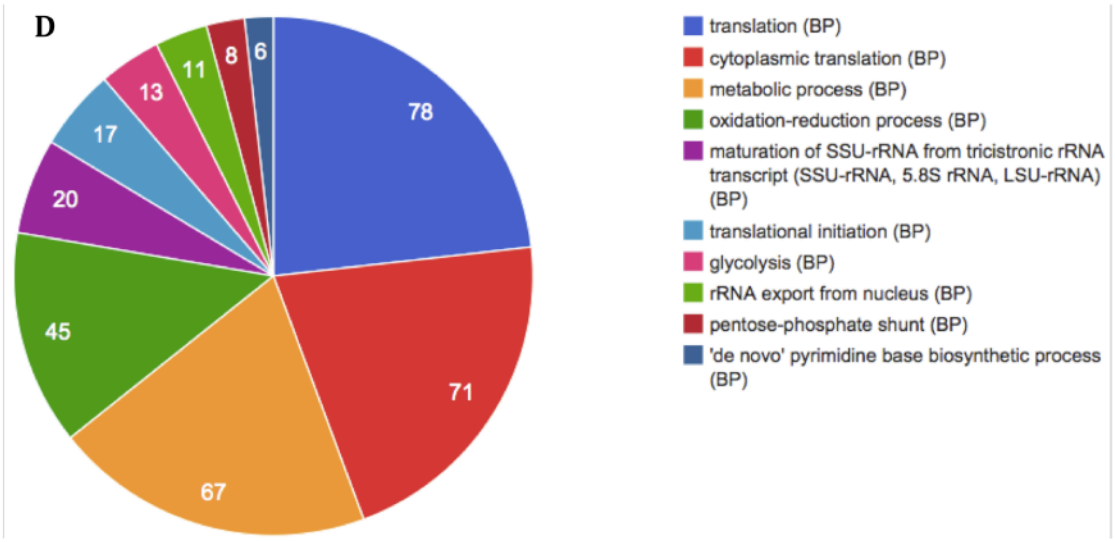
D
78
71
67
45
20
17
13
11
8
6
translation (BP)
cytoplasmic translation (BP)
metabolic process (BP)
oxidation-reduction process (BP)
maturation of SSU-rRNA from tricistronic rRNA transcript (SSU-rRNA, 5.8S rRNA, LSU-rRNA) (BP)
translational initiation (BP)
glycolysis (BP)
rRNA export from nucleus (BP)
pentose-phosphate shunt (BP)
'de novo' pyrimidine base biosynthetic process (BP)

Figure 3.

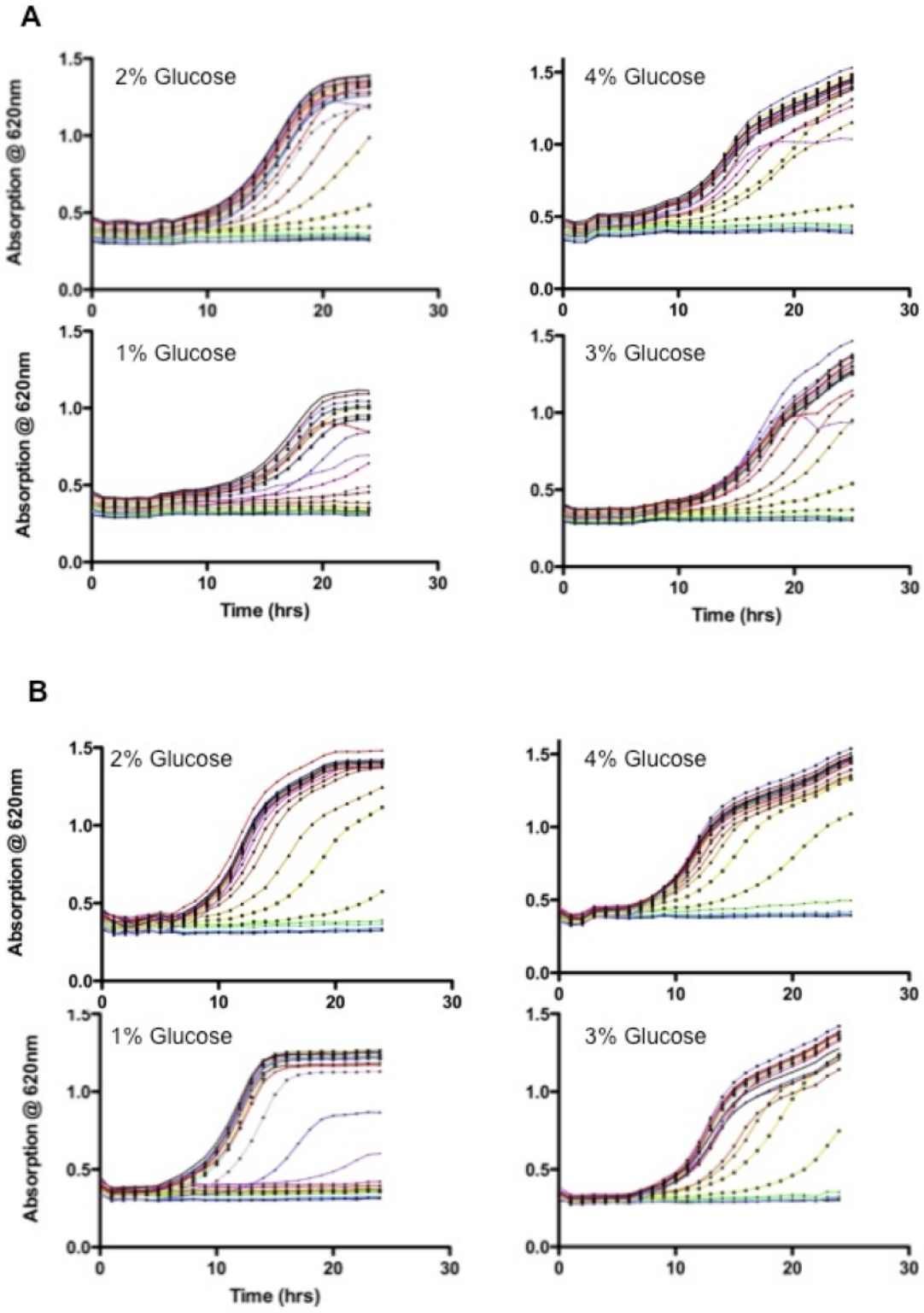
A
2% Glucose
4% Glucose
1% Glucose
3% Glucose
Absorption @ 620nm
Time (hrs)
B
2% Glucose
4% Glucose
1% Glucose
3% Glucose
Absorption @ 620nm
Time (hrs)

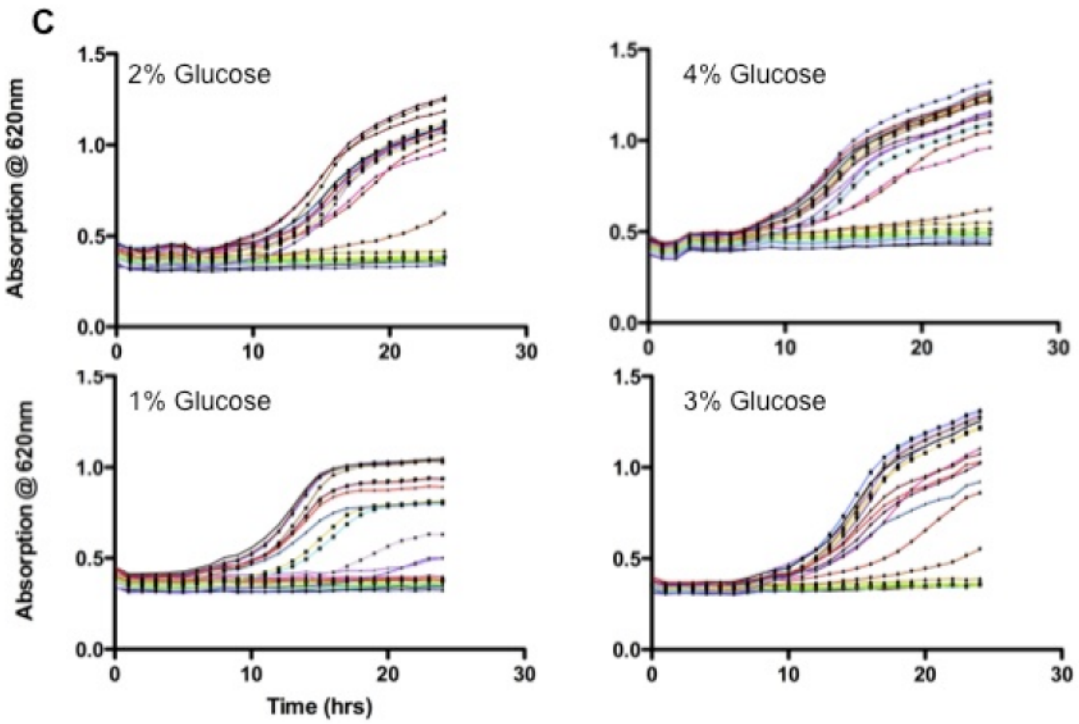
C
2% Glucose
4% Glucose
1% Glucose
3% Glucose
Absorption @ 620nm
Absorption @ 620nm
Time (hrs)

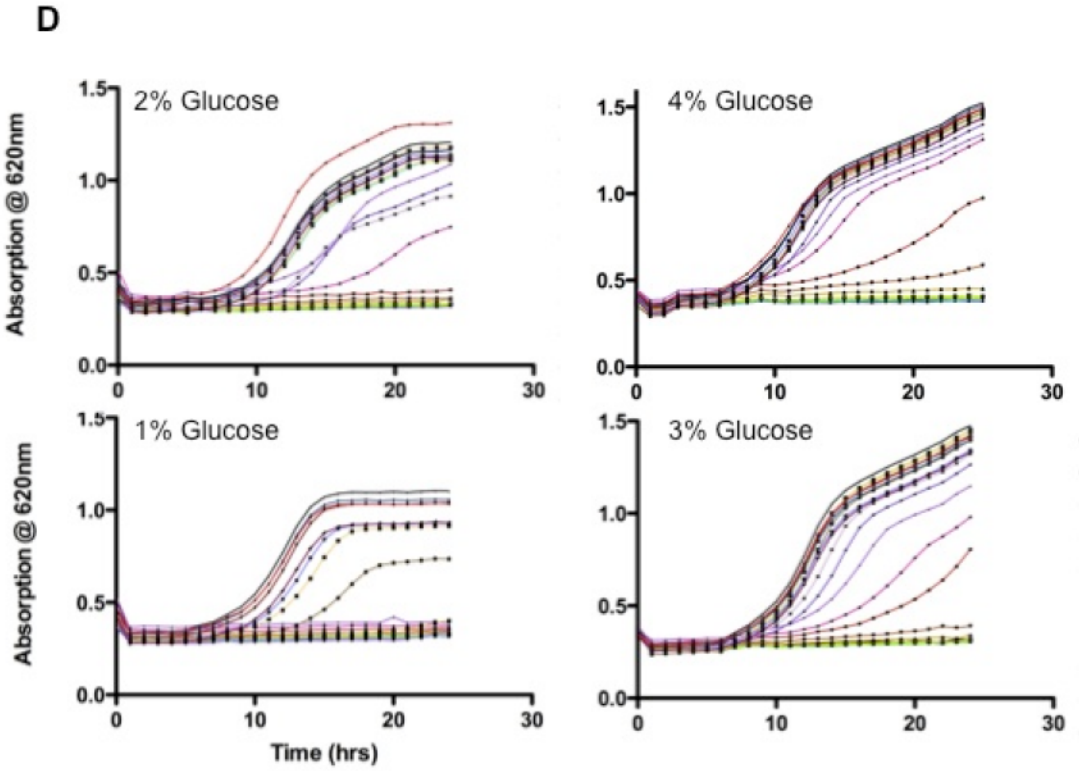
D
2% Glucose
4% Glucose
1% Glucose
3% Glucose
Absorption @ 620nm
Absorption @ 620nm
Time (hrs)

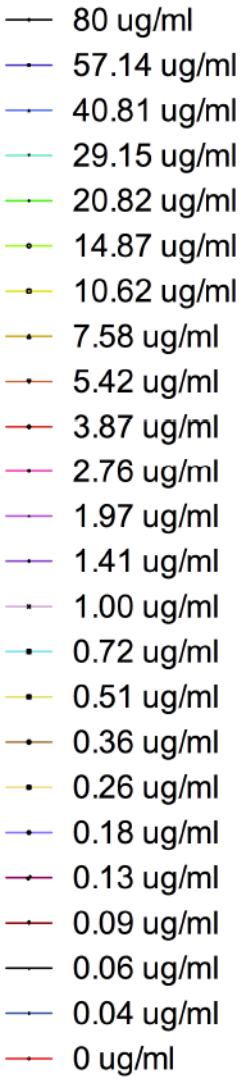
80 ug/ml
57.14 ug/ml
40.81 ug/ml
29.15 ug/ml
20.82 ug/ml
14.87 ug/ml
10.62 ug/ml
7.58 ug/ml
5.42 ug/ml
3.87 ug/ml
2.76 ug/ml
1.97 ug/ml
1.41 ug/ml
1.00 ug/ml
0.72 ug/ml
0.51 ug/ml
0.36 ug/ml
0.26 ug/ml
0.18 ug/ml
0.13 ug/ml
0.09 ug/ml
0.06 ug/ml
0.04 ug/ml
0 ug/ml

Proportionate work on the manuscript: 80%

Status: Manuscript in preparation

Discussion

Structural and functional role of the degenerate nucleotide binding site

Our work concerning replacement of non-consensus amino acids in the degenerate nucleotide binding site by consensus ones led to several important findings. The details are elaborated in Paper I. It was observed that single point mutations did not severely impact ATP hydrolysis rates while affecting rhodamine 6g transport to varying levels. Liquid drug assays with rhodamine 6g, cycloheximide, fluconazole and ketoconazole revealed similar patterns of drug resistance. Interestingly, the combination of mutations viz. AHC loop (Walker A, H loop and C loop) and ABHC loop (Walker A, Walker B, H loop, and C loop) displayed significantly reduced ATPase activities and no rhodamine 6g transport. Liquid drug assays also showed significantly reduced resistance towards all drugs except rhodamine 6g for these mutants (investigations regarding this contradicting result is discussed later). These results lead us to believe that artificially engineering a second functional NBS in Pdr5 actually disrupts the ATP hydrolysis occurring at the consensus NBS in addition to not contributing fruitfully to the new NBS. It also means that there are probably significant architectural alterations in the NBDs following the mutations that lead to a complete breakdown of the function. The co-ordination as well as communication between the two NBS as well as the TMDs and NBDs is crucial for proper ABC transporter function. In this regard the D loops have been proposed to play a very important role in communication between the two NBS (28, 29). The Q loops are the ones proposed to co-ordinate movements between the NBDs and

TMDs (29), this goes together with the proposed X loops right at the junction between the NBDs and TMDs which are thought to act as gatekeepers controlling the substrate binding pocket (30). In our study we think that it is the essential inter-domain NBS communication that has been broken down due to the introduced mutations and hence ATP binding and hydrolysis at one NBS is not 'sensed' by the other. This ultimately leads to complete non-functionality of the transporter. Figure 9 displays the predicted change in the degenerate NBS after introducing the mutations.

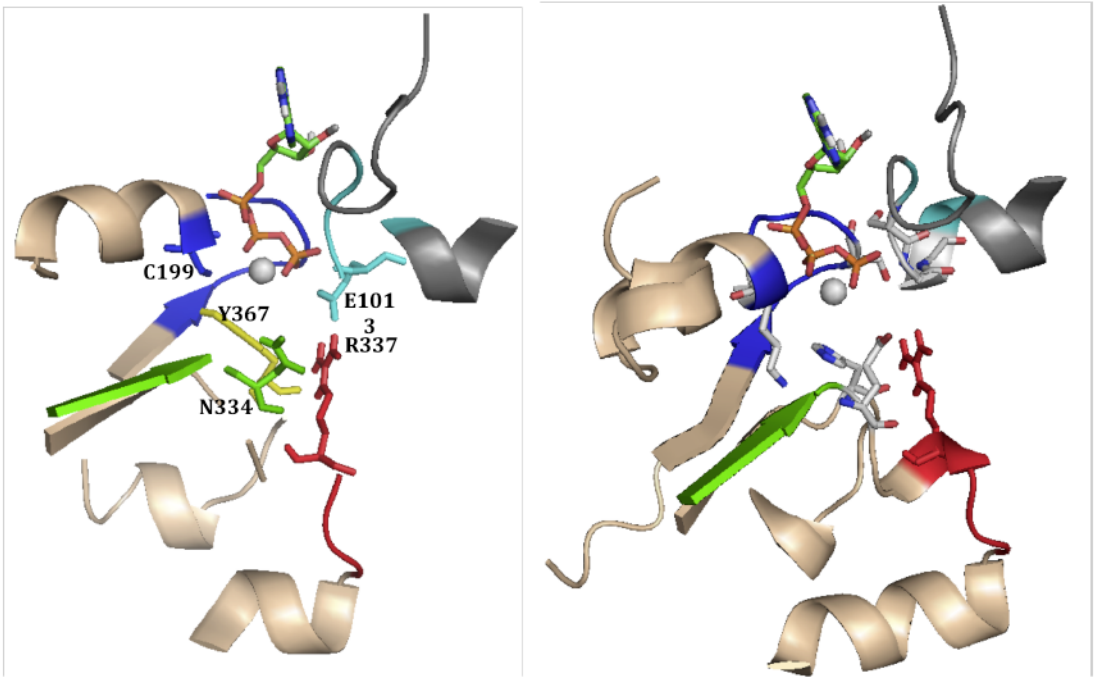

Figure 9. Comparison of the degenerate NBS before and after introducing the mutations. Based on the Pdr5 model proposed by Rutledge *et al*. (17).

To get a complete view of the NBDs with all the vital sequences necessary for nucleotide binding and hydrolysis as well as the communication machinery we introduced the mutations *in silico* and observed the changes in structure as shown in figure 10.

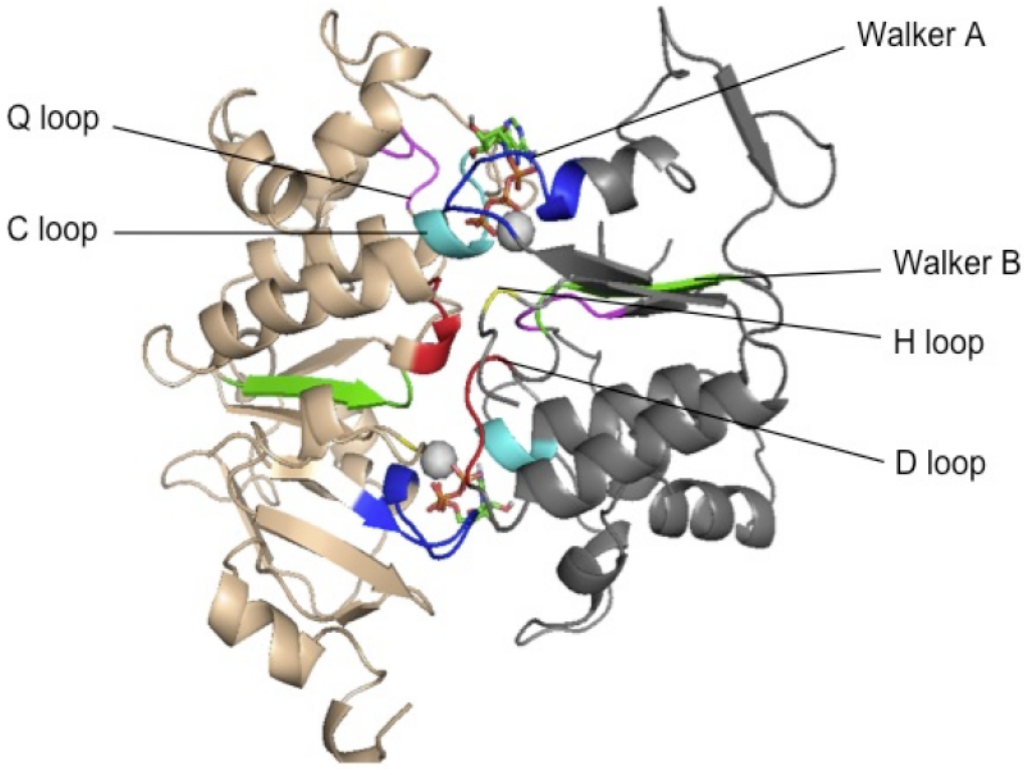

Figure 10. Pdr5 model with the altered bases and the predicted structural changes. Based on Rutledge *et al*. (17).

Substrate dependent stochastic stoichiometry of rhodamine 6g transport

Coupling of ATP hydrolysis to substrate transport is a basic feature of ABC transporters and has been extensively studied (22, 31). Pgp for instance is a strictly coupled ABC transporter in the sense that presence of a substrate increases the ATP hydrolysis rate and vice versa (32). It also makes sense from the cell's point of view to possess such a

regulatory handle on the protein to avoid futile ATP hydrolysis. On the other hand lies Pdr5, which so far has not displayed any substrate stimulated ATPase activity and maintains a relatively high level basal activity. This goes hand-in-hand with the presence of a degenerate NBS, which practically cannot hydrolyze ATP. Such a feature is seen in yeast ABC transporters and is remarkably different than the ones from higher eukaryotes.

We study Pdr5 functionality in crude membrane preparations using mainly two assays: Oligomycin sensitive ATPase activity determination and rhodamine 6g transport assay. Although the ATPase activity can also take place in a protein molecule that can no longer transport a substrate, the rhodamine 6g assay essentially requires structural integrity and functionally active protein to get a positive read-out. This is the basis of our work concerning the selection of the rhodamine 6g transport assay for stoichiometry determination. Our approach was a rather simple one of attempting to measure the amount of ATP hydrolyzed while monitoring active rhodamine 6g transport. Rhodamine 6G is a fluorescent substrate and it fluoresces in its monomeric state while dimers and higher oligomers are non-fluorescent (27). Our crude membrane preparations of highly enriched Pdr5 are oriented inside-out i.e the NBDs face the outside while the substrate is transported to the lumen of the vesicle. In the presence of ATP the transport activity takes place, which leads to a drop in fluorescence intensity and can be monitored in real time using a spectrofluorometer. Our results are elaborated in Paper II. Basically our findings report stoichiometric ratios of 0.3 i.e about 3 molecules of ATP are hydrolyzed per molecule of substrate transported. But in our

observation this ratio is stochastic due to its dependence on substrate concentration. As mentioned earlier Pdr5 constantly hydrolyzes ATP regardless of any substrate being present, hence it turns out it is only a matter of chance that Pdr5 encounters a substrate and pumps it out. This is completely dependent and directly proportional to the concentration of the substrate present. This relation holds true until the substrate itself becomes inhibitory to the protein and locks the possibly locks the protein in the outward facing conformation at high concentration. This in turn affects ATP hydrolysis and the stoichiometric coupling goes down. In our case the optimum substrate concentration was determined as 600nM rhodamine 6g beyond which we observed a decrease in the coupling ratios.

Possible alternate mechanisms of overcoming drug resistance

Our mutagenesis study concerning the degenerate NBS led to some very interesting observations. Among these was an increased resistance towards rhodamine 6g of two mutants AHC loop and ABHC compared to WT. This was contradictory to our biochemical data that displayed very low ATPase activity and no active transport of rhodamine 6g by these mutants. As a result we tried to take a new approach to better understand the reasons behind this. Direct fluorescence microscopy of the mutant cells exposed to rhodamine 6g during the liquid drug assay showed that while WT cells have no intracellular rhodamine 6g, the mutants have huge accumulation of the dye in the cells. This is intriguing because the mutants can withstand almost twice as much rhodamine 6g than the WT cells while maintaining cell viability.

These observations pointed in the direction of possible alternate mechanisms of drug resistance in action in the mutants. To investigate this we subjected the WT and mutants exposed to rhodamine 6g to complete proteome analysis by LC-MS. The results are elaborated in Paper VI. In essence what we discovered is that in the presence of rhodamine 6g the mutant cells up-regulate the glycolytic enzymes significantly more than the WT cells. This is crucial for cell survival in the absence of functional ATP generation from the mitochondria. It was also observed from growth assays that the mutants were much better adept at utilizing glucose at low concentrations than the WT. Protein interactome studies indicate that Pdr5 can interact with hexose transporters present in the membrane (33, 34). It is plausible that such an event does take place and the interaction between hexose transporters and Pdr5 does alter the amount of glucose import within the cell. This interaction between the two proteins might be different between the WT and the mutants due to alterations in the post-translational modifications of the proteins. Preliminary results with γ-P^{32} ATP comparing WT and ABHC mutants did display higher phophorylation of the mutant. It is quite possible that other post-translational modifications are involved as well. This hypothesis is in agreement with the data because the cells lacking Pdr5 show no such behaviour and are way more sensitive to rhodamine 6g than the mutant. Real time measurements of vital parameters such as glucose and oxygen consumption, pH measurement and biomass increase will shed more light on the mechanisms in action. A recent study does point towards accumulation of glucose within the yeast cells as an anticipatory measure to counteract stress (35). This clearly supports

our hypothesis that when yeast cells are exposed to a substrate like rhodamine 6g, which is not very toxic, the cells have time to respond and put in action alternate mechanisms of cell survival. We also suspect the retrograde phenomenon to play a role in this that involves communication between mitochondria and nucleus through transcription factors that lead to metabolic flux changes during stress (36).

References

1. Aller SG*, et al.* (2009) Structure of P-glycoprotein reveals a molecular basis for poly-specific drug binding. (Translated from eng) *Science* 323(5922):1718-1722 (in eng).
2. Csanady L, Mihalyi C, Szollosi A, Torocsik B, & Vergani P (2013) Conformational changes in the catalytically inactive nucleotide-binding site of CFTR. (Translated from eng) *J Gen Physiol* 142(1):61-73 (in eng).
3. Ouellette M, Legare D, & Papadopoulou B (2001) Multidrug resistance and ABC transporters in parasitic protozoa. (Translated from eng) *J Mol Microbiol Biotechnol* 3(2):201-206 (in eng).
4. Balzi E & Goffeau A (1994) Genetics and biochemistry of yeast multidrug resistance. (Translated from eng) *Biochim Biophys Acta* 1187(2):152-162 (in eng).
5. Balzi E & Goffeau A (1991) Multiple or pleiotropic drug resistance in yeast. (Translated from eng) *Biochim Biophys Acta* 1073(2):241-252 (in eng).
6. Kolaczkowska A & Goffeau A (1999) Regulation of pleiotropic drug resistance in yeast. (Translated from Eng) *Drug Resist Updat* 2(6):403-414 (in Eng).
7. Carvajal E, van den Hazel HB, Cybularz-Kolaczkowska A, Balzi E, & Goffeau A (1997) Molecular and phenotypic characterization of yeast PDR1 mutants that show hyperactive transcription of various ABC multidrug transporter genes. (Translated from eng) *Mol Gen Genet* 256(4):406-415 (in eng).
8. Katzmann DJ, Hallstrom TC, Mahe Y, & Moye-Rowley WS (1996) Multiple Pdr1p/Pdr3p binding sites are essential for normal expression of the ATP binding cassette transporter protein-encoding gene PDR5. (Translated from eng) *J Biol Chem* 271(38):23049-23054 (in eng).
9. Zaidi AH*, et al.* (2008) The ABC-type multidrug resistance transporter LmrCD is responsible for an extrusion-based mechanism of bile acid resistance in Lactococcus lactis. (Translated from eng) *J Bacteriol* 190(22):7357-7366 (in eng).
10. Thor Straten P, Kirkin AF, Seremet T, & Zeuthen J (1997) Expression of transporter associated with antigen processing 1 and 2 (TAP1/2) in malignant melanoma cell lines. (Translated from eng) *Int J Cancer* 70(5):582-586 (in eng).

11. Decottignies A*, et al.* (1998) ATPase and multidrug transport activities of the overexpressed yeast ABC protein Yor1p. (Translated from eng) *J Biol Chem* 273(20):12612-12622 (in eng).
12. Rogers B*, et al.* (2001) The pleitropic drug ABC transporters from Saccharomyces cerevisiae. (Translated from eng) *J Mol Microbiol Biotechnol* 3(2):207-214 (in eng).
13. Golin J, Ambudkar SV, & May L (2007) The yeast Pdr5p multidrug transporter: how does it recognize so many substrates? (Translated from eng) *Biochem Biophys Res Commun* 356(1):1-5 (in eng).
14. Kolaczkowska A, Kolaczkowski M, Goffeau A, & Moye-Rowley WS (2008) Compensatory activation of the multidrug transporters Pdr5p, Snq2p, and Yor1p by Pdr1p in Saccharomyces cerevisiae. (Translated from eng) *FEBS Lett* 582(6):977-983 (in eng).
15. Golin J*, et al.* (2007) Complete inhibition of the Pdr5p multidrug efflux pump ATPase activity by its transport substrate clotrimazole suggests that GTP as well as ATP may be used as an energy source. (Translated from eng) *Biochemistry* 46(45):13109-13119 (in eng).
16. Zaitseva J*, et al.* (2006) A structural analysis of asymmetry required for catalytic activity of an ABC-ATPase domain dimer. (Translated from eng) *EMBO J* 25(14):3432-3443 (in eng).
17. Rutledge RM, Esser L, Ma J, & Xia D (2011) Toward understanding the mechanism of action of the yeast multidrug resistance transporter Pdr5p: a molecular modeling study. (Translated from eng) *J Struct Biol* 173(2):333-344 (in eng).
18. van Veen HW, Higgins CF, & Konings WN (2001) Multidrug transport by ATP binding cassette transporters: a proposed two-cylinder engine mechanism. (Translated from eng) *Res Microbiol* 152(3-4):365-374 (in eng).
19. Tombline G*, et al.* (2008) ATP occlusion by P-glycoprotein as a surrogate measure for drug coupling. (Translated from eng) *Biochemistry* 47(10):3294-3307 (in eng).
20. Sauna ZE*, et al.* (2007) Catalytic cycle of ATP hydrolysis by P-glycoprotein: evidence for formation of the E.S reaction intermediate with ATP-gamma-S, a nonhydrolyzable analogue of ATP. (Translated from eng) *Biochemistry* 46(48):13787-13799 (in eng).

21. Sharom FJ (2006) Shedding light on drug transport: structure and function of the P-glycoprotein multidrug transporter (ABCB1). (Translated from eng) *Biochem Cell Biol* 84(6):979-992 (in eng).
22. Sauna ZE & Ambudkar SV (2001) Characterization of the catalytic cycle of ATP hydrolysis by human P-glycoprotein. The two ATP hydrolysis events in a single catalytic cycle are kinetically similar but affect different functional outcomes. (Translated from eng) *J Biol Chem* 276(15):11653-11661 (in eng).
23. George AM & Jones PM (2012) Perspectives on the structure-function of ABC transporters: the Switch and Constant Contact models. (Translated from eng) *Prog Biophys Mol Biol* 109(3):95-107 (in eng).
24. Ernst R*, et al.* (2008) A mutation of the H-loop selectively affects rhodamine transport by the yeast multidrug ABC transporter Pdr5. (Translated from eng) *Proc Natl Acad Sci U S A* 105(13):5069-5074 (in eng).
25. Decottignies A, Kolaczkowski M, Balzi E, & Goffeau A (1994) Solubilization and characterization of the overexpressed PDR5 multidrug resistance nucleotide triphosphatase of yeast. (Translated from eng) *J Biol Chem* 269(17):12797-12803 (in eng).
26. Serrano R (1988) H+-ATPase from plasma membranes of Saccharomyces cerevisiae and Avena sativa roots: purification and reconstitution. (Translated from eng) *Methods Enzymol* 157:533-544 (in eng).
27. Toptygin D, Packard BZ, & Brand L (1997) Resolution of absorption spectra of rhodamine 6G aggregates in aqueous solution using the law of mass action. *Chemical Physics Letters* 277(5,Äì6):430-435.
28. Ananthaswamy N*, et al.* (2010) The signaling interface of the yeast multidrug transporter Pdr5 adopts a cis conformation, and there are functional overlap and equivalence of the deviant and canonical Q-loop residues. (Translated from eng) *Biochemistry* 49(21):4440-4449 (in eng).
29. Jones PM & George AM (2012) Role of the D-loops in allosteric control of ATP hydrolysis in an ABC transporter. (Translated from eng) *J Phys Chem A* 116(11):3004-3013 (in eng).
30. Dawson RJ & Locher KP (2006) Structure of a bacterial multidrug ABC transporter. (Translated from eng) *Nature* 443(7108):180-185 (in eng).

31. Al-Shawi MK, Polar MK, Omote H, & Figler RA (2003) Transition state analysis of the coupling of drug transport to ATP hydrolysis by P-glycoprotein. (Translated from eng) *J Biol Chem* 278(52):52629-52640 (in eng).
32. Senior AE, al-Shawi MK, & Urbatsch IL (1995) ATP hydrolysis by multidrug-resistance protein from Chinese hamster ovary cells. (Translated from eng) *J Bioenerg Biomembr* 27(1):31-36 (in eng).
33. Nourani A, Wesolowski-Louvel M, Delaveau T, Jacq C, & Delahodde A (1997) Multiple-drug-resistance phenomenon in the yeast Saccharomyces cerevisiae: involvement of two hexose transporters. (Translated from eng) *Mol Cell Biol* 17(9):5453-5460 (in eng).
34. Snider J*, et al.* (2013) Mapping the functional yeast ABC transporter interactome. (Translated from eng) *Nat Chem Biol* 9(9):565-572 (in eng).
35. Dikicioglu D*, et al.* (2013) Yeast cells with impaired drug resistance accumulate glycerol and glucose. (Translated from eng) *Mol Biosyst* 10(1):93-102 (in eng).
36. Butow RA & Avadhani NG (2004) Mitochondrial signaling: the retrograde response. (Translated from eng) *Mol Cell* 14(1):1-15 (in eng).

Declaration

The dissertation presented here has been made independently and without unauthorized assistance. The dissertation has not been submitted in this or any similar form to any other institution. I have not taken any unsuccessful promotion exams so far.

Duesseldorf, 20th January 2014

Rakeshkumar P. Gupta

Acknowledgements

First and foremost I thank Lutz for his ever-cheerful nature, patience, enthusiasm and constant encouragement towards our work. I have thoroughly enjoyed brainstorming discussions with you and shall always cherish them. Had it not been for your motivation and freedom to pursue my ideas I could not have come this far. Your 'Just do it' attitude and 'Good data is worth a million theories' motto are something I shall take with me.

Nils and Patrick: It was a privilege to share the office with you two in the beginning stages of my study. Tossing around ideas on boring afternoons was wonderful and rewarding when I look back at it. Nils thank you for everlasting discussions, in most of which I was merely a listener. I am thankful to both of you.

Sander and Uli: I must thank Sander for his sharp criticisms at times that made us look at the problems in a different way and also for your excellent suggestions. I thank Uli for being there always whenever I needed an external opinion about my hypothesis, and sharing his time and ideas with me without ever complaining.

Petra: Thank you for teaching me the basics of working with Pdr5 and your friendly nature.

Jan: Dear Sir, thank you for the joy you always bring along. I wish you all the very best, and thank you for the wonderful time we had in the lab.

Sabrina, Susanne, Diana and Iris L: Dear 2nd floor office friends thank you all very much for a cheerful atmosphere in the office at all times. Crazy girl thank you for never complaining to my teasing. I thank all of you and wish you all the very best.

Miro, Vero, Tatu, Nino and Nacera: I miss all of you guys. Tatu and Vero thank you for your ever cheerful smiles, hope you two are doing great. Miro and Nino my buddies at the weekends at the Institute, thanks for the company.

Philipp, Andre and Christian: Thank you guys for all the fun we had during parties and barbeques. Philipp- the sailor, keep sailing and conquer new frontiers. I wish all of you the very best.

Michael, Sven, Kerstin, Kalpana, Sakshi, Eleanor, Katharina, Jens, Marcel and Sandra: Welcome to all the newbies and wish you all the best. Thank you all for the cheer and fun.

Zainab, Ricarda, Iris G, Martina, Marianne, Silke and Isa: Thanks to all you girls for all the help and good times. Thank you Martina for your help with technical things whenever I needed.

Frau Rasid and Frau Blum: Thank you Frau Blum for taking care of all the administrative stuff for me every time I needed. My sincere thanks to Frau Rasid,

you have been like a family member to me away from home. Thanks to you I learnt German and I wish you good health and happiness for the future.

Pallavi: Dear Palla, thank you for always being there as a friend and your constant support and motivation. I consider myself blessed to have friends like you. I wish you all the best, may you find lots of success and happiness wherever you go.

Pritesh: Dear Pritesh, thank you for your pragmatic advice over the years and your friendship.

And last but not least I wish to thank my parents, sister, Sandeep and little Advik for all your support and blessings throughout. I would not have been anyone or anything without all of you being there for me always. Words are not enough to express my gratitude for you.